



VIETNAM INSTITUTE OF METEOROLOGY HYDROLOGY AND CLIMATE CHANGE

ISSN 2525-2496

JOURNAL OF CLIMATE CHANGE SCIENCE

No.19 - Sep. 2021



JOURNAL OF CLIMATE CHANGE SCIENCE

EDITOR-IN-CHIEF
Nguyen Van Thang

DEPUTY EDITOR-IN-CHIEF
Huynh Thi Lan Huong

EDITORIAL BOARD

HEAD OF EDITORIAL BOARD: Tran Thuc

MEMBERS:

Duong Hong Son
Mai Van Khiem
Nguyen Ky Phung
Doan Ha Phong
Hoang Minh Tuyen
Truong Duc Tri
Do Tien Anh
Le Ngoc Cau
Do Dinh Chien
Bach Quang Dung
Nguyen Xuan Hien
Vu Van Thang

MANAGING EDITOR

Tran Thanh Thuy

HEAD OF ADMINISTRATION:

Tran Thanh Thuy

PUBLICATION LICENCE:

No. 604/GP-BTTTT

30th December 2016

Ministry of Information and
Communications

JOURNAL OFFICE:

23/62 Nguyen Chi Thanh Str,
Dong Da Dist., Hanoi

Tel:+84.2437731410

Email: tapchibdkh@imh.ac.vn

Website: <http://imh.ac.vn>

PRINTED IN:

Le Giang jsc

87/192 Le Trong Tan Str,
Hoang Mai Dist, Ha Noi

- 1 **Tran Thuc:** An introduction to the working version of the ninth phase of the intergovernmental hydrological programme, 2022-2029
- 5 **Bui Duc Hieu, Ta Dinh Thi, Nguyen Dang Huy Anh, Nguyen Anh Tuan:** Effectiveness of measures to improve water security in Quang Ngai province in the context of climate change
- 14 **Luong Huu Dung, Doan Huy Phuong, Ngo Thi Thuy, Chu Nguyen Ngoc Son:** Impact of urbanization on flooding in Khanh Hoa province
- 20 **Nguyen Van Hong, Nguyen Phuong Dong, Pham Thanh Long, Pham Anh Binh, Ho Cong Toan:** Study on forecasting tidal water levels in the Sai Gon Dong Nai river for assessment of flood impacts in Ho Chi Minh city
- 29 **Le Quoc Huy, Pham Tien Dat, Tran Van My, Nguyen Hong Hanh, Nguyen Thi Lan, Dang Linh Chi:** Characterizing effects of different ENSO phases on Sea Surface Temperature in the Viet Nam East Sea
- 37 **Le Hung Chien, Doan Ha Phong, Tran Xuan Truong, Ngo Thi Dinh:** Determination of evapotranspiration using solar radiation and meteorological data applying different methods: A case study Hoa Binh province
- 49 **Truong Ba Kien, Tran Duy Thuc, Nguyen Quang Trung, Nguyen Binh Phong, Vu Van Thang:** Radar extrapolation in very short-range rainfall forecasting in Ho Chi Minh city
- 59 **Vu Thanh Hang, Pham Thi Thanh Nga, Doan Thi The, Pham Thanh Ha, Nguyen Thi Phuong Hao, Nguyen Tien Cong:** The ability of RCA4 regional climate model to simulate and project surface solar irradiation over Viet Nam
- 72 **Nguyen Xuan Hien, Nguyen Thi Thanh, Ngo Thi Thuy, Du Duc Tien:** Developing tropical cyclone risk warning system for North Central Viet Nam
- 80 **Le Ngoc Cau, Pham Van Sy, Ngo Thi Van Anh, Le Van Quy, Mai Trong Hoang:** Assessing climate change risk and vulnerability for agricultural sector in Hoa Binh province
- 92 **Doan Thi The, Duong Hai Yen, Nguyen Van Son, Le Thi Thu, Nguyen Hong Son, Le Thi Thu Ha:** Review of assessment of agricultural meteorology in Viet Nam crops 2020
- 103 **Ngô Thi Thuy, Tran Van Tra, Cung Hong Viet, Nguyen Dinh Hoang:** Changes in air quality during COVID-19 social distancing in Ha Noi city

AN INTRODUCTION TO THE WORKING VERSION OF THE NINTH PHASE OF THE INTERGOVERNMENTAL HYDROLOGICAL PROGRAMME, 2022 - 2029

Tran Thuc

Chairman of Viet Nam National Committee for the UNESCO-IHP

Received: 03 August 2021; Accepted: 23 August 2021

1. Background

The UNESCO Intergovernmental Hydrological Programme (IHP), founded in 1975, is a long-term programme executed in phases of 8-year duration. Its programmatic focus has gone through a profound transformation from a single discipline mode to a multi-disciplinary undertaking, aimed at advancing hydrological knowledge through supporting scientific research and education programmes. Recently, with the increased presence of social science components, including important growth in the quality and quantity of citizen science inputs, IHP is evolving into a truly transdisciplinary undertaking. This progress has capitalized on the recognition that solutions to the world's water-related problems are not just technical, engineering or natural science issues, but have strong human and socio-cultural dimensions, where social sciences play an increasingly important role. IHP facilitates an interdisciplinary and integrated approach to watershed and aquifer management, which incorporates the social dimension of water resources, promotes and develops international research in hydrological and freshwater sciences. The ever-increasing pace of environmental changes intertwined with human dimensions calls for a better understanding of hydrology. The interaction between human activities and water systems needs to be considered to develop scenarios for water resources management.

For decades, water-related challenges have

grown significantly in terms of complexity and frequency. As challenges related to water resources have become more serious, it is time for people to take action to protect water security. To handle the issue, it is fundamental to create and disperse information through strong public and worldwide approaches to support more developments. The IHP of UNESCO in its Eighth Phase has been the current apparatus for the UN Member States to make this a reality worldwide. Phase Eight of IHP, from 2014 to 2021 has been conceived, among other goals, to help implement the international post-2015 agenda and the forthcoming Sustainable Development Goals. The Programme can help develop flexible and adaptable solutions in various contexts that help in transforming societies of all cultures into societies resilient to global changes and increase their potential to develop in a sustainable manner.

IHP-IX continues to offer a platform and venue to extend cooperation within the international scientific community, and thus contribute to addressing many unsolved problems in hydrology. The main objective of the IHP ninth phase (IHP-VIII 2014 - 2021) is to outline a compelling and strategic focus for the Intergovernmental Hydrological Programme for the 2022 - 2029 period. This is an important goal which requires strengthening the cooperation and synergies between the IHP and programmes of other UN agencies and other relevant organisations on a global level and on the ground. The following content will introduce Priority Areas, Vision, Mission as well as Strategic Objectives of the IHP-IX local and nearby scale.

*Corresponding author: Tran Thuc
E-mail: tranthuc.vkttv@gmail.com*

2. Priority Areas

The IHP-IX priority areas, identified and elaborated by UNESCO's Member States, are presented as five transformative tools that will enable water security to sustain development in a changing world for the period 2022 - 2029:

a. Scientific Research and innovation

The development of hydrological science and research has provided practical knowledge and information for society about water fluxes, transport and management, however, ever-increasing and uncertain environmental changes demands for a continued effort on research innovation and application. Scientific research incorporating human interactions with nature in the context of complex water sciences and management problems provide fundamental feedback for water resources management, along with the application of new tools, approaches, and technologies.

b. Water education in the Fourth Industrial Revolution

It is undeniable that the success of Agenda 2030 for Sustainable Development and water-related SDGs and associated targets depend on a profound transformation in human values and, consequently, human behaviour and actions, directly impacting how we live our lives. Achieving that end can only be envisioned when society recognizes the need to reintegrate itself with nature in ways that embrace a common understanding of the importance and limits of our natural resource base to improving the quality of life. Water education at all levels for an improved water culture, in a context of global change, is undoubtedly a formidable tool for the Member States to practice inclusive, evidence-based water governance and management in order to move towards resilient and sustainable societies.

c. Bridging the data-knowledge gap

By the year 2029, significant advances will have occurred in transparency and accessibility of water data, which made possible further development of open access science platforms and generated facilitating instruments for

integrated watershed management, particularly in the case of transboundary water resources.

Transparency and accessibility of data are among the main pillars that sustain the advancement of open science - a coming commitment of UNESCO. Hydrological measurements are essential for decision-making and sustainable water resources management. The absence or inaccessibility of comprehensive or long-term data about water quantity, quality, distribution, access, risks, use, etc. often leads to partial or ineffective management and investments. Therefore, both sufficient data and its accessibility needs to be ensured and, in many cases, improved, as recommended by the UN Mar del Plata conference in 1977.

d. Inclusive water management under conditions of global change

By 2029, most societies have managed to adapt to or mitigate water risks derived from, among others, climate change and the human factor, such as global pandemics, generating better participatory management practices and new opportunities for the future of our planet.

Healthy rivers, lakes, wetlands, aquifers, and glaciers do not just supply safe drinking water and maintain all ecosystems on the planet; they also support agriculture, hydropower, industry, recreation, communications, and transportation of goods. Although water is considered the core of sustainable socio-economic development, it is frequently ignored in the investment debate. Additionally, water management is not considered in an integrated, inclusive manner and it is frequently disbursed; considered a shared responsibility among many different governmental institutions.

e. Water governance based on science for mitigation, adaptation, and resilience

Water governance refers to the political, social, economic, legal, and administrative systems in place that influence water's access and use, protection from pollution, and management in general. It determines the equity and efficiency in water resources and services allocation and distribution, and balances water use between socio-economic activities

and the goods and services provided through ecosystem preservation. It includes formulation, establishment, and implementation of water policies, with clear and practical standards based on science, including water ethics, legislation and institutions, and the roles and responsibilities of all stakeholders. By 2029, Member States have significantly reduced water governance gaps, generating greater equity and efficiency in the allocation, distribution, and conservation of water resources and services, and designing and implementing water policies in an inclusive and participatory way with standards based on science while developing ongoing efforts addressing the adaptation and mitigation to climate change.

3. IHP Vision

IHP envisions a water-secure world where people and institutions have adequate capacity and scientifically based knowledge for informed decisions on water management and governance to attain sustainable development and to build resilient societies.

4. IHP-IX Mission

Our mission for the period 2022 - 2029 is to support the Member States to accelerate the implementation of water-related SDGs and other relevant agendas through water science and education. To this end IHP-IX will:

a. Leverage intersectorality for sustainable water management and sustainable water security;

b. Promote international scientific research and cooperation for improved knowledge to address water and climate challenges incorporating the interaction between human and water systems.

c. Mobilize and disseminate effectively scientific relevant expertise, knowledge, and tools for informed decisions in addressing water challenges.

d. Reinforce institutional and human capacities and train the present and upcoming generation of water professionals capable of providing water solutions for SDGs and building climate resilience through the water.

e. Raise awareness and promote a water

culture and water ethics at all levels for conserving, protecting, and mainstreaming the crucial role of water in all sectors.

f. Support Member States in better understanding and managing their water resources.

g. Support the UN SDG6 Global Accelerator Framework implementation including the associated water and climate coalition in terms of understanding and implementing solutions to global water challenges

5. Strategic Objectives

As several challenges arise from achieving water security, which range from the effects of global change such as water-related disasters to operational aspects such as understanding of the value of water as this is expressed by local water rates. The Intergovernmental Hydrological Programme's approach to these challenges is to expand the human capital, scientific base and knowledge at all levels to "understand the impacts of global changes on water systems and to link scientific conclusions to policies for promoting sustainable management of water resources".

The above-identified outcome of IHP-IX is aligned with UNESCO's overall Medium-Term Strategy and will serve two of its Strategic Objectives: Strategic Objective 1: Reduce inequalities and promote learning and creative societies in the digital age through quality education for all; Strategic Objective 2: Work towards sustainable societies by preserving the environment through the promotion of science, technology and the natural heritage.

A prerequisite to evidence-based water governance and management is available, accessible and current scientific knowledge provided by trained and aware human resources. Strategies and activities addressing global changes that are science-based and inclusive of all sectors of civil society in the context of the long-term resilience of decisions taken, enhance the overall resilience of societies. Building communities and societies that are resilient in the face of changing and ever more complex environmental conditions requires that science

inform policy. Improving this aspect of the decision process permits greater involvement of civil society with the government, including the ability of decision-makers to benefit from the use of indigenous knowledge.

The following performance indicators have been identified to monitor progress towards the achievement of the desired result (Outcome 1):

- PI 1: Number of Member States/stakeholders use improved water science, research and apply the strengthened capacities to expand knowledge and better manage services and related risks at all levels.

- PI 2: Number of Member States with enhanced water informal, formal, and non-formal education at all levels.

- PI 3: Number of Member States which use scientific data, and knowledge to sustainably manage their water resources.

- PI 4: Number of Member States practice inclusive and cross-sectoral water management to address global challenges.

- PI 5: Number of Member States implementing mechanisms and tools based on science to strengthen water governance for mitigation, adaptation, and resilience.

EFFECTIVENESS OF MEASURES TO IMPROVE WATER SECURITY IN QUANG NGAI PROVINCE IN THE CONTEXT OF CLIMATE CHANGE

Bui Duc Hieu⁽¹⁾, Ta Dinh Thi⁽²⁾, Nguyen Dang Huy Anh⁽³⁾, Nguyen Anh Tuan⁽⁴⁾

⁽¹⁾Office of the Ministry of Natural Resources and Environment

⁽²⁾Congressman of the 15th National Assembly, Viet Nam Administration of Seas and Islands

⁽³⁾Department of Climate change

⁽⁴⁾Viet Nam Institute of Meteorology, Hydrology and Climate change

Received: 12/8/2021; Accepted: 01/9/2021

Abstract: *As one of the countries most adversely affected by climate change and sea level rise, Viet Nam is facing many challenges threatening its water security. Currently, there have not been many studies assessing water security in the context of climate change, especially the quantification of the water security at national and provincial levels. The study used the method of developing a set of indicators to assess the water security in the context of climate change. On that basis, the study proposed measures to improve the water security in Quang Ngai province. The analysis results show that among the 17 proposed sub-indicators on water security, there are 5 sub-indicators that cannot be affected, namely: flood frequency; number of days of drought; ratio of flooded area; the average annual rainfall and the average annual temperature. The remaining 12 sub-indicators can be improved by measures and hence the study has selected prioritized measures to ensure water security in Quang Ngai in the direction of focusing on improving these 12 indicators.*

Keywords: *Water security; Climate Change; Set of indicators.*

1. Introduction

Water is an essential part of life, a basic need and foundation for the ecosystem and social activities, so water plays an important role in contributing to conflicts that can threaten human security and the environment [6].

Water security is not simply about “appropriate access to water” – it is about sustainable access to water in an appropriate quantity and quality to meet the needs of survival, production, socio-economic development and protection of ecosystems. Water security is central to achieving a broader sense of security, sustainability, development and human affairs [8]. Specifically, according to the United Nations Water (UN-Water), the most complete definition of water security is “*The capacity of*

a population to safeguard sustainable access to adequate quantities of acceptable quality water for sustaining livelihoods, human well-being, and socio-economic development, for ensuring protection against water-borne pollution and water-related disasters, and for preserving ecosystems in a climate of peace and political stability”.

Measuring the water security is not a simple task and many tools have been established to quantify it [10]. In an assessment for the Asia-Pacific region [7], the water security of 46 countries with different conditions on water resource and socio-economic development was assessed through 5 indicators including: basic needs, food production, environmental flows, risk management and independence. In the study of water security indicators [9], in order to calculate the water security, 03 groups of sub-indicators are needed including water

Corresponding author: Bui Duc Hieu
E-mail: duchieulect@gmail.com

resources, water environment and socio-economic conditions, which used 15 factors selected for establishing an integrated assessment of water security in the Yellow River basin. Specific targets include: (i) Water resource component; (ii) Water environment component; and (iii) Socio-economic component. The Asian Water Development Outlook Report of the Asian Bank (ADB) published in 2020 [18] has introduced a method to measure water security using five main indicators, including: (1) the water security of rural households, (2) economic water security, (3) security on urban water, (4) security on water environment, and (5) security on water-related disaster.

In Viet Nam, although there is not much research on water security, some research related to water security can be mentioned, including:

In 2015, the study on “Development and application of a framework for assessing water security for Ha Noi city” [4] showed the water security index of Ha Noi and the integrated water security index (WSI) in 2005, 2010 and 2015, with respectively. Thereby, the study showed that the water security index of Ha Noi City has increased gradually over time. Based on the arithmetic average method and weighting of indicators for groups, and regions, the research has divided Ha Noi into 4 areas (Center, North, West and South) and categorized 5 groups of indicators according to the following criteria: Household; Economy; Environment; Disasters and governance, management.

One of the recent studies on water security in Viet Nam [5] is the study on water security for sustainable development of the Ma river basin. The study developed a set of water security indicators in Viet Nam's river basin, which includes 18 indicators divided into 6 groups of sub-indicators: (i) Water flowing to the river basin; (ii) Clean water supply for people; (iii) The economic level of water use of the river basin; (iv) Protection of river ecosystems and environment; (v) Risks and damages caused by natural disasters; (vi) Management of water resource and river basin, and decentralization of water security assurance levels in the basin. On that basis, the study proposed a number

of structural and non-structural measures to ensure water security in the basin.

Therefore, it can be seen that it is possible to evaluate and quantify the level of water security and apply a set of indicators in the assessment, which serves as a basis for proposing measures to ensure the water security. Regarding Viet Nam's situation, although numerous issues on water security have arisen nationwide in general and in Quang Ngai in particular. Viet Nam has a few studies on water security, even in the State's legal documents, especially in the context of climate change. From that perspective, this study was conducted to assess the level of water security in the context of climate change in Quang Ngai through a set of indicators, which also serves as a basis for proposing and selecting response solutions.

2. Research method and used data

2.1. Method of selection and calculation of water security indicators

2.1.1. Preliminary index selection

Through a literature review and based on the UN-Water's definition of water security, the study identified the factors that need to be achieved to ensure water security, including: (i) The community has enough water for domestic use and serving socio-economic development; (ii) Guaranteed water quality, using clean water; (iii) Not affected by water-related disasters; (iv) All of the above factors must be maintained in the condition that the ecosystem is still preserved, the community lives in peace, and the political system is stable.

The study has preliminarily identified indicators to assess water security (before consulting experts) including 04 main groups of indicators showing 4 aspects of UN-Water's water security concept, specific:

- (1) Ecosystem indicator group: Ecosystem conditions are still preserved;
- (2) Indicator group of Natural disasters and water-related hazards: Water resources are not affected by water-related disasters;
- (3) Socio-economic indicators group: Ensuring enough water for domestic use and serving socio-economic development;

(4) Water resources and people: Water quality is guaranteed, using unpolluted water. Each main group of indicator includes sub-indicators, there are 27 sub-indicators in total. This set of indicators will be consulted by experts to choose appropriate indicators.

2.1.2. Applying the expert method to choose the right indicator

The method of expert consultation was selected to determine the set of indicators on water security [3].

The process of selecting water security indicators was carried out specifically through 8 steps, categorized into 3 stages including before, during and after consultation as follows:

- Stage before expert consultation:

+ Step 1: Select a group of experts related to the consultation process. The number of experts was 10 people (including scientists and managers working on the relevant research content from the Institute of Hydrology, Meteorology and Climate Change, Institute of Water Resources Science, Ha Noi University of Natural Resources and Environment, Department of Water Resources Management, Department of Climate Change, Viet Nam Meteorological and Hydrological Administration and Department of Natural Resources and Environment in Quang Ngai Province).

+ Step 2: Develop indicators of water security based on literature review and conformity assessment.

+ Step 3: Develop questions to consult experts and relevant scientists.

- Stage of expert consultation:

+ Step 4: Conduct the first round consultation. An expert consultation meeting was held. Experts were asked to assess the level of consensus with the given set of indicators. The consensus level is ranked from 1 - 5 as follows: (i) Very irrelevant; (ii) Not relevant; (iii) More or less relevant; (iv) Relevant; and (v) Very relevant.

+ Step 5: Analyze the data from round 1. After collecting data by Delphi method, each group of authors selected different rules to synthesize and analyze results, two commonly used rules are KAMET and DPSIR framework

(Kendal value was used to assess the appropriateness of the indicators that need being consulted. The level of consensus was scored according to the thresholds 0.0 - 0.1; > 0.1 - 0.3; > 0.3 - 0.5; > 0.5 - 0.7; > 0.7 - 1.0, which means very weak; weak; moderate; strong; very strong consensus, with respectively).

Based on the evaluation results, the Median values (Md); Quartile deviation (Q); Mean (qi) and Variance (%) according to KAMET rule were calculated.

+ Step 6: Apply the method of expert consultation in round 2. The questionnaire was sent to experts in round 2 to consult the level of consensus or stability in the answers of the members. Indicators were not used when an expert could not answer the questions with certainty [2].

- Stage after expert consultation:

+ Step 7: Analyze data in round 2. After the data was collected in round 2, the results were analyzed. The analysis was based on the above-mentioned KAMET rule. The value of Median (Md); Quartile deviation (Q); Mean (qi) and Variance (%) were recalculated at this step.

In case all questions were approved or rejected; or the Mean value was higher than 3.5 and the Variance value was less than 15%, the method of expert consultation finalized [2].

Step 8: Analyze and summarize the results. Based on the results from the above steps, the final indicators were selected to perform the calculation.

2.1.3. Determination of water security indicator

The set of water security indicators for Quang Ngai province includes sub-indicators, the value of the water security indicator is calculated by the formula shown below:

$$ANN = \frac{1}{n} \sum_{i=1}^n ANN_i$$

where:

ANN: Water Security Indicator

ANN_i: Ith sub-indicator; n is the total number of indicator groups.

The water security hierarchy is divided by regular intervals (Table 1).

Table 1. Water security classification applied to Quang Ngai province

Range	Classification
$0 < ANN \leq 0.2$	Very low water security
$0.2 < ANN \leq 0.4$	Low water security
$0.4 < ANN \leq 0.6$	Moderate water security
$0.6 < ANN \leq 0.8$	High water security
$0.8 < ANN \leq 1$	Very high water security

2.2. Data used for the calculation

The used data for the calculation of this study included:

- The climate change scenario of Quang Ngai province was extracted from the scenario of climate change and sea level rise for Viet Nam updated in 2016 by the Institute of Meteorology, Hydrology and Climate Change [1]. The scenario was developed according to two scenarios of greenhouse gas concentration, namely the medium scenario RCP4.5 and the high scenario RCP8.5.

- The climate data measured up to 2014 were used for model calibration and comparison of calculated results with actual measured data.

This data was from the following stations: An Chi, Ba To, Ly Son, Quang Ngai, and Son Giang.

- The natural, economic and social data were analyzed from the results of surveys, investigation and related collected documents.

3. Results and Discussion

3.1. A set of indicators on water security

The final set of indicators after expert consultation includes 04 main indicators and 17 sub-indicators. These indicators have closely followed the UN–Water definition as presented in the Introduction section. Specifically, the indicators were described and interpreted according to the calculation formulas as Table 2.

Table 2. The indicators on water security index for the whole year at present

Main indicators	Sub-indicators
Ecosystem	Pollution status
	Water resource pressure
	Water resource indicators
	Green coverage ratio
	Coefficient of ecosystem degradation
Water-related disasters and hazards	Flood frequency
	Number of days of drought
	Portion of flooded area
	Average annual precipitation
	Average annual temperature
Socio-economy	Cost of water and sanitation
	Payment for water and wastewater services
Water resources and people	Water scarcity coefficient
	Coefficient of change of water coming to river basin
	Water extraction coefficient
	Population with access to clean water
	Percentage of people having access to a standard wastewater collection system

3.2. Application of a set of indicators to evaluate the effectiveness of measures to ensure water security in Quang Ngai

3.2.1. Analyze, evaluate and select suitable measures

Among the above-mentioned 17 indicators of water security, there are 05 indicators that cannot be affected, namely: flood frequency, number of days of drought, rate of flooded area, the average annual precipitation and the average annual temperature. The remaining 12 indicators can be improved by measures and hence the selection of prioritized measures to ensure water security in Quang Ngai should focus on improving these 12 indicators. On that basis, the study proposed measures to prioritize implementation until 2030, with a vision to 2050 as follows:

- Measures to maintain and expand the forest area in order to achieve the goal of maintaining the current forest coverage:

- + Focus on investigation, planning, zoning and protection of existing forest areas, reducing forest degradation and promoting new plantation, ensuring the improvement of the ecological environment. In the near future, in addition to the management and protection of special-use forests, the province needs to mainly develop protection forests and production forests; renew production plans and implement measures to develop planted forests, ensuring a sufficient number of laborers to participate in afforestation.

- + Implement synchronously measures on science and technology and human resources as well as policies to attract investment; encourage all economic sectors to participate in forest development effectively; strengthening the capacity of state management, administrative reform, as well as clearly defining the functions and tasks of managing forestry activities in the locality.

- + Continue to maintain and promote the investment policy to develop concentrated material afforestation areas, in which clearly define the rights to use land and forest resources for forestry companies, forestry enterprises, other economies and households, ensuring long-term production investment. Land is allocated

to each household for use, and a part of the area is allocated for agro-forestry production, ensuring for the planting, maintenance and protection of forests. Communes with special difficulties when allocating land to households must allocate capital and investment in techniques and seedlings so that people can feel secure in forestry development.

- Measures for wastewater management and treatment to achieve the goal of 100% of wastewater is collected and treated before being discharged into lakes, rivers, and streams:

- + Focus on monitoring and controlling key waste sources. Continue to invest in and build a monitoring system to monitor continuously, automatically and virtually the water discharge activities of large wastewater discharge facilities that are at risk of polluting water sources.

- + Strictly control projects, works, industrial, agricultural, medical, craft villages, mining zones and clusters... with strict regulations on environmental impact assessment, compliance with the regulation of synchronously constructing the wastewater discharge system with the non-discrete drainage system, avoiding increased pollution and having a policy to increase discharge fees for waste dischargers. Specifically, it is necessary to thoroughly implement Decree No. 53/2020/ND-CP dated May 5, 2020 of the Government on regulations on environmental protection fees for wastewater, which have new articles on the subject of charge as well as the fee level. Particularly, according to the regulation the organizations, households and individuals that discharge wastewater are the payers for environmental protection fees for wastewater. In case organizations, households, and individuals discharge wastewater into the centralized wastewater treatment system and pay for wastewater treatment services to the managing and operating unit of that centralized wastewater treatment system following the service price mechanism, the managing and operating unit will be the one to pay the environmental protection fee for wastewater.

- + Actively propagate to raise the awareness of water saving and water reuse in order to reduce the amount of direct wastewater, in parallel with the awareness of environmental protection.

- Measures to ensure the population of Quang Ngai is at an appropriate level in both quantity and structure to achieve the goal of maintaining the current fertility rate: In fact, the fertility rate in Quang Ngai is decreasing sharply, particularly, the rate of delivering the third child tend to decrease continuously from 2015 to present, with the current value of 11.63%. From that perspective, it is necessary that the province urgently changes its communication, advocacy, and planning strategies, in line with the focus of population work in the new situation. Therefore, Quang Ngai must have its own plan on population work, in which the most important thing is to shift the focus of policy from family planning to population and development, comprehensively solving problems of population size, structure, quality, and distribution in relation to socio-economic development, and ensuring national defense and security of the province.

- Measures to ensure water demand for daily life, agriculture, industry, and services to achieve the goal of ensuring 100% demand in terms of quantity and quality:

+ Regarding domestic water supply: focus on upgrading and repairing concentrated rural clean water supply works. Particularly, the priority is given to the repair of clean water works in rural areas and areas contaminated with alum and lacking clean water. The pipeline system is upgraded, with modern filtering technology, ensuring that the water meets the standards to be supplied to the people. At the same time, there is a plan to protect and manage clean water supplying works. It is necessary to improve the efficiency of using clean water works in rural areas to ensure the supply of clean water to the people. In the long term, there are incentive mechanisms and policies to encourage enterprises to invest in rural clean water supply systems according to Decree No. 57/2018/ND-CP dated April 17, 2018 of the Government on mechanisms and policies to encourage enterprises to invest into agriculture and rural areas and Decision No. 131/2009/QĐ-TTg dated November 2, 2009 of the Prime Minister on a number of policies to encourage investment and management and exploitation of rural clean water supply works.

+ About ensuring water for agriculture (especially in the dry season): The first important measure to avoid burden on the irrigation water in the dry season is to appropriately rearrange the structure of crops, livestock, actively change the structure of crops (from rice to upland crops that use less water in areas with water shortages), and not to produce in areas where water supply is not guaranteed during the crop season. It is necessary to conduct research and apply new techniques and technologies for water-saving irrigation, particularly application of modern irrigation technologies such as sprinkler irrigation, drip irrigation to supply the right amount of water for growth and development. In addition, water resources should be prioritized for critical periods of productivity, and be limited in other periods. The construction of irrigation works should be complete to promptly put them into use and serve production. It is important to monitor regularly the meteorological and hydrological forecasts, weather trend and inventory of water sources to have a reasonable water use plan.

+ According to the calculation, the demand for water use in the industry now and in the future up to 2030 will be fully satisfied.

+ Regarding water demand for tourism and services, in fact, in Quang Ngai, the area with the highest water shortage is Ly Son district (both for domestic and tourism purposes). In order to meet the demand for fresh water in the future, it is necessary to have solutions to provide sustainable fresh water to the island, especially to conserve natural groundwater. Specifically, in addition to strictly protecting groundwater sources, it is very important and urgent to research and invest in one of the two following technological solutions: a purifier of seawater into fresh water and installation of a system to bring fresh water from the mainland to the island. However, each solution has advantages and disadvantages. Regarding utilization of the sea water purifier into fresh water, although the initial investment is not significant, the process of operation and maintenance is quite expensive. In terms of the investment into the water supply pipeline system from the mainland to island, although

the initial investment is high, it is less expensive to operate. Therefore, local authorities need to calculate specifically to both save money and ensure the water demand for people and tourists.

- The overall solution to raise incomes and improve people's lives in order to achieve the goal of reaching USD 4,400/person/year by 2030, with an orientation to reach USD 33,400/person/year by 2050 according to the Resolution of the 20th Party Congress of Quang Ngai Province:

+ Continue to promote administrative reform, particularly improving the ranking of indicators on administrative reform, efficiency in public governance and administration, and provincial competitiveness. In addition, it is necessary to promote tourism development, gradually becoming a spearhead economic sector as well as foster the socio-economic development and sustainable poverty reduction in mountainous districts.

+ Mobilize and effectively use resources to promote the industrial development, in which, the proportion of high-tech industries must be increased and the attraction and development of supporting industries and non-oil industries must be fostered. Besides, it is important to

comprehensively review mechanisms and policies, consider renewing investment promotion methods and reform the operating model of economic zones.

+ Harmonious and sustainable development among economic regions.

3.2.2. Calculation results of water security indicators after applying measures

After proposing the above-mentioned measures, the study conducted a recalculation of the water security indicators to evaluate the effectiveness of the measures. The evaluation results are as follows:

In case the measures mentioned in Section 3.2.2 are implemented synchronously and effectively, the water security indicators in all districts and the whole province will be increased with the difference ranging from 0.08 to 0.04. Specifically, the water security indicators in 03 districts of Ly Son, Tay Tra and Tra Bong improved with a difference of 0.08. Besides, Ba To, Duc Pho, Minh Long, Mo Duc, Nghia Hanh, Son Ha, Tu Nghia districts reached the difference of 0.07. Overall, water security of the the whole province was improved from the average level of 0.55 to the high level of 0.62 (the difference of 0.07) (Table 3).

Table 3. Comparison of water security in case of application of measures

No.	District	Water security indicators without measures	Water security indicators with measures	Difference
1	Ba To	0.59	0.66	0.07
2	Binh Son	0.53	0.57	0.04
3	Duc Pho	0.53	0.59	0.07
4	Ly Son	0.44	0.52	0.08
5	Minh Long	0.58	0.65	0.07
6	Mo Duc	0.52	0.59	0.07
7	Nghia Hanh	0.57	0.64	0.07
8	Son Ha	0.59	0.66	0.07
9	Son Tay	0.57	0.63	0.06
10	Son Tinh	0.55	0.61	0.06
11	Tay Tra	0.57	0.65	0.08
12	Quang Ngai city	0.57	0.61	0.04
13	Tra Bong	0.58	0.65	0.08
14	Tu Nghia	0.55	0.62	0.07
PROVINCE		0.55	0.62	0.07

It can be seen from the table that water security of all 10 districts changes from medium to high level, particularly: Ba To (from 0.59 to 0.66), Minh Long (from 0.58 to 0.65), Nghia Hanh (from 0.57 to 0.64), Son Ha (from

0.59 to 0.66), Son Tay (from 0.57 to 0.63), Son Tinh (from 0.55 to 0.61), Tay Ninh Tra (from 0.57 to 0.65), Quang Ngai city (from 0.57 to 0.61), Tra Bong (from 0.58 to 0.62) and Tu Nghia (from 0.55 to 0.62) (Figure 1).

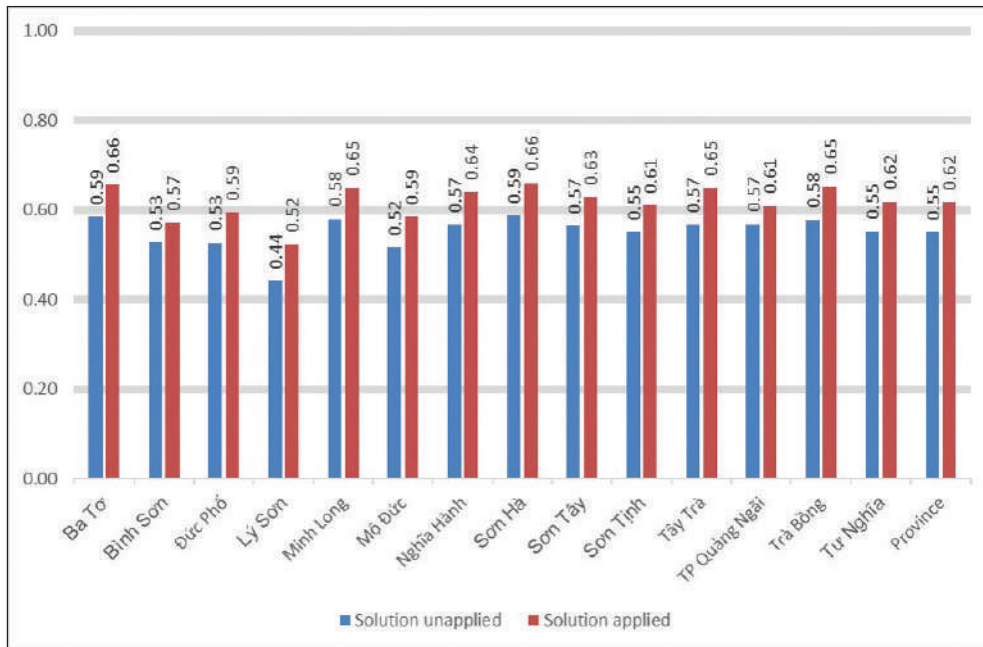


Figure 1. Comparison of water security indicators with and without solution

4. Conclusion

Based on the results of the water security assessment using a set of indicators, the following measures have been proposed to improve the state of water security in Quang Ngai:

(1) Measures to maintain and improve the forest area in order to achieve the goal of maintaining the current forest coverage;

(2) Measures for wastewater management and treatment to achieve the goal of 100% of wastewater is collected and treated before being discharged into water bodies;

(3) Measures to ensure the population of Quang Ngai is at an appropriate level in both quantity and structure to achieve the goal of maintaining the current fertility rate;

(4) Measures to ensure water demand for daily life, agriculture, industry and services to achieve the goal of ensuring 100% demand in terms of quantity and quality;

(5) The overall solution to raise incomes and improve people's lives in order to achieve the goal of reaching USD 4,400/person/year by 2030, with an orientation to reach USD 33,400/person/year by 2050 according to the Resolution of the 20th Party Congress of Quang Ngai Province.

Once all above-mentioned solutions are implemented synchronously and effectively, the water security indicator will be significantly improved, from medium to high level (0.55 to 0.62), reaching a difference of 0.07.

References

1. Ministry of Natural Resources and Environment (2016), *Climate change and sea level rise scenarios for Viet Nam*.
2. Chu, H.C.; Hwang, G.J. (2007), *A Delphi-based approach to developing expert systems with the*

cooperation of multiple experts.

3. Bui Duc Hieu, Ta Dinh Thi, Huynh Thi Lan Huong, Dang Quang Thinh, Nguyen Van Dai, Nguyen Thi Lieu, Nguyen Anh Tuan (2021), "Assessment of water security in Quang Ngai province in the context of climate change", *Journal of Hydrology and Meteorology*, 729, 79-90; doi:10.36335/VNJHM 2021(729).79-90.
4. Hai, N.D. (2015), *Development and application of a water security assessment framework for Ha Noi city.*
5. Mui, N.T. (2019), *Research on water security for sustainable development of Ma river basin.* Doctoral thesis at the University of Water Resources.
6. Lozet F., Edou K. (2013), *Water and Environmental Security for Conflict Prevention in Times of Climate Change.*
7. GWP. (2014), "Assessing water security with appropriate indicators", *Proceedings from the GWP workshop.*
8. UN-Water. (2014), *Water Security & the Global Water Agenda A UN–Water Analytical Brief.*
9. Xiaoli, J.; Chunhui, L.; Yanpeng, C.; Xuan, W.; Lian, S. (2015), *An improved method for integrated water security assessment in the Yellow River basin, China.*
10. WaterAid (2012), *Water security framework.*

IMPACT OF URBANIZATION ON FLOODING IN KHANH HOA PROVINCE

Luong Huu Dung, Doan Huy Phuong, Ngo Thi Thuy, Chu Nguyen Ngoc Son
Viet Nam Institute of Meteorology Hydrology and Climate Change

Received: 30 July 2021; Accepted: 20 August 2021

Abstract: Currently, natural disasters such as floods and inundation are increasing both in the quantity and degree of impact. The areas most heavily affected by flooding are low-lying areas such as coastal cities and countries. The characteristics of natural disasters such as floods and inundation are not only affected by changes in climate factors but also by urbanization and human activities. This paper uses the MIKE FLOOD (DHI) model to analyze the impact of urbanization on flood and inundation characteristics in the downstream areas of Cai river in Khanh Hoa province. The results show that the change of urban topography during the urbanization period has significant effects on the floodplain areas in terms of location and intensity, thereby changing the characteristics of flood and inundation distribution spatially.

Keywords: Urbanization, flooding, coastal areas, Khanh Hoa province, Viet Nam.

1. Introduction

Flooding is one of the most dangerous natural disasters with about 70 million people impacted by flood every year [13]. Under climate change context, flooding is more severe especially in urban cities [1, 16]. Flooding is not only a global concern, but also one of the main hazards in Viet Nam that frequently causes severe economic losses and casualties [7]. It was estimated that as of 2010 about 930,000 people in the country are exposed to flood risk, with total annual losses to flooding of approximately 2.6 billion USD [17].

Flood risk is not only a popular threat to riverine areas but also to many densely populated cities and coastal regions. Furthermore, urbanization is rising in Viet Nam that has one of the highest growth rates in the urban population in East Asia. Based on the historical records, in 2013, there were 770 officially designated urban areas in Viet Nam [14]. It was estimated that by the end of 2015, 20 new urban areas had been formed [12]. With the acceleration of urbanization since Doi Moi (social, economic, and political

renovation starting in 1986), flood risk has increased in urban areas [4]. This trend is aggravated by population growth, economic development and the associated expansion of buildings and infrastructure into flood-prone areas [4, 10, 11]. During the period 2012 - 2015, several major floods occurred in Viet Nameese cities, notably in Ha Noi, Quang Ninh, Da Nang, Can Tho, and Ho Chi Minh City [5]. The number of flood and inundation events has been rising in recent years and therefore flood risk is anticipated to increase due to population and economic development. The major impact of urbanization on the hydrological characteristics of a catchment is to decrease the amount of infiltration into the ground and to increase the speed of surface runoff. Because of the urbanization and road construction, overland flow and drainage were impeded, leading to deeper flooding and longer inundation.

ISET (2016) indicated that the urbanization an infrastructure construction within the floodplain areas of the Vu Gia - Thu Bon river system caused more flood risk in the upstream areas of the floodplain. The natural capacity of floodplains for absorbing and slowing floodwater flow is decreased due to the rising land

Corresponding author: Luong Huu Dung
E-mail: dungluonghuu@gmail.com

surface elevation and urban activities. As a consequence of this, the behavior of extreme flood events is different from what occurred in the past. The flood risks will be transferred from the new planned urban areas to other lower areas. In these lower areas, the risk levels are higher, the flood events may occur faster, the water depth is deeper and finally, flood inundation drains more slowly [5].

Urbanization increases regional impervious surface area, which generally reduces hydrologic response time and therefore increases flood risk [2]. In order to assess urbanization impact on flood risk, two common types of data sources used to analyze and estimate are historical records and flood modeling results. Early studies implemented urbanization impact evaluation on the magnitude and frequency of urban inundation through historical data from the gauging stations [3, 8]. The studies of Villarini, et al (2009) and Prosdoci, et al (2015) have employed advanced model systems to indicate that the urbanization has a statistically considerable impact on the magnitude and frequency of flood events.

Briefly, the information about river flow, flood and inundation and how they are affected by topography changes associated with urbanization development can help communities reduce their current and future vulnerability to floods. In this study, the impacts of urbanization on flooding are retrieved by assessing the

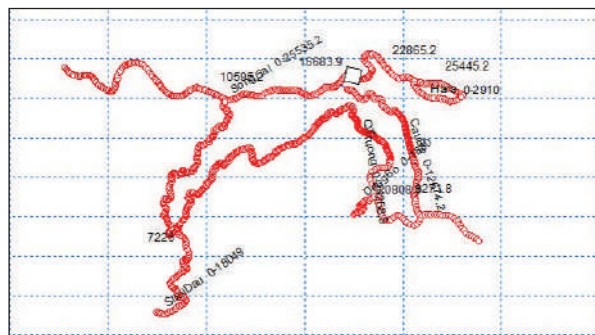


Figure 1. Schetch of river network in MIKE 11 model

- Boundary conditions:
 - Upper boundary: Observed flow discharge data at Dong Trang station
 - Midstream boundary: The flow discharge

change of topography characteristics in Khanh Hoa province located in Viet Nam over time and flooding exposure consequently.

2. Study area and methodology

2.1. Study area

Cai River is the largest river in Khanh Hoa province, located in the range of 120°03' - 120°37' North latitude, 108°41' - 109°12' East longitude. The Cai River basin area is 2,000 km² and covers the whole of Nha Trang City, Dien Khanh and Khanh Vinh districts and part of the area of Cam Lam district of Khanh Hoa province and MaDrak of Dak Lak province.

Khanh Hoa Province is located in the South Central Coastal Region of Viet Nam. The total population of the province in 2019 was around 1,336,143. The province has core developed areas such as Nha Trang city and Cam Ranh Bay port. Khanh Hoa Province has set a goal to become a centrally-governed type 1 city by 2025. The province has approved many planning projects at a total cost of VND61 billion. These projects mainly invest in urban residential and housing areas and traffic roads.

2.2. Input data

Using the hydrological stations and observed flow data, the simulated river network for hydraulic estimation of the Cai River was established with the total main river length of 31 km as shown in Figure 1.

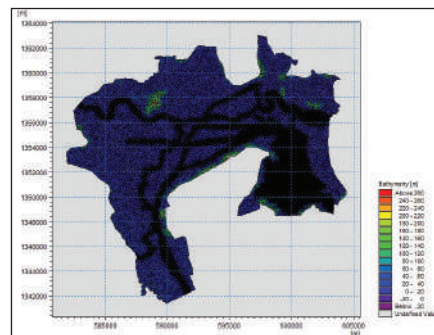


Figure 2. Grid calculation on Mike 21 FM model

process of tributaries entering the Cai River, simulated from the Mike NAM model based on the observed meteorological data (rainfall and evaporation) in Nha Trang, Dong Trang and

Khanh Vinh station.

- Lower boundary: The observed water level process at the estuary of Cai river.

- Topographic data: Topographic data which covers the whole Cai basin is collected with the scale 1:10,000 then analyzed and used for the flexible mesh generation (calculation grid setting up) by the ArcGIS software.

- Setting up the calculation grid for the study area: Depending on the different areas in simulation, the resolution of calculation grid would be different. For riverside areas, the possibility of flooding is higher then need more detailed simulation, so the calculation grid is divided into thicker, while for the areas far from the river and the possibility of flooding is lower, grid is set up into sparser net. The calculation grid for the study area is presented in Figure 2.

2.3. Numerical techniques

In order to present the change of flooding status in Khanh Hoa province in the different topographic situations, the hydraulic software MIKE package i.e. MIKE FLOOD coupling MIKE-11HD and MIKE 21FM is used. The change of topography under urbanization is illustrated in the digital elevation model (DEM) that integrated in MIKE 21FM in the form of the flexible mesh system to visually present the change of flooding characteristic in 2D space.

In order to combine the advantages of both 1-D and 2-D models and overcome their disadvantages, MIKE FLOOD allows coupling the MIKE 11 and MIKE 21 models in the simulation process, reducing the computation time but still being able to simulate both the flow in the channel and on the field sites or flood plains as well as simulating the hydro-hydraulic process within the whole system. This is the final stage in setting up the hydraulic model system. In this study, based on the MIKE-11HD and MIKE 21FM models set up above, the two are connected in the MIKE FLOOD model through the linkage type called "Lateral". The simulated results of the MIKE FLOOD model then are converted into GIS file format to estimate and calculate the flooding area corresponding to the flooding depth range.

3. Results and discussion

In this study, to evaluate the effects of urbanization on flood characteristics, the research team conducted inundation simulation process using MIKE FLOOD model with the hydrological data input corresponding to the flood event occurred in 2009 with the frequency of 1% and 2 topographic data in 2010 and 2018 respectively.

The topographic data in 2010 is selected to represent the topographic feature of the study area before the urbanization period and the topographic data (with some planned areas) in 2018 is selected to represent the topography characteristic after the urbanization period. The main difference between the two topographic inputs is that, for the topographic data in 2018, the terrain elevation of the areas including Dien Toan, Dien An, and Dien Thanh communes of Dien Khanh District, Vinh Chung, Vinh Hiep, Vinh Thanh communes and other the southern wards of Nha Trang city located in the lower part of the Cai river are planned to be raised by 2 - 3 m for the building constructions compared to the terrain elevation in 2010 of the same areas.

The results of inundation simulation in the downstream area of Cai river using the MIKE FLOOD model corresponding to the two scenarios of topography in 2010 and 2018 show that the flooded area occurs in Dien Khanh districts and the Nha Trang city, the specific results are as follows:

The topography scenario in 2010:

In Dien Khanh district, there are 18 affected communes with a total flooded area of 75.4 km², of which 4 communes are most affected with over 80% of the flooded area, including: Dien Thanh, Dien Lac, Dien Phu and Dien Khanh town. The flooding depth in the communes of Dien Khanh district is mainly at a depth of less than 1.5 m, only Dien An, Dien Thanh and Dien Toan communes have the largest inundation depth from 2.5 - 3 m. The agricultural land area affected by flooding is mainly in Dien Khanh district with a total area of 24.80 km², the flood depth ranges from 1 - 1.5 m. The flooded residential area in Dien Khanh district is 1.54 km², most of the flooded depth is less than 1.5 m.

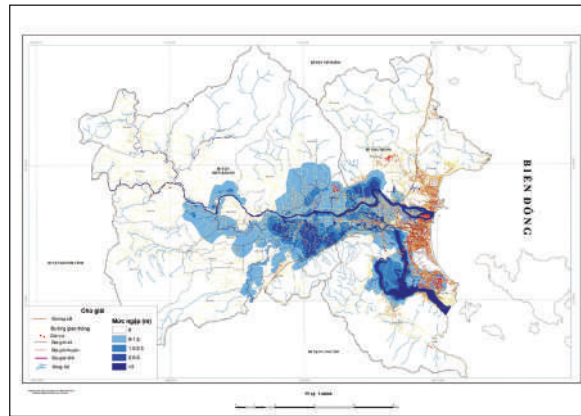


Figure 3. Inundation map corresponding to the topography scenario in 2010

In Nha Trang city, there are 17 affected communes/wards with a total flooded area of 30.57 km², in which the most affected places include Vinh Ngoc, Vinh Thanh, Vinh Hiep, Vinh Trung communes and Ngoc Hiep, Phuoc Hai, Phuoc Long wards. Flooding depth in Nha Trang city is mostly below 1.5 m. The communes/wards with the greatest flooding depth include: Ngoc Hiep Phuoc Hai and Xuong Huan wards with over 10% of the ward areas being flooded up to 3 m. The flooded residential area in Nha Trang city is 3.14 km², most of the flooded depth is less than 1.5 m.

The topography scenario in 2018:

In Dien Khanh district, there are 15 affected

communes with a total flooded area of 47.64 km² in which there are 4 communes most affected including: Dien Khanh, Dien Binh, Dien Lac, Dien Phu and Dien Khanh town. The degree of flooding in the communes of Dien Khanh district is mainly common at the depth of less than 1.5 m, the communes of Dien Lac, Dien Thanh, Dien Phu and Dien Khanh town are the places with the largest inundation depth (over 2 m). The agricultural land area affected by flooding is mainly in Dien Khanh district with a total area of 18.40 km², the common flood depth is from 1 - 1.5 m. The flooded residential area in Dien Khanh district is 1.14 km², most of the flooded depth is less than 1.5 m.

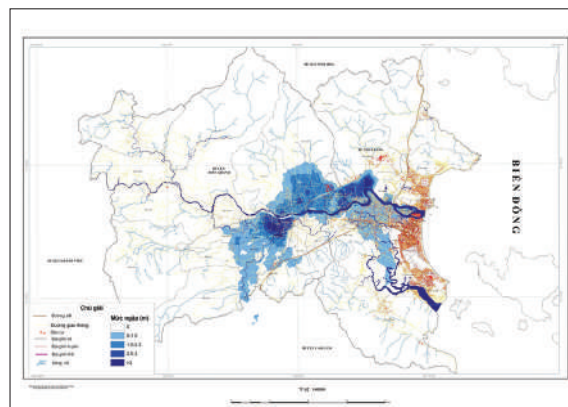


Figure 4. Inundation map corresponding to the topography scenario in 2018

In Nha Trang City, there are 12 affected communes/wards with a total flooded area of 17.82 km², in which, the most affected places including Vinh Hiep, Vinh Thanh and Ngoc Hiep wards with a proportion of flooded area above 50% of the area of communes. The flooding

depth in the Nha Trang is mostly below 1.5 m. The communes/wards with the greatest inundation depth include: Xuong Huan and Ngoc Hiep wards with inundation depth from 2.5 - 3 m. The flooded residential area in Nha Trang city is 1.39 km², most of the flooded depth is less

than 1.5 m.

Comparison of inundation characteristics

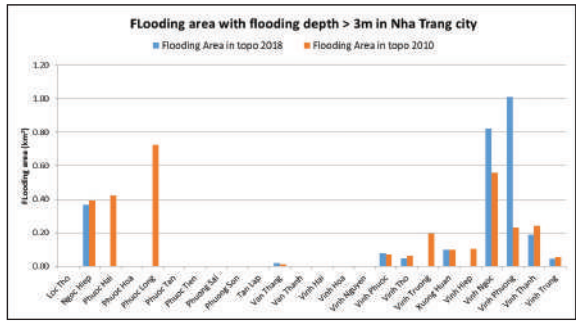
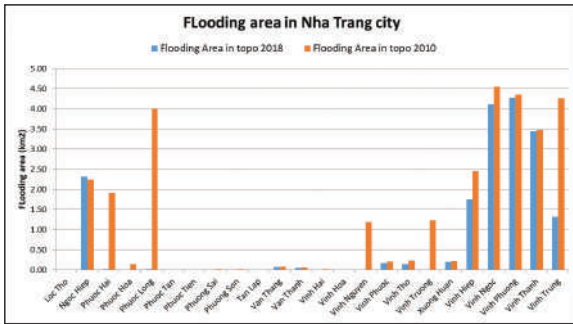


Figure 5. Comparison of flooded areas in Nha Trang city between 2 topographic scenarios in 2010 and 2018

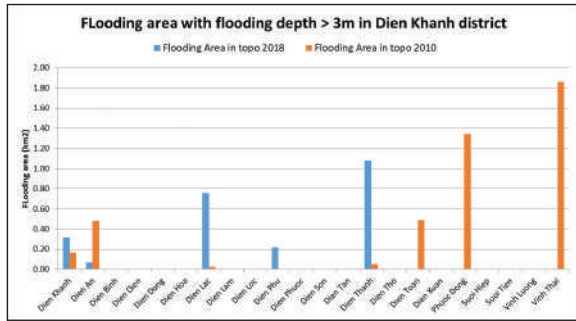
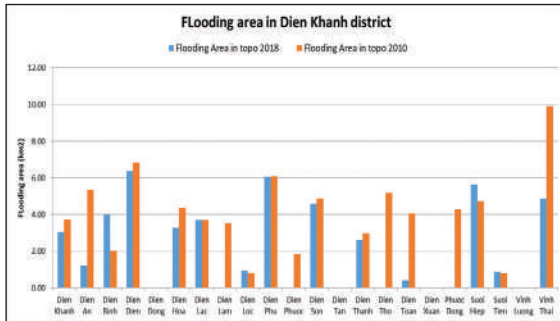


Figure 6. Comparison of flooded areas in Dien Khanh district between 2 topographic scenarios in 2010 and 2018

Based on the data observed from the inundation area graphs and maps, it can be seen that the inundation area in the whole study area caused by the flood event in 2009 on the 2010 terrain is larger than on the 2018 terrain. However, it can be observed that the inundation area corresponding to the flooding depth over 3 m in the 2018 topographic scenario is greater than that in the 2010 topographic scenario occurring at some wards and communes of Nha Trang city and Dien Khanh district. Meanwhile, other wards and communes which have quite large flooded area in the 2010 topographic scenario are not inundated in the 2018 topographic scenario. These no flooding areas coincide with the areas planned to be raised in terms of topography elevation. Therefore, it can be concluded that the difference in flooded area of some areas between the two scenarios may be caused by the change of the base elevation in the floodplains downstream. In summary, it can be concluded that the urbanization development through leveling or raising the

caused by flood event in 2009 between two topographic scenarios in 2010 and 2018:

ground elevation can indirectly change the location of low floodplain areas. This leads to the inundation area and inundation depth being changed accordingly.

4. Conclusion

The paper presented the main results of the study on the impact of urbanization on flood characteristics. The study implemented an inundation simulation caused by the flood event in 2009 for the downstream areas of Cai river in Khanh Hoa province, corresponding to two topographic scenarios in 2010 and 2018. In the study, the MIKE FLOOD model coupling 1-dimensional models MIKE 11 and 2-dimensional MIKE 21 is used to simulate flooding and inundation for the study area. The results show that the total flooded area in the 2010 topographic scenario is generally larger than that in the 2018 topographic scenario. However, for the case with the flooding depth over 3 m, the results showed that the flooded area of some areas corresponding to the

2018 topographic scenario is larger when compared to the 2010 topographic scenario. In addition, for the 2018 topographic scenario, the areas which have no inundation are the areas planned to rise the topography

elevation. Therefore, it can be concluded that urbanization and urban planning have indirectly changed the location of floodplains at the river downstream, thereby changing the spatial distribution of flooding and inundation.

References

1. Dottori, F. et al., (2018), "Increased human and economic losses from river flooding with anthropogenic warming", *Nature Climate Change*, (8), 781–786.
2. Feng, B., Zhang, Y. & Bourke, R., (2021), "Urbanization impacts on flood risks based on urban growth data and coupled flood models", *Natural Hazards*, (106), 613-627.
3. Hollis, G. E., (1975), *The effect of urbanization on floods of different recurrence interval*, Water Resources Research.
4. Huong, H. & Pathirana, A., (2013), "Urbanization and climate change impacts on future urban flooding in Can Tho city, Viet Nam", *Hydrol. Earth Syst. Sci.*, (17), 379-394.
5. ISET, (2016), "Urban Development and Flood Risk in Viet Nam: experience in three cities".
6. Konrad, C. P., (2003), "Effects of urban development on floods", USGS Fact Sheet FS-076-03.
7. Luu, C., von Meding, J. & Mojtahedi, M., (2019), "Analyzing Viet Nam's national disaster loss database for flood risk assessment using multiple linear regression-TOPSIS", *International Journal of Disaster Risk Reduction*, (40).
8. Moscrip, A. L. & Montgomery, D. R., (2007), "Urbanization, Flood Frequency, And Salmon Abundance In Puget Lowland Streams", *Journal of the American Water Resources Association*, 33(6), 1289-1297.
9. Prosdocimi, I., Kjeldsen, T. R. & Miller, J. D., (2015), "Detection and attribution of urbanization effect on flood extremes using nonstationary flood-frequency models", *Water Resources Research*, 51(6), 4244-4262.
10. Storch, H. & K. Downes, N., (2011), "The Dynamics of Urban Change in Times of Climate Change - the Case of Ho Chi Minh City", REAL CORP 2011.
11. Sudmeier-Rieux, K. et al., (2015), "Protected areas as tools for disaster risk reduction : a handbook for practitioners".
12. Tran, T., (2016), "Climate Change Challenges and Solutions to Improve Climate Change Adaptation Capacity of Cities in Viet Nam", *Presentation at the Interim Workshop on National Urban Development Strategy, Ha Noi*.
13. (UNDRR) United Nations Office for Disaster Risk Reduction, (2011), *Global assessment report on disaster risk reduction*, Geneva: Switzerland.
14. Viet Nam Ministry of Construction, (2014), *Annual report on urban development in Viet Nam*, Ha Noi, Viet Nam.
15. Villarini, G. et al., (2009), "Flood frequency analysis for nonstationary annual peak records in an urban drainage basin", *Advances in Water Resources*, 32(8).
16. Willner, S. N., Otto, C. & Levermann, A., (2018), "Global economic response to river floods", *Nature Climate Change*, (8), 594–598.
17. World Bank, (2018), "Climate risk country profile-Viet Nam", The World Bank Group and the Asian Development Bank, Washington DC.

STUDY ON FORECASTING TIDAL WATER LEVELS IN THE SAI GON DONG NAI RIVER FOR ASSESSMENT OF FLOOD IMPACTS IN HO CHI MINH CITY

Nguyen Van Hong, Nguyen Phuong Dong, Pham Thanh Long,
Pham Anh Binh, Ho Cong Toan
Sub-Institute of HydroMeteorology and Climate Change

Received: 06 September 2021; Accepted: 20 September 2021

Abstract: In recent years, due to the impact of extreme weather, the evolution of rain and tides in Ho Chi Minh City (HCMC) has many changes. Particularly, rainfall and rainfall intensity have been increasing more and more, duration of rainfall has been longer and longer, the number of some heavy rains with a volume of 50 - 100 mm has been boosted, the high tide level on the river has also multiplied in recent year. As the result, the flooding situation of the city is heavily and seriously impacted, causing inevitable damage and challenges for the socio-economic activities of city people. Therefore, research on the impact of coastal water levels on flooding in the city is very necessary. In this paper, UTide software is applied to calculate and forecast tidal water levels along the coastal areas and inland stations of the Sai Gon River, thereby assessing the impacts of flooding due to high tides on HCMC with water level forecast results for 3 stations Nha B, Phu An and Vung Tau respectively 0.82, 0.83 and 0.97.

Keywords: UTide, flood, high tide, forecast, Ho Chi Minh City.

1. Preface

Sea level fluctuation is a combination of tidal components due to the gravitational pull of the moon, sun and non-tidal factors such as wind, storm, waves, etc. Tidal phenomenon has been studied very early; it is predicted quite accurately in the deep sea. However, there are some certain difficulties in tidal prediction in the coastal area (the area less affected by tides) [10].

HCMC is one of the megacities in the world thanks to its urban scale, role and size in economic development. However, in addition to the opportunity creation for development, urbanization also increases the risk due to climate change for coastal urban dwellers. HCMC is easy flooded due to urbanization, rainfall, runoff from upstream and rising sea levels. Besides, the city is also ranked in the top 10 cities in the world most affected by climate change [6].

The spatial area of HCMC has been expanded from 86.2 km² in 1990 to 351.1 km² in 2010, and nearly 60% of the total area of HCMC is below the elevation of 1.50 m above sea level. As a result, the city usually faces flooding problems during the rainy season from June to November and the high tide cycle from September to December every year due to semi-diurnal influence and discharge from the upstream of the Saigon - Dong Nai River. There are several causes for flooding in Ho Chi Minh City, including the objective causes, such as climate change (CC), sea level rise (NBD), increased rainfall and tidal peaks, and increasing urbanization resulting in the sharply increase in population beyond the capacity of the drainage system. Previously, there were only studies on sea level rise to inundation patterns and there were no detailed studies on coastal tidal water affecting inland stations and flooding urban areas. Therefore, the study of the impact of coastal tide levels has a very important role in assessing and finding out the causes for flooding in HCMC [3].

Corresponding author: Nguyen Van Hong
E-mail: nguyenvanhong79@gmail.com

In this paper, UTide software is applied by the research team to analyze fluctuations and forecast water levels at some stations in the coastal area and some stations of HCMC such as Vung Tau marine station, Phu An hydrological station (on the Saigon River) and Nha Be hydrological station (on the Saigon River) and Nha Be hydrological station (on Nha Be River) by the Least Squares Method [11]. The hourly water level data at the stations in 2018 will be used to analyze the set of harmonic constants and test the water level in April 2020, thereby forecasting the monthly water level in 2021. Research above results is the part of the purpose for the assessment of impacts on flooding situation of the city [10].

2. Study method

2.1. Study area

HCMC is located in the southwest of the Southeast region, adjacent to Binh Duong Province in the North, adjacent to Tay Ninh province in

the Northwest, adjacent to Dong Nai province in the East and Northeast, adjacent to Ba Ria - Vung Tau province and the East Sea in the Southeast and adjacent to Long An and Tien Giang Province in the West and Southwest.

HCMC is located at the downstream of major rivers, including Dong Nai River, Saigon River, Be River, on the fringe of the Mekong Delta. HCMC is located in an area with a sub-equatorial monsoon tropical climate. The amount of radiation is abundant, and the average sunshine is 6.10 hours/day. The average annual temperature is about 28.4°C. Monsoon brings a large amount of moisture from the West and Southwest. The relatively low natural topography of HCMC along with different purposes of land use results in a clear distribution of space and rainfall, even depending on the difference of the inner - city districts. Total rainfall in HCMC ranges from 1,200 to 2,100 mm/year [4 - 8].

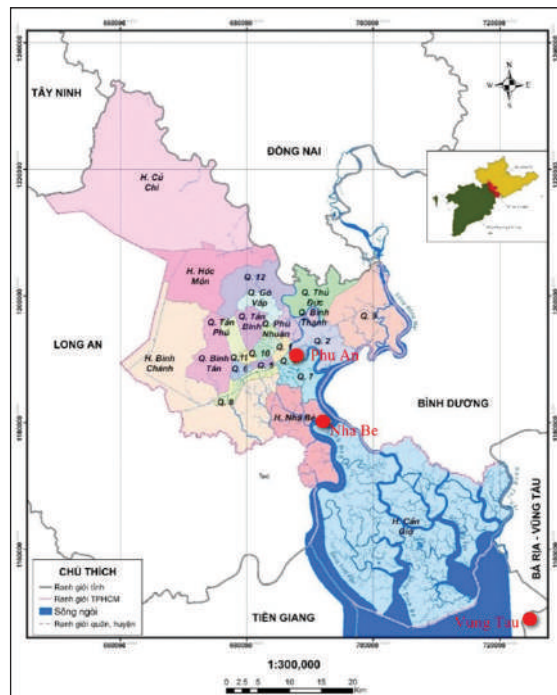


Figure 1. Map of the study area

2.2. Research Methods

2.2.1. Basic system of equations

The first step is to analyze the real tides using the Least Squares Method for the component

waves in order to find their suitable harmonic constants (phase and amplitude).

The formula for tidal height (y) by harmonic tidal analysis method is rewritten as follows [2]:

$$y_i = C_0 + \sum_{j=1}^M A_j \cos[2\pi(\sigma_j t_i - \phi_j)]$$

$$= C_0 + \sum_{j=1}^M [C_j \cos(2\pi\sigma_j t_i) + S_j \sin(2\pi\sigma_j t_i)] \quad (2.1)$$

In there:

t_i : Time of monitoring series; M : Number of waves to be analyzed; σ_j : Angular frequency of the wave; C_0 : Average water level; $A_j = (C_j^2 + S_j^2)^{1/2}$: Tidal amplitude; $\phi_j = (1/2\pi) \cdot (\arctan S_j / C_j)$:

Wave phase.

In N number of hourly water levels, the sum of squared error of the observed water level and the analyzed water level is calculated as formula (2.2) below:

$$\varepsilon = \sum_{i=1}^N [y_i - C_0 - \sum_{j=1}^M (C_j \cos 2\pi\sigma_j t_i + S_j \sin 2\pi\sigma_j t_i)]^2 \quad (2.2)$$

The formula (2.3) - (2.5) is the derivative of the above equation with respect to $C_0, C_j, S_j (j=1, M)$:

$$0 = \frac{\partial \varepsilon}{\partial C_0} = 2 \sum_{i=1}^N \left(y_i - C_0 - \sum_{j=1}^M C_j \cos 2\pi\sigma_j t_i + \sum_{j=1}^M S_j \sin 2\pi\sigma_j t_i \right) (-1) \quad (2.3)$$

$$0 = \frac{\partial \varepsilon}{\partial C_j} = 2 \sum_{i=1}^N \left(y_i - C_0 - \sum_{j=1}^M C_j \cos 2\pi\sigma_j t_i + \sum_{j=1}^M S_j \sin 2\pi\sigma_j t_i \right) (-\cos 2\pi\sigma_j t_i) \quad (2.4)$$

$$0 = \frac{\partial \varepsilon}{\partial S_j} = 2 \sum_{i=1}^N \left(y_i - C_0 - \sum_{j=1}^M C_j \cos 2\pi\sigma_j t_i + \sum_{j=1}^M S_j \sin 2\pi\sigma_j t_i \right) (-\sin 2\pi\sigma_j t_i) \quad (2.5)$$

From formulas (2.1) to (2.5) it is possible to set up a matrix to solve the system of equations as follows:

$$\begin{pmatrix} N & C_1 & C_2 & \dots & C_M & S_1 & S_2 & \dots & S_M \\ C_1 & CC_{11} & CC_{12} & \dots & CC_{1M} & CS_{11} & CS_{12} & \dots & CS_{1M} \\ C_2 & CC_{21} & CC_{22} & \dots & CC_{2M} & CS_{21} & CS_{22} & \dots & CS_{2M} \\ \vdots & \vdots & \vdots & \dots & \vdots & \vdots & \vdots & \dots & \vdots \\ C_M & CC_{M1} & CC_{M2} & \dots & CC_{MM} & CS_{M1} & CS_{M2} & \dots & CS_{MM} \\ S_1 & SC_{11} & SC_{12} & \dots & SC_{1M} & SS_{11} & SS_{12} & \dots & SS_{1M} \\ \vdots & \vdots & \vdots & \dots & \vdots & \vdots & \vdots & \dots & \vdots \\ S_M & SC_{M1} & SC_{M2} & \dots & SC_{MM} & SS_{M1} & SS_{M2} & \dots & SS_{MM} \end{pmatrix} \begin{pmatrix} C_0 \\ C_1 \\ C_2 \\ \vdots \\ C_M \\ S_1 \\ \vdots \\ S_M \end{pmatrix} = \begin{pmatrix} \sum_{i=1}^N y_i \\ \sum_{i=1}^N y_i \cos 2\pi\sigma_1 t_i \\ \sum_{i=1}^N y_i \cos 2\pi\sigma_2 t_i \\ \vdots \\ \sum_{i=1}^N y_i \cos 2\pi\sigma_M t_i \\ \sum_{i=1}^N y_i \sin 2\pi\sigma_1 t_i \\ \vdots \\ \sum_{i=1}^N y_i \sin 2\pi\sigma_M t_i \end{pmatrix} \quad (2.6)$$

Thanks to solving the above matrix equation, the harmonic constants (including tidal amplitude and oscillation phase) to be analyzed are determined. Once we have obtained the amplitude and oscillation phase of each component tidal wave, we can insert them into the formula (2.1) to calculate and predict the water level fluctuation in any time.

2.2.2. The Unified Tidal Analysis and Prediction (UTide) software

The development of the Unified Tidal Analysis and Prediction (UTide) software is based on the harmonic tidal analysis theory given by [1] and with the support of Fortran Software, in addition to the methods analysis from previous platforms such as T_tide, r_T_tide and "versatile" [2].

The software is built with the following criteria:

The software can be taken into account with two-way cases for flow velocity data or one-way for sea level forecasting. The software is specially designed to handle recording times that are unevenly distributed and/or blank adaptable of analyzing data at regular or irregular intervals of time, providing accurate cycle correction results for series of time up to 18.6 years [2]. It is also able to provide easy-to-use and comprehensive diagnostics to aid the component selection process.

Regarding the water level processing (amplitude and phase), for missing data series, or difference in amplitude and phase error, Utide software has processing tools such as Fourier transform (for uniformly distributed time), Lomb-Scargle (for irregular time) and residuals between unprocessed input data, appropriate harmonic constants, etc.

The Least Squares Method is incorporated strongly with the iterative adjustment of L1/L2 [1] to minimize the effect of extrinsic values and reduce confidence intervals.

With the software Matlab, it is possible to analyze groups of chronological series by calling a function *.m. The flexible and interchangeable interface of the analysis configurations can be easily used by the arguments to the *.m function.

Regarding calculation requirements:

Utide software may have higher computational requirements than previous software like Ttide... (More requirements about memory and longer processing time) [2], because:

Perform phase correction and amplitude calculation using validation time. Build complex value formulas of the matrix system to solve.

In the case of irregular times, the Lomb-

Scargle periodogram calculations are slower than their counterparts for uniformly distributed times. Calculating the new confidence interval takes a little more time than previous versions. The selection of characteristic components requires additional calculations. In the Software, the confidence interval estimation is taken into account to consider the instability of the sin/cos model parameters.

Using software:

The functions of Signal Processing Toolbox (pwelch(), cpsd(), hanning()) and Statistic Toolbox (robustfit(), mvrnd()) functions in Matlab (Daniel, 2011; Website MathWorks.com) are utilized in Utide. Therefore, if these toolsets are not available, it will cause errors in the default configuration of UTide.

UTide software includes 3 functions:

- ut_solv.m (for harmonic analysis for tidal flows and water levels);
- ut_reconstr.m (use analysis results to forecast tidal flows and water levels);
- ut_constants.mat contains calculated constants including 146 component tidal waves.
- Utide software runs on Matlab platform.

2.2.3. Software testing

The test results between the measured and calculated water level data of Vung Tau, Phu An and Nha Be stations in April 2020 are presented in Figure 2 - 4. According to the comparison results, the predicted tides are lower in comparison with actual measurements, proving that non-tidal factors such as wind, waves, etc. have an influence on the total water level fluctuation. The largest error in April 2020 was 0.20 m, the correlation between the calculated and measured results was quite good, with a correlation coefficient R^2 greater than 0.80 (Table 1)

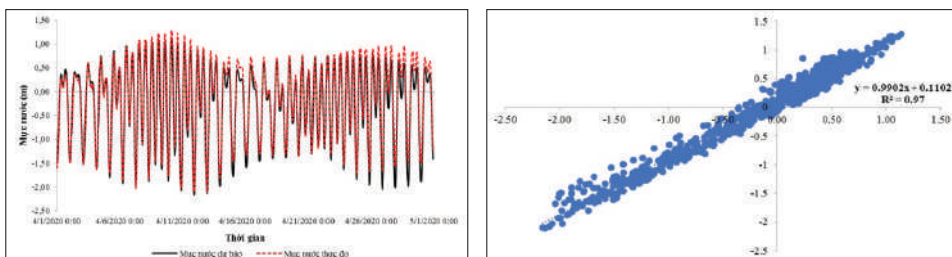


Figure 2. Test the water level (a) and the correlation graph (b) between the forecast water level and the calculated water level in April 2020 at Vung Tau station

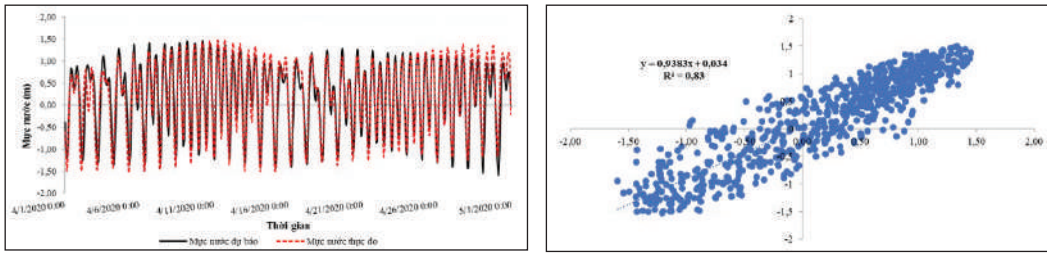


Figure 3. Test the water level (a) and the correlation graph (b) between the forecast water level and the calculated water level in April 2020 at Phu An station

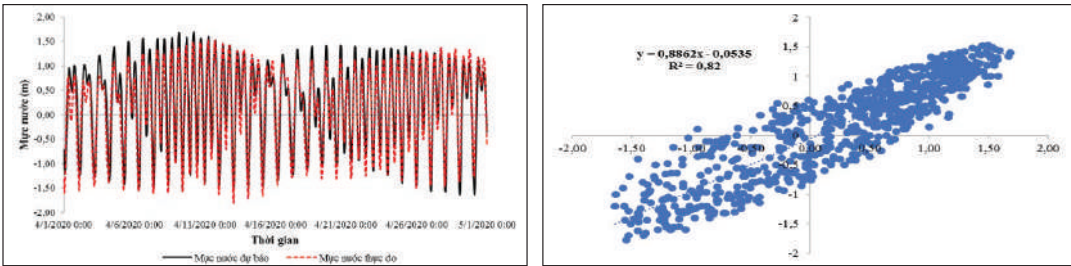


Figure 4. Test the water level (a) and the correlation graph (b) between the forecast water level and the calculated water level in April 2020 at Nha Be station

Table 1. Result of correlation coefficient between forecasted water level and actual water level measured at four stations, April 2020

Station	Correlation value
Vung Tau	0.97
Phu An	0.83
Nha Be	0.82

The result of comparing the data extracted from the tide table of Phu An station provided by the Southern Regional HydroMeteorological Center with the data calculated by Utide software

for 10 days from November 1 to November 10 are presented in Table 2, showing the reliability and accuracy of Utide software in case of comparing errors in the range of 0.05 to 0.1.

Table 2. Comparison of the measured data at Phu An station of Southern Region HydroMeteorology Center and calculation data of Utide

Time	Time to appear	Actual water level measured by SRHC	Water level calculation software by UTide
1/11/2020	4:00	1.49	1.39
2/11/2020	18:00	1.48	1.38
3/11/2020	5:00	1.43	1.36
4/11/2020	5:00	1.42	1.34
5/11/2020	5:00	1.43	1.35
6/11/2020	1:00	0.32	0.3
7/11/2020	6:00	1.06	1.18
8/11/2020	15:00	-1.3	-1.16
9/11/2020	8:00	0.73	0.76
10/11/2020	10:00	0.41	0.43

3. Research results and discussion

3.1. Water level analysis and forecast results

The data in this study is a series of hourly water level monitoring data from 2010 to 2018 at Nha Be station (located in Nha Be district of HCMC), Phu An station (located in District 1 of HCMC) and Vung Tau station (located in Ward 2, Vung Tau City) and there are 77,760 real hourly-measured data at each station. Based on the analysis results, harmonic constants are used as input for forecasting. To test the water level forecasting ability of UTide software, we calculate the water levels at the three stations as above using the set of the harmonic constants in April 2020 to verify with real measured data as well as forecast the water level in January 2021.

The analysis results of the harmonic constants will have 68 wave components; Due to the structure of the article, only 20 wave components have the largest oscillation amplitude and are

typical for irregular semidiurnal tides of Vung Tau station are presented. The harmonic constants at Vung Tau station are presented in Table 3. The calculated amplitudes of component waves M2, K1, O1 and S2 are 0.77 m, 0.59 m, 0.45 m and 0.30 m, respectively.

The contribution by variation of each component wave is shown in Figure 5. Accordingly, the component tidal waves are mainly concentrated at the frequency of 0.04 and 0.08 (cycle/hour). Correspondingly, diurnal and semi-diurnal tidal components have the largest contribution to the water level fluctuations. Most of the tidal waves are concentrated at an insignificant amplitude of less than 4 cm. 8 component waves with the largest amplitude above these 68 component waves calculated in Vung Tau is shown in Figure 5. Where the component wave with the highest amplitude and the largest percentage of energy is wave M2, the second component wave with amplitude and energy percentage is wave K1.

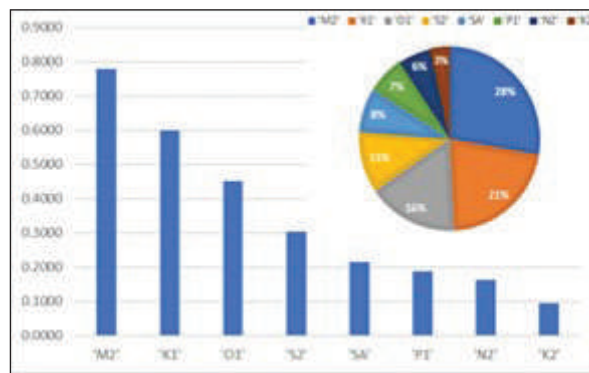


Figure 5. Component waves in Vung Tau with the largest amplitude and percentage of component waves

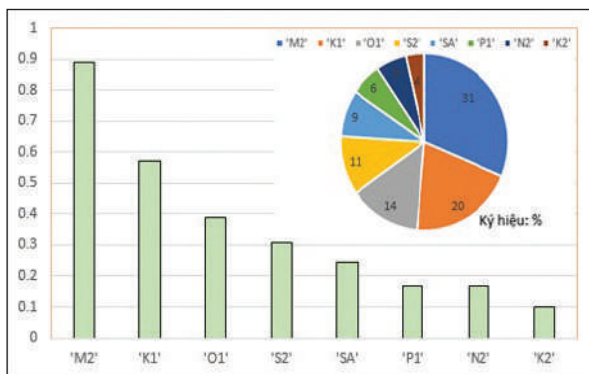


Figure 6. Component waves at Nha Be with the largest amplitude and percentage of component waves

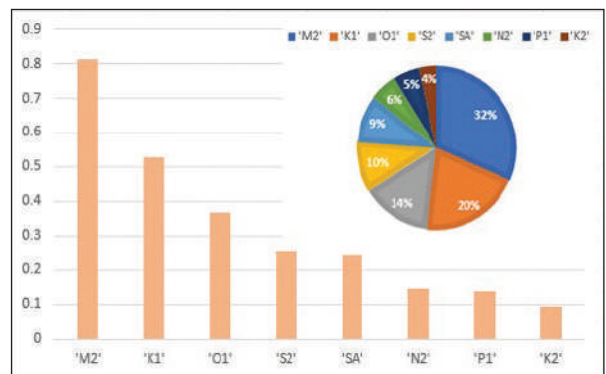


Figure 7. Component waves at Phu An with the largest amplitude and percentage of component waves

Table 3. Air conditioning constant of Vung Tau station from 2010 - 2018

Wave	Frequency	Amplitude	Amplitude error	Phase	Phase error	Signal Noise (SNR)
'M2'	0.08	0.77	0.0013	38.84	0.09	1441152.21
'K1'	0.04	0.59	0.0008	312.92	0.07	1946113.21
'O1'	0.03	0.45	0.0008	263.41	0.09	1486431.39
'S2'	0.08	0.30	0.0013	80.63	0.20	312634.18
'SA'	0.0001	0.22	0.0038	354.09	1.20	8575.71
'P1'	0.04	0.18	0.0007	308.76	0.23	204161.37
'N2'	0.07	0.16	0.0012	15.94	0.46	99561.22
'K2'	0.08	0.09	0.0011	94.26	0.69	28834.75
'Q1'	0.03	0.08	0.0008	243.03	0.42	44167.48
'SSA'	0.0002	0.05	0.0045	97.78	4.08	616.67
'NU2'	0.08	0.03	0.0012	21.44	2.16	3499.46
'MK3'	0.12	0.02	0.0007	188.56	1.42	6240.88
'NO1'	0.04	0.02	0.0008	290.76	1.67	5000.79
'2N2'	0.07	0.02	0.0012	351.55	2.74	1350.99
'H1'	0.08	0.02	0.0013	27.24	3.23	2060.63
'MU2'	0.07	0.02	0.0012	319.14	3.19	1339.12
'J1'	0.04	0.02	0.0007	351.78	1.95	2752.38
'L2'	0.08	0.02	0.0014	60.36	2.81	792.83
'H2'	0.08	0.01	0.0011	244.49	3.64	967.42
'MO3'	0.11	0.01	0.0007	130.47	2.42	3014.33

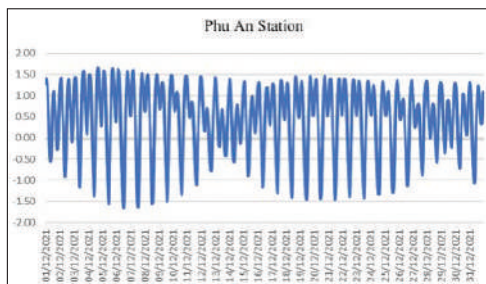


Figure 8. Water level forecast in December 2021 in Phu An

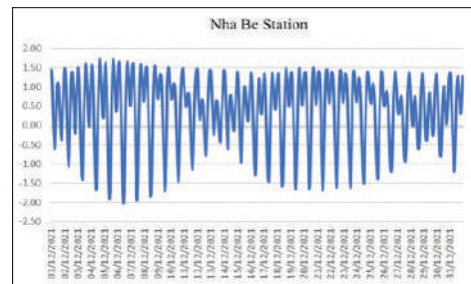


Figure 9. Water level forecast in December 2021 in Nha Be

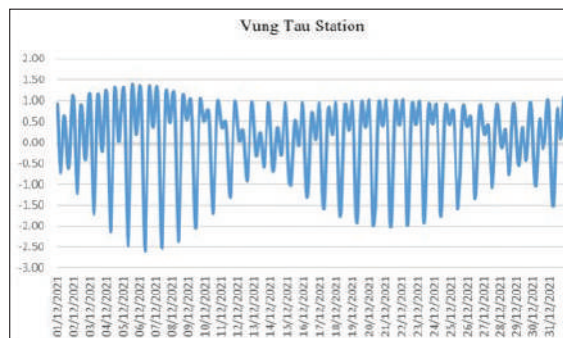


Figure 10. Water level forecast in December 2021 in Vung Tau

3.2. Assessment of the impact of tidal level on flooding in HCMC

According to the tidal level forecast results, the impact of tidal level in HCMC, especially the inner - city area, is very serious at the end of 2021. The forecasted maximum water level in 2021 at Vung Tau station is 1.41 m, while that at Phu An and Nha Be stations is 1.75 and 1.81 m, respectively, revealing that the coastal water level has a great influence on the water level in rivers and canals. The water level on the Saigon River at Phu An station is 0.34 m higher than that of Vung Tau station, and the water level on the Soai Rap river at Nha Be station is 0.40 m higher than that of Vung Tau station. The maximum water level exceeds the alarm level III of 1.60 m, which will cause flooding in HCMC. It is very necessary to have more research on the impact of tidal levels in HCMC in the future.

4. Conclusion

The results of analysis and calculation of water levels at Vung Tau, Phu An and Nha Be stations using UTide software archived good results, with a high correlation coefficient from 0.81 to 0.97. The comparison results between

forecast and actual water levels in April 2020 have negligible deviations in both phase and amplitude. The results of water level analysis show that tidal waves M2, K1, O1 and S2 have the largest amplitude among tidal waves.

Based on the results of analysis and prediction of water level fluctuations at Vung Tau station, Phu An station and Nha Be station, it can be concluded that the software has the ability to analyze well the set of harmonic constants, have a reliable forecast of water level fluctuations. Based on that, UTide software can be applied for coastal tidal forecasting and river water level forecasting for the southern region.

From the calculated results, it is shown that the hydrographic station, namely Vung Tau station, archives high result in the correlation coefficient of 0.97 compared to the ones of hydrological stations such as Phu An and Nha Be of approximately 0.83 and 0.82. This shows that the hydrographic stations subject to the strong influence of the tide have higher accuracy. The hydrological stations located deeply in the field are less affected by tides and subject to the influence of river flows, they have lower accuracy.

Contributions of authors: Developing research ideas: N.V.H., C.T.H.; Selection of a research method: N.P.D., C.T.H., P.A.B.; Data processing: N.P.D.; Writing the paper: P.A.B., C.T.H., N.P.D.; Paper editing: N.V.H., P.A.B., C.T.H., N.P.D..

References

1. Codiga, DL and Aurin, DA (2007), "Residual circulation in eastern Long Island Sound: Observed transverse-vertical structure and exchange transport". *Continental shelf research* 27, 103-116.
2. Codiga, DL (2011), "Unified Tidal Analysis and Prediction Using the U_tide Matlab Function", *Technical Report*, Graduate School of Oceanography, University of Rhode Island, Narragansett, RI. 59 pp.
3. Asian Development Bank (2010), *Ho Chi Minh City Adaptation to climate change - Summary report*.
4. Sub-Institute of Meteorology, Hydrology and Climate Change (2008), *Research and build a database of hydro-meteorological characteristics for flood prevention in Ho Chi Minh City*.
5. Sub-Institute of Meteorology, Hydrology and Climate Change (2011), "Research and build a model to assess the impact of climate change on natural and human socio-economic factors in HCMC".
6. Sub-Institute of Meteorology, Hydrology and Climate Change (2015), "Calculating inundation in the basin of District 12 - Ho Chi Minh City using the MIKE FLOOD model".
7. Hoang, T.T.; Nam, B.C.; Thinh, N.N (2012), "Study on calculation of showers into the downstream flow of the Saigon River as input to the anti-flooding problem", *Journal of Hydrometeorology*, October 2012, (17-21).
8. Sub-Institute of Meteorology, Hydrology and Climate Change (2020), "Develop and update action

- plans responding to climate change for the period of 2021 - 2030 with a vision to 2050 in Ho Chi Minh City*", Project of the Department of Natural Resources and Environment of Ho Chi Minh City.
9. Tuan , LN. (2017), *"Research and update of the climate change scenarios of Ho Chi Minh City according to the new methodology and scenarios of the Intergovernmental Panel on Climate Change (IPCC) and the Ministry of Natural Resources and Environment"*, Project of the Department of Science and Technology of Ho Chi Minh City.
 10. Pham Van Huan and Nguyen Tai Hoi (2007), *"Viet Nam coastal sea level fluctuations"*, *Hydrometeorological Journal*, No. 556, 30-37.
 11. Nguyen Phuong Dong, Tran Tuan Hoang et al (2020), *"Researching and applying utide software to calculate and analyze water levels for forecasting in the southern region"*, *12th Scientific Conference in 2020 - Ho Chi Minh City School of Natural Sciences*.

CHARACTERIZING EFFECTS OF DIFFERENT ENSO PHASES ON SEA SURFACE TEMPERATURE IN THE VIET NAM EAST SEA

Le Quoc Huy⁽¹⁾, Pham Tien Dat⁽²⁾, Tran Van My⁽¹⁾, Nguyen Hong Hanh⁽¹⁾,
Nguyen Thi Lan⁽¹⁾, Dang Linh Chi⁽¹⁾

⁽¹⁾Viet Nam Institute of Meteorology, Hydrology and Climate change

⁽²⁾VNU University of Science

Received: 13 September 2021; Accepted: 29 September 2021

Abstract: *The effect of different ENSO phases on Sea Surface Temperature (SST) has been an intensive effort to find the link between this basin-scale climate pattern and one of the most critical marine parameters. This issue, however, has not been well-studied in the Viet Nam East Sea (VES). This study examined the effect of different ENSO phases on SST in the VES by applying a series of statistical techniques on both satellite data and observed data from coastal stations. We find a significant correlation between ENSO and satellite-based SST data in the winter season ($r = 0.56$). We recognize a stronger relationship of ENSO-SST in the southern stations (with r varies from 0.47 - 0.83). We then compared the impact of different ENSO phases for the period of 1990 - 2019. Our results reveal that the extreme El Nino event 1997/98 had impacted SST strongly than any other event. In addition, we find that the response of SST to ENSO phases does not depend on intensity. The outcomes of this work may significantly contribute to the understanding of the effects of ENSO on marine parameters in the VES.*

Keywords: ENSO, SST, EEMD, EOF.

1. Introduction

ENSO (El Niño - Southern Oscillation) is a large-scale climate pattern in the tropical Pacific region but has global impacts. ENSO occurs every 2 - 7 years and includes two opposite phases: El Nino (warm phase) and La Nina (cold phase), with a significant change of atmospheric circulation [1]. This change, in turn, strongly impacts many weather parameters such as temperature, rainfall, etc.... Those impacts have been intensively reported and studied in many works, but a large portion of them has focused on land. In contrast, the effects of ENSO on sea surface parameters have been less well-studied. The sea surface temperature (SST) is the most crucial parameter since it has been used as a monitoring indicator of ENSO via several ENSO indices (e.g., NINO3.4, Multivariate ENSO Index - MEI). However, the

response of SST to different ENSO phases (i.e., El Nino and La Nina) varies in each event. In a recent paper [9], Rao and Ren (2017) compared the impacts of different ENSO extreme events on SST and other parameters in the tropical Pacific region. Their results reveal distinctive effects of El Nino 1982/83, 1997/98, and 2015/16 on SST. This study suggests a different mechanism of each El Nino will have a distinct influence on various parameters. The work of Rao and Ren (2017) has led to an interesting research question: Do different ENSO events (both El Nino and La Nina) have the same impacts on SST in a small-scale ocean basin such as the Viet Nam East Sea? If they do differently, can we compare their effects?

The Viet Nam East Sea (VES) is one of the largest marginal seas in the world. There is a complex air-sea coupled system in this region, including unique climatic-oceanic related phenomena: Monsoons, ENSO, and ocean currents. The link between ENSO and SST

Corresponding author: Le Quoc Huy
E-mail: huylq2@gmail.com

has been discovered in several studies [8, 10]. They used EOF analysis to find the main pattern of SST in the VES and found a significant correlation between ENSO and SST. However, they did not compare in more detail the effects of each ENSO event on SST. In Viet Nam, the impact of ENSO on SST has been investigated in numerous studies [5, 6, 7, 11, 12, 13], but very few works paid attention to sea surface parameters.

In this study, we present detailed research for the first time on the comparison of different ENSO phases on SST in the VES. We used both satellite data (from 1993 - 2020) and observes data from coastal and island stations (from 1990 - 2019) for this study. The data and methods will be presented in section 2; results and discussions will appear in section 3, and finally, we conclude some key findings in section 4.

2. Data and Methodology

2.1. Data sets

We collected monthly satellite SST data sets from CMEMS (1993 - 2020) with a $0.25^\circ \times 0.25^\circ$ degree spatial resolution. The data cover the area from $0 - 25^\circ\text{N}$ to $99 - 121^\circ\text{E}$ in the western tropical Pacific. The monthly observed data from coastal and offshore stations came from 07 stations expanding from the North to the South of Viet Nam: Cua Ong, Bai Chay, Son Tra, Quy Nhon, Phu Quy (island), Truong Sa (island), and Vung Tau. We processed observed SST data sets to make sure that they meet the quality and have a common period. We chose a period of 1990 - 2019 for all seven stations so that the correlation analysis will be comparable between them.

There are several ENSO indices such as: Nino3.4, MEI, or SOI, but in this study we used Nino3 index to present the evolution of ENSO phases. Nino3 index is considered as the best index to capture El Nino extreme events since it uses the maximum SST anomalies that are in the same region ($5^\circ\text{S} - 5^\circ\text{N}$, $150^\circ\text{E} - 90^\circ\text{W}$) [9]. The monthly time series of Nino3 will be used in analysis along with data of SST in this study.

2.2. Methodology

2.2.1. Link with ENSO

For satellite data, we applied Empirical Orthogonal Function (EOF) analysis to determine the spatial and temporal patterns of SST in the VES. We then selected only the first principal component (PC1) time series of SST from EOF analysis to examine the relationship between SST and ENSO via the Nino3 index. Before applying EOF, we had removed the trend and seasonal signals from the data set so that EOF only analyzed the SST anomalies (SSTA). This is necessary as Nino3 is calculated by using SSTA in region of $5^\circ\text{S} - 5^\circ\text{N}$, $150^\circ - 90^\circ\text{W}$. The two time series (PC1-SST and Nino3) are analyzed by cross correlation analysis. We then further explore the co-variations of both SST and Nino3 by using coherence-wavelet analysis [Grinsted et al., 2004]. This step aims to find out the common period that two time series co-vary throughout the length of data sets.

For SST data from stations, we used Ensemble Empirical Mode Decomposition (EEMD) method to obtain the 2 - 7 year signals (the ENSO re-occurrence) from monthly SST data and Nino3. EEMD is an adaptive and data-driven method to decompose a raw time series to different modes with their amplitudes and frequencies [14]. This method has been recently used in a work led by Le et al., 2017 to analyze SST for coastal stations along Viet Nam's coastlines.

2.2.2. Comparison of different ENSO phases on SST

To compare the effects of different ENSO phases on SST in the VES we mainly focus on the difference between El Nino events (warm phase) and La Nina events (cold phase). We also measure the power of some extreme events [e.g., El Nino 1997/98 and 2015/16 events] against other events from 1990 - 2019. To do that, we used the Hovmoller diagram and other statistical plots to characterize the strength of events and their impacts on SST.

3. Results and Discussions

3.1. Impacts of ENSO on SST

The results of EOF analysis are presented in Fig. 1. We chose to present the first three EOFs and PCs because they account for about 82% of total variance of SST in the VES from 1993 - 2020. Here, we focus on the first EOF and PC. The EOF1 (62%) increases of SST for the entire study area with the maximum increasing SST $\sim 2^{\circ}\text{C}$. It can be seen from Fig. 1 that; the coastal and offshore Southern Central and Southern coasts of Viet Nam are warmest regions. Results from Fig. 1 indicates a rising trend of SST recently in the VES, which has also been reported in other studies.

The correlation coefficient of monthly PC1-Nino3 is $r = 0.3$ but that increases to $r = 0.56$ when we average values of three months: 12, 1 and 2 - DJF (Fig. 2). This result proves the effect of ENSO on SST in the winter when ENSO is in its mature phase. In addition, the result also shows

the positive correlation between SST and ENSO: SST increases/decreases in warm/cold phase of ENSO. Our results agree well with other studies (e.g.,) but we further prove the effect of ENSO on SST by using the winter-averaged SSTA and Nino3. Results from coherence-wavelet analysis also reveal that PC1-SST and Nino3 co-vary in a high power period of 4 - 6 years during 1993 - 2005 (Fig. 3). The high power is strongest in the extreme El Nino 1997/98 event compared to other events. After 2005, Nino3 and PC1-SST show high correlation in the 2 - 4 year band indicating another process dominates variations of SST in the VES (Fig. 3).

ENSO also shows the effect on SST from coastal and island stations. The ENSO-related signals from each data set after using EEMD were analyzed with Nino3 (note that, the trend in each data had been removed in EEMD analysis). The correlation coefficients vary from 0.4 - 0.66 for monthly data and from 0.36 - 0.83 for winter-averaged data (Table 1).

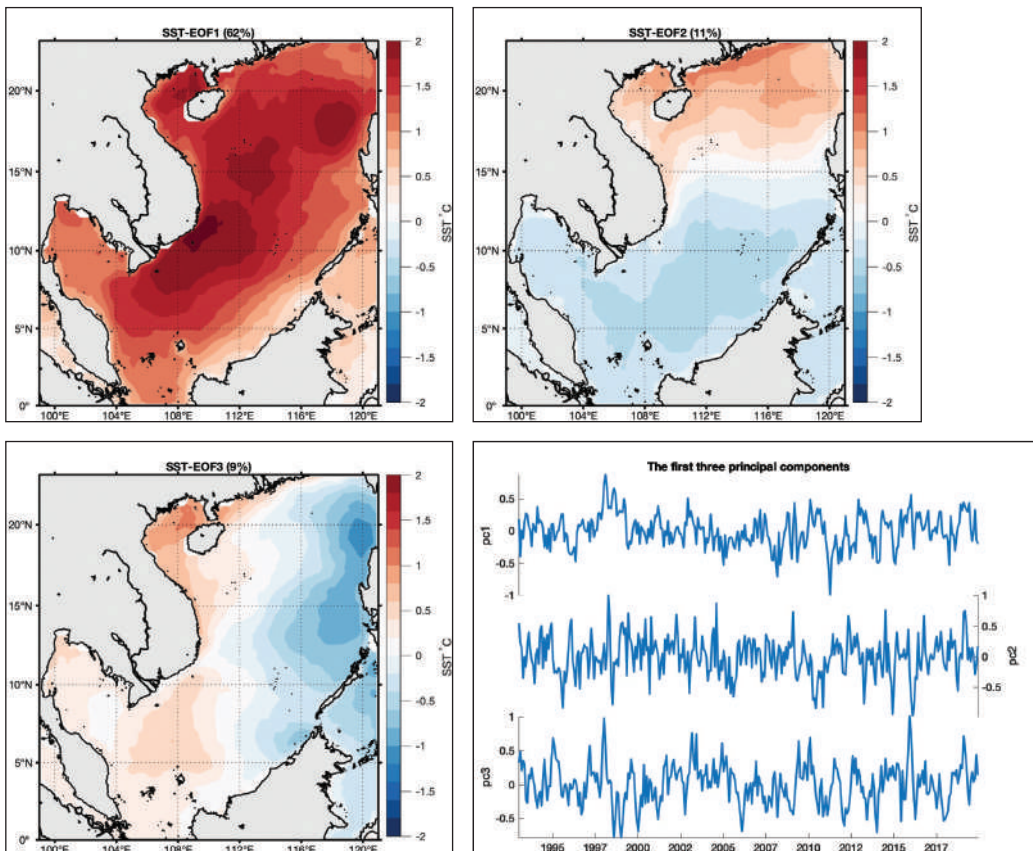


Figure 1. The three first EOF and PCs of SST from EOF analysis

Unlike moderate correlations between Northern stations and Nino3, Southern stations show higher correlations with ENSO, particularly in the mature phase. This indicates that the imprint of ENSO is more clear and more increased of south VES, which agrees with the results from EOF analysis above. Phu Quy and Truong Sa have the highest correlations with $r = 0.83$ and $r = 0.71$, respectively (Fig. 4). Table 1 also reveals that the El Nino 1997/98 strongly

impacted on SST in 4 stations (Son Tra, Quy Nhon, Phu Quy and Truong Sa) with the largest change in Quy Nhon station (0.8°C). Nevertheless, La Nina events also show remarkable impact on SST in Cua Ong, Bai Chay and Quy Nhon. Interestingly, the extreme El Nino 2015/16 event does not significantly impact SST, although 2015/16 is considered a powerful event after 1997/98 and 1982/83 events.

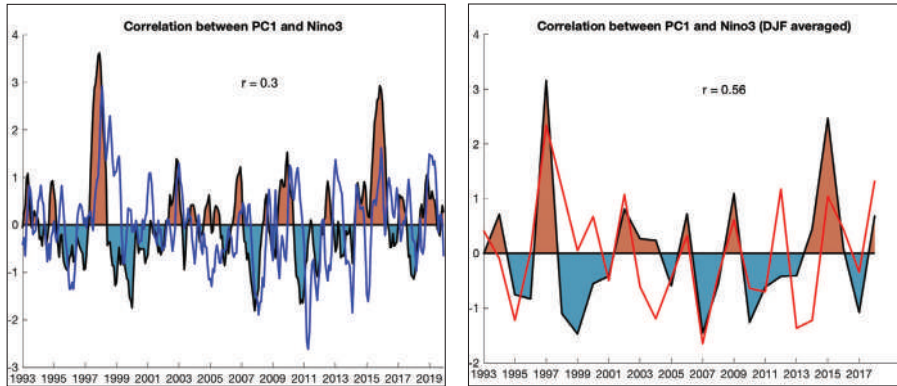


Figure 2. Cross-correlation analysis between PC1-SST and Nino3 in: monthly data (left) and winter-averaged data - DJF (right). The shaded anomaly graph shows Nino3 data

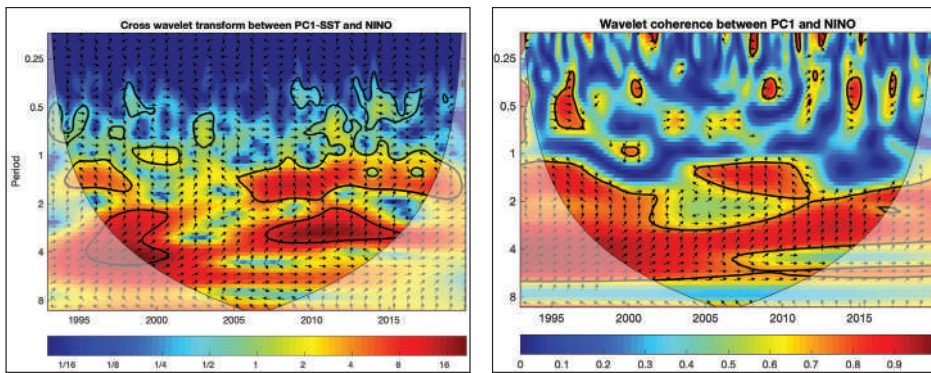


Figure 3. Coherence wavelet analysis for PC1-SST and Nino3 during 1993-2020

Table 1. Correlation coefficients between SST-Nino3 at 07 stations

Station	Length of Data	$r_{\text{SST-Nino3}}$	$r_{\text{SST-Nino3-DJF}}$	The changes in ENSO phases ($^{\circ}\text{C}$)
Cua Ong	1990 - 2019	0.40	0.36	-0.75(2007)**
Bai Chay	1990 - 2019	0.41	0.42	-0.92(2010)**
Son Tra	1990 - 2019	0.40	0.42	0.62(1997)*
Quy Nhon	1990 - 2019	0.42	0.47	0.8 (1997)*, -0.8 (2011)**
Phu Quy	1990 - 2019	0.66	0.83	0.72(1997)*
Truong Sa	1990 - 2019	0.56	0.71	0.67(1997)*
Vung Tau	1990 - 2019	0.44	0.60	0.58(2015)*

*: El Nino events; **: La Nina events

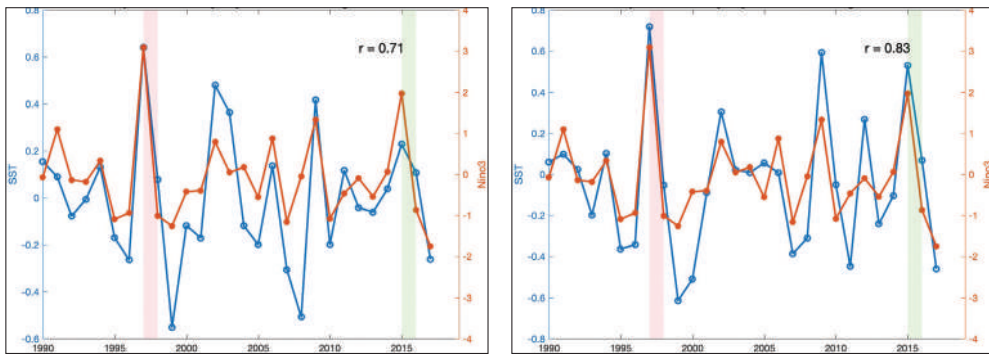


Figure 4. Correlations between SST and Nino3 using winter mean at Truong Sa (left) and Phu Quy (right). The shaded band shows El Niño 1997/98 (pink) and El Niño 2015/16 (green) phase.

3.2. Comparison of different ENSO phases

This section defines intense/extreme El Niño events as 1997/98 and 2015/16; strong La Niña events are 1998/99, 1999/00, 2007/08, and 2010/11. Other events will be considered as weak events (for both El Niño and La Niña phases).

First, we used Hovmöller to present the evolution of SST in the time-longitude dimension. We averaged along latitudes monthly SST and in DJF period to truly see the mature phase of ENSO. To focus on the coastal regions of Viet Nam, we only plot Hovmöller diagram for an area from 104°E to 112°E (Fig. 5). Fig. 5 shows that SSTA in

the El Niño 1997/98 event increased up to more than 1°C, highest among other events indicating the most powerful El Niño event in history. The increase of SSTA in the El Niño 1997/98 expanded from the center of the VES to coastal regions of Viet Nam (104°E - 105°E, Fig. 6). The 2015/16 event also made an increase of SSTA but with lower values. Overall, SSTA increased and was warmer than normal conditions in El Niño events, except for the 2004/05 event (a decrease of -0.2 ÷ -0.3°C). Conversely, La Niña reduced SST anomalies, except for the 1998/99 event (an increase of 0.1 - 0.2°C). This contrast is clearly shown in Fig. 5 and Fig. 6.

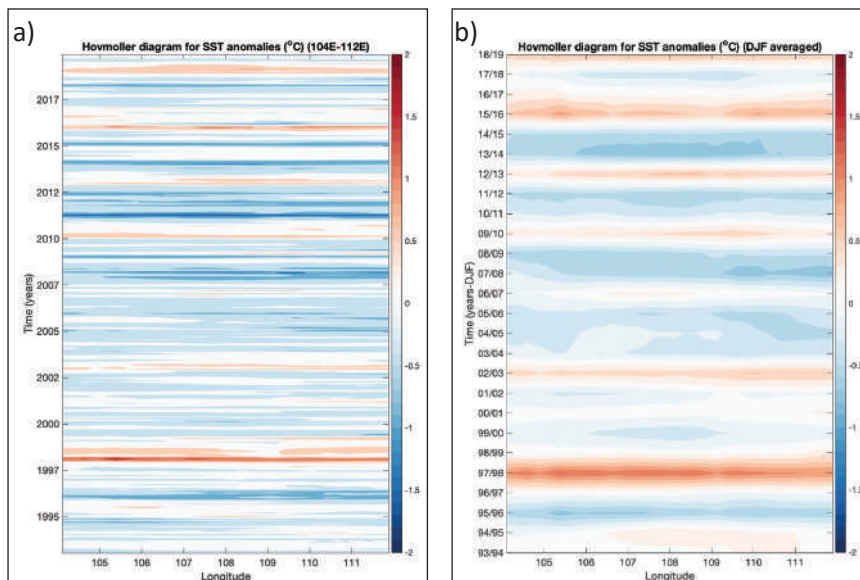


Figure 5. Hovmöller diagram of SST for: monthly data (a) and winter mean data (b)

To further certify the differences between ENSO phases, we show in Fig. 7 the normalized values of PC1-SST from EOF analysis and Fig. 8

the scatter plot between PC1-SST and Nino3 index for each winter year. In these Figs, we used standard deviations as an indicator to

measure the strength of each event. It shows that not many El Nino and La Nina events strongly impact SST anomalies in the VES regions, but we still observe some significant features.

Firstly, among El Nino events outside the $\pm 1\sigma$ area, the extreme El Nino 1997/98 event

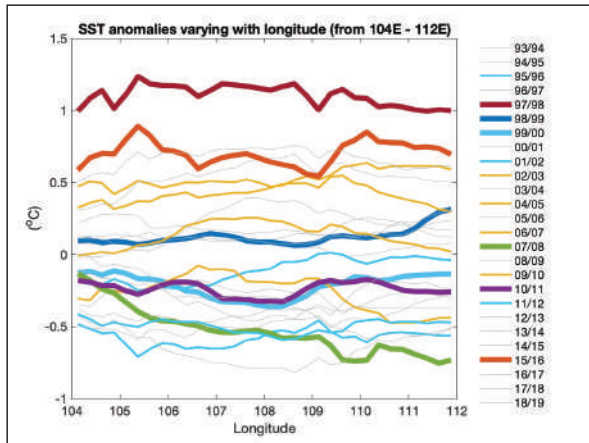


Figure 6. Evolution of SST anomalies with longitude using DJF data. The grey lines show neutral phases

Secondly, only two La Nina events have significant impacts on SST anomalies: 1995/96 and 2007/08 cases but the latter event has much more influence. Meanwhile, the strong

has strongest impact on SST anomalies as all its statistical values surpass other events (Figs 7 and 8). The 2015/16 and 2002/03 events have little impacts on SST anomalies whereas the 2004/05 event shows “strange” behavior with negative sign on SST anomalies.

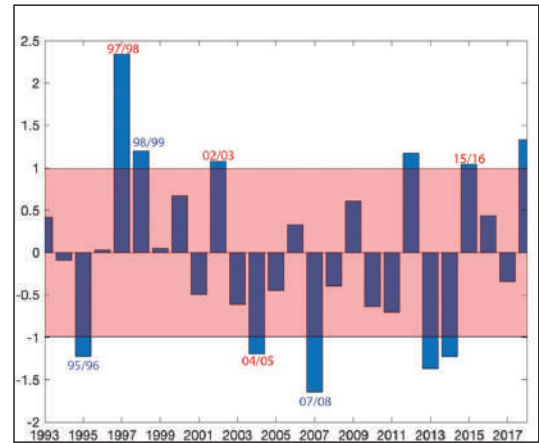


Figure 7. The normalized PC1-SST values from EOF analysis for each winter year. The shaded area indicates the area of $\pm 1\sigma$

1998/99, 1999/00 and 2010/11 cases do not show their effects and the 1998/99 case even observes a positive sign of SST anomalies (Figs 7 and 8).

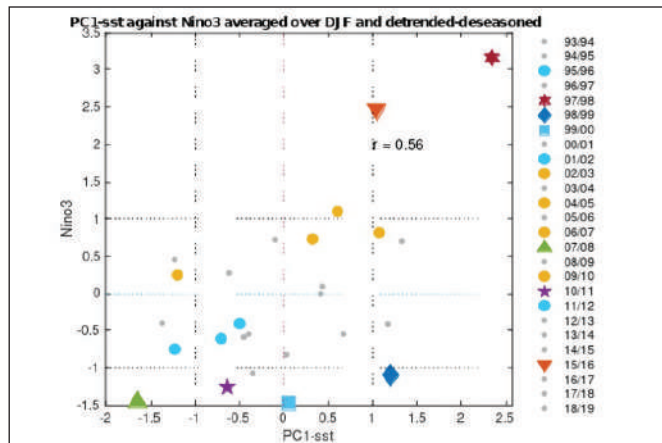


Figure 8. Scatter plot between PC1-SST and Nino3 index for each winter year. The dash lines show area of $\pm 1\sigma$

The difference between ENSO phases in this study agrees well with other studies and suggests a debate on different underlying mechanisms between ENSO events. There have been several studies trying to reveal how El Nino events differ

from each other in terms of influence on SST anomalies [4, 9]. For example, Paek [4] discussed that the two extreme El Nino events 1997/98 and 2015/16 have distinct underlying dynamics and climate impacts. They suggested that

the maximum SST anomalies in the 2015/16 event did not propagate westward as far as to the 1997/98 events. By looking at the peak magnitude of the westerly wind anomalies in the two events, the authors found that the wind in the latter event was 35% smaller than during the 1997/98 event. This might be why the maximum SST anomalies in the VES were much higher during the 1997/98 event in our study. Paek [4] also discussed that the type of the two events was not the same leading to the different behavior in the mature phase. While the 1997/98 event was pure eastern Pacific (EP) ENSO, the 2015/16 even showed a mixture of both the EP and central Pacific (CP) ENSO, causing the departure of the 1997/98 event.

4. Conclusions

Impacts of ENSO have been reported in other studies but here we present the first work of combining satellite data and observed data from coastal stations to study the imprints of ENSO in the VES. We also introduce the first study of comparison of different ENSO phases

from 1993 - 2020. Our results show that ENSO has stronger impacts on SST in the south central to southern Viet Nam coastline than the North. These imprints are more prominent in the mature phase of ENSO (i.e., wintertime) when the correlation between Nino3 index and PC1-SST is $r = 0.56$.

Our findings reveal that the extreme 1997/98 El Nino event was the most powerful event and has most impact on SST anomalies in the VES. The second extreme El Nino 2015/16 did not produce the effect as strong as the 1997/98 event. This difference might be due to the variance of underlying dynamics (e.g., the westerly wind intensity). But to fully explain this matter, there is a need for a detailed study in the future.

It should be noted that, the response of SST to ENSO is not related to the intensity of each event. A weak ENSO case could show a remarkable effect on SST while a strong one could not. This might be an important insight for the following research to study on the impact of ENSO in the VES.

Acknowledgments: This study is supported by the national project (code number ĐTDL.CN-28/17); project TNMT.2018.06.12. We would like to express our sincere thanks to the Projects Management Board and colleagues in the research group for their comments and support to help us complete this paper.

Reference

1. Clarke, A.J., (2008), *An Introduction to the Dynamics of El Nino & the Southern Oscillation*. Burlington: Elsevier, 2008.
2. Chunli Liu, Xue Li, Sufen Wang, Danling Tang & Donghe Zhu (2020), "Interannual variability and trends in sea surface temperature, sea surface wind, and sea level anomaly in the South China Sea", *International Journal of Remote Sensing*, 41:11, 4160-4173, DOI: 10.1080/01431161.2020.1714777
3. Grinsted, A., J. C. Moore, S. Jevrejeva (2004), *Application of the cross wavelet transform and wavelet coherence to geophysical time series*, *Nonlin. Process. Geophys.*, 11, 561566
4. Paek, H., J.-Y. Yu, and C. Qian (2017), "Why were the 2015/2016 and 1997/1998 extreme El Niños different?", *Geophys. Res. Lett.*, 44, doi:10.1002/2016GL071515.
5. Pham Duc Thi (2014), "Sea surface temperature regime over ENSO areas, Viet Namese territory and East Sea in ENSO development stages in the under of climate change" [*Chế độ nhiệt độ mặt nước biển trên các khu vực ENSO, lãnh thổ Việt Nam và Biển Đông trong các giai đoạn phát triển của ENSO trong bối cảnh biến đổi khí hậu*], *Viet Nam Journal of Hydrometeorology*, No 10-2014, 29-34.
6. Le Quoc Huy, Nguyen Xuan Hien, Tran Thuc, Pham Tien Dat (2017a), "Analysis of the variations in sea surface temperature and the influence of ENSO in the coastal region of the south central of Viet Nam" [*Phân tích sự biến động của nhiệt độ bề mặt biển và ảnh hưởng của ENSO ở khu vực ven biển Nam Trung Bộ*], *Journal of Climate Change Science*, No 1, 3-2017; 67-74.

7. Quoc Huy Le, Thuc Tran, Xuan Hien Nguyen and Van Uu Dinh (2017b), "Effects of ENSO on the intraseasonal oscillations of sea surface temperature and wind speed along Viet Nam's coastal areas". *Viet Nam Journal of Science, Technology and Engineering*, 59(3), 85-90.
8. Qiu, F., P. Aijun. Z. Shanwu. C. Jing. S. Haowei. (2015) "Sea surface temperature anomalies in the South China Sea during mature phase of ENSO". *Chinese Society for Oceanology and Limnology, Science Press, and Springer-Verlag Berlin Heidelberg*. <http://dx.doi.org/10.1007/s00343-016-4290-3>.
9. Rao, J., and R. C. Ren, (2017) "Parallel comparison of the 1982/83, 1997/98 and 2015/16 super El Niños and their effects on the extratropical stratosphere". *Adv. Atmos. Sci.*, 34(9), 1121–1133, doi: 10.1007/s00376-017-6260-x
10. Siti Maisyarah et al (2019), "The Effect of the ENSO on the Variability of SST and Chlorophyll-a in the South China Sea", *IOP Conf. Ser.: Earth Environ. Sci.* 246 012027. doi:10.1088/1755-1315/246/1/012027
11. Tran Van Chung et al (2018), "Anomaly variations of temperature fields and its relationship with ENSO phenomenon in Ninh Thuan - Binh Thuan", *Journal of Marine Science and Technology*; Vol 18, No 1; 2018: 79-87; DOI: 10.15625/1859-3097/18/1/8765.
12. Vu Van Tac et al (2017), "Sea surface temperature anomaly in South Central Viet Nam Waters related to ENSO phenomenon" [Bất thường của nhiệt độ nước tầng mặt tại vùng biển Nam Trung bộ Việt Nam liên quan đến hiện tượng ENSO]. *Viet Nam Journal of Marine Science and Technology*, 17(2), 111–120; DOI: 10.15625/1859-3097/17/2/10153.
13. Vu Van Tac et al (2019), "Sea surface temperature anomaly in the coastal waters of Viet Nam related to ENSO phenomenon" [Bất thường của nhiệt độ nước tầng mặt tại vùng biển ven bờ Việt Nam liên quan đến hiện tượng ENSO], *Viet Nam Journal of Marine Science and Technology*; Vol. 20, No. 1; 2020: 1–11, DOI: <https://doi.org/10.15625/1859-3097/20/1/15038>.
14. Z.H. Wu, N.e. Huang (2009), "ensemble empirical mode decomposition: A noise-assisted data analysis method", *Adv. Adapt. Data. Anal.*, 1(1), pp.1-41.

DETERMINATION OF EVAPOTRANSPIRATION USING SOLAR RADIATION AND METEOROLOGICAL DATA APPLYING DIFFERENT METHODS: A CASE STUDY HOA BINH PROVINCE

Le Hung Chien⁽¹⁾, Doan Ha Phong⁽²⁾, Tran Xuan Truong⁽³⁾, Ngo Thi Dinh⁽¹⁾

⁽¹⁾ Viet Nam National University of Forestry

⁽²⁾ Viet Nam Institute of Meteorology, Hydrology and Climate Changer

⁽³⁾ Ha Noi University of Mining and Geology

Received: 19 August 2021; Accepted: 08 September 2021

Abstract: *Evapotranspiration (ET) is a significant parameter that needs to be determined and accurately estimated in many practical applications such as the management and use of water domestic, agricultural production, and forestry. The content of the article presents four methods that include the Makkink method (1957), Abteu method (1996), Priestley & Taylor method (1972), Hargreaves & Samani method (1982, 1985) to calculate evapotranspiration from meteorological data at monitoring stations in Hoa Binh province. The results of evapotranspiration calculated from the methods are compared and evaluated for accuracy with direct measurement data at the province's hydro-meteorological stations, attend to the management, forecasting water demand in agriculture and forestry, and design of irrigation works with climate conditions of Hoa Binh province. The results indicate that the average evapotranspiration values at the hydro-meteorological stations of Makkink method (1957), Abteu method (1996), Priestley & Taylor method (1972), Hargreaves & Samani method (1982, 1985) to calculate evapotranspiration from meteorological data at monitoring stations in Hoa Binh province. The results of evapotranspiration calculated from the methods are compared and evaluated for accuracy with direct measurement data at the province's hydro-meteorological stations, attend to the management, forecasting water demand in agriculture and forestry, and design of irrigation works with climate conditions of Hoa Binh province. The results indicate that the average evapotranspiration values at the hydro-meteorological stations of Makkink method (1957), Abteu method (1996), Priestley & Taylor method (1972), Hargreaves & Samani method (1982, 1985) on 04th June 2017 were 8.1 mm, 5.8 mm, 7.8 mm and 11.3 mm, respectively. The average error of evapotranspiration at meteorological stations calculated according to the methods compared with the average evapotranspiration at meteorological stations measured directly is 5.2%, 24.7%, 1.3%, 46.7%, respectively. Calculating evapotranspiration by the Makkink method with coefficients $a = 0.9$ and $b = 0$ gives the most accurate results with the highest correlation coefficients $R^2 = 0.969$ and $RMSE = 0.346$. According to the results, the Priestley-Taylor and Makkink method is proposed to calculate the evapotranspiration for the Hoa Binh area.*

Keywords: *Evapotranspiration, Makkink method, Priestley - Taylor method, , Hoa Binh Meteorological station.*

1. Introduction

Evaporation is the process whereby liquid water is converted to water vapor or gaseous state. Evaporation is the first step in the water cycle that water is changed from the liquid into

the vapor in the atmosphere. Evaporation is the return of water into the atmosphere through the diffusion of water molecules from soil, vegetation, water bodies, and other wet surfaces [1]. Transpiration is the phenomenal release of water vapor into the air from the surface of the leaves of a plant stem as a physiological response of the plant to combat the dryness around it.

Corresponding author: Doan Ha Phong
E-mail: doanhaphong.imhen@gmail.com

The total amount of water lost through the diffusion of water molecules into the atmosphere is known as transpiration. Other factors affecting evaporation are solar radiation, air humidity, temperature and wind velocity.

Evapotranspiration is a term used to describe the total amount of plant evaporation and transpiration from the earth's surface to the atmosphere over a long period of time to clarify the relationship with annual precipitation [2]. This is an important variable in hydrological research. ET is useful information for agricultural planning, urban planning, irrigation scheduling for crop growth patterns, regional water balance study, agro-climatic zoning, and design and operation irrigation systems [3]; [4]; [5]. Direct measurements of ET around the world are rare, therefore, there is a lack of actual observational data to provide a qualitative improvement opportunity for various hydrological methods, since direct measurements of ET are costly and usually performed by high micro-quantum techniques. It is predicted that the direct impact of climate change on water resources is mainly evapotranspiration. Hydrological change creates one of the most important potential impacts on global climate change in the tropical areas [6]. It is clear that climate change will increase temperature and changes in precipitation. High temperatures will cause high evaporation, affecting hydrological systems and water resources. Therefore, accurate quantification of the ET is important and necessary not only for the long-term management of water resources but also for the design and operation of irrigation facilities specifically for the heavily cropped land region under climate change conditions. For many years, scientists around the world have tried to find many experimental methods to calculate ET values for different types of climate zones. These methods estimate ET by mathematical formula based on research and experimental results [7]. The typical methods are Penman method [8], Jensen-Haise method [9], Blaney-Criddle method [10], Hargreaves-Samani method [11]; Thorn-Thwaite method [12], and Van Bavel method [13]. Each method has its own advantages and is applicable to

each specific climate zone. Some methods are essentially modified versions of others. The main concern in ET estimation is the reliability and accuracy of the methods [3]. Many methods have been developed from a certain point of view for a particular climate area, so it often fails to estimate the amount of evapotranspiration that might occur under other climatic conditions. This is also a challenging problem in accurately forecasting the ET value. For these reasons, it is essential to select an appropriate method for the regional climate as well as the availability of data. In this research, Makkink method (1957), Abtew method (1996), Priestley & Taylor method (1972) and Hargreaves & Samani method (1982, 1985) are used to compare the effectiveness and reliability in estimating ET for climate zones in Hoa Binh province.

2. Materials and Methods

2.1. Research location

Hoa Binh is a mountainous province in the Northwest region, adjacent to the Red River Delta, located 73 km away from Ha Noi on the National Highway 6 Ha Noi - Hoa Binh - Son La. The whole province has an area of about 4,578.1 km². It borders Phu Tho province to the North, Ha Nam and Ninh Binh provinces to the south, Ha Noi to the east and Northeast, Son La province to the west and Northwest, and Thanh Hoa province to the southwest. The distinct features of Hoa Binh's topography are low and medium-high mountains, complicatedly divided terrain, steep slopes and stretching in the direction of Northwest - Southeast, divided into two distinct regions: The average high mountain area in the Northwest has an average altitude of 600 - 700 m, the highest place is the top of Phu Canh (Da Bac) 1,373 m. The average slope is from 20° to 35°, some places are over 40°, accounting for about 46% of the province's area. Low mountains and hills (Southeast) has an area of 246,895 hectares, accounting for 54% of the province's area, with an average slope 10 - 25°, an average altitude of 100 - 200 m. Alternating mountainous terrain, there are low valleys, narrow valleys stretching along large rivers and streams.

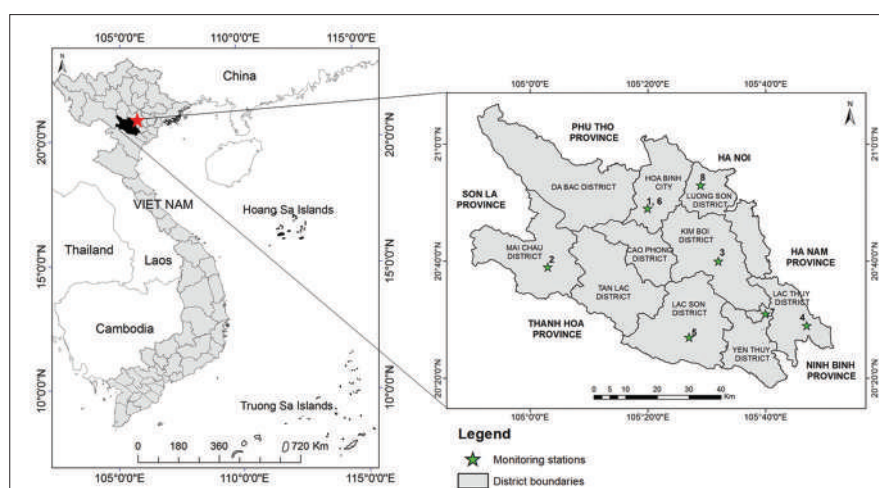


Figure 1. Research area and monitoring stations

Hoa Binh is located in the tropical monsoon climate with characteristics following hot, humid, cold winter. The average temperature in the year is 23°C, average rainfall is 1,800 mm/year, relative humidity 85%, and average annual evaporation of 704 mm. The climate of the year is divided into two distinct seasons. The summer begins in April and ends in September. The average temperature is above 25°C, reach a peak on the day around 43°C. The average monthly rainfall is over 100 mm, and the average monthly rainfall highest is 680 mm (in 1985). Rain usually concentrates in July and August, which accounts for 85 - 90% of the whole year's rainfall. The winter begins in October of the previous year and ends in March of the following year, the average temperature in the month fluctuates between 16 - 20°C, the lowest temperature is 3°C. Rainfall in October about 20 mm [14]. Due

to topographical features, Hoa Binh also has Northwest climate with dry and cold winters, hot and humid summers (in the Northwest high mountains), and the climate in the Northern Delta is more temperate (in the low mountainous areas).

2.2. Meteorological data

Meteorological data for the calculation of evapotranspiration from various methods were collected from Hoa Binh hydro-meteorological stations on 4th June 2017 provided by the Center for Hydro-Meteorology of Hoa Binh Province (Table 1). According to Table 1, the wind speed of the monitoring points ranges from 4 m/s to 8 m/s, the average humidity is from 50% to 71%, the total number of sunshine hours is from 9.3 to 12.3 hours, and the amount of actual water evaporation from 4.6 mm to 9.6 mm.

Table 1. Hydrometeorological data at meteorological monitoring stations in Hoa Binh area on 04/06/2017

No.	Station	Coordinates			Strongest wind (m/s)		Average humid ity (%)	Sunshine duration (hours)	Temperature (°C)		Actual water evaporation (mm)
		Longi tude	Lati tude	Altitude (m)	Direc tion	Wind speed			T (max)	T (min)	
1	Hoa Binh Meteorology	105.20	20.49	22.7	South west	5	50	12.1	41.0	31.0	9.6
2	Mai Chau Meteorology	105.03	20.39	165.5	North west	8	65	10.0	40.0	25.3	5.7
3	Kim Boi Meteorology	105.32	20.40	61.1	North west	4	64	10.6	40.9	27.5	7.0
4	Chi Ne Meteorology	105.47	20.29	11.3	North west	6	71	11.6	40.3	29.6	7.8

No.	Station	Coordinates			Strongest wind (m/s)		Average humidity (%)	Sunshine duration (hours)	Temperature (°C)		Actual water evaporation (mm)
		Longitude	Latitude	Altitude (m)	Direction	Wind speed			T (max)	T (min)	
5	Lac Son Meteorology	105.27	20.27	41.2	North west	4	69	9.3	40.1	27.2	4.6
6	Hoa Binh Hydrological	105.20	20.49	22.6	South west	6	52	12.0	40.8	30.7	9.5
7	Hung Thi Hydrological	105.40	20.31	20.1	North west	5	70	11.4	40.5	30.0	8.0
8	Lam Son Hydrological	105.29	20.53	25.4	South west	7	67	12.3	40.9	30.5	9.2

2.3. Evapotranspiration calculation methods

2.3.1. Makkink method (1957)

The Makkink method (1957) [15] is currently widely used due to the simplification of some of the field measurement index used by the FAO 56 Penman - Monteith method. Makkink proposes the following method of calculating evapotranspiration from solar radiation:

$$ET = a \frac{\Delta}{\Delta + \gamma} \frac{R_s}{\lambda} + b \quad (1)$$

Where: ET - the amount of evapotranspiration (mm/day); R_s - solar radiation (MJ/m²/day); Δ - slope of saturation vapour pressure curve (kPa/°C), γ - psychrometric constant (kPa/°C), λ - latent heat of vaporization (MJ/kg) to; a , b - linear coefficient of the Makkink method.

The linear coefficients of the Makkink method used in the calculation of evapotranspiration from determined surface at the method's proposal time (1957) were: $a = 0.61$ and $b = 0.12$. However, linear coefficients a and b depend on climatic conditions and topographical factors of each region in the world. According to Hasen's research in the Netherlands, 1984, the coefficients a , b have the values $a = 0.70$ and $b = 0$. On the other hand, a combination of Uppsala University (Sweden) and Louisiana University (USA) by Xue and Singh conducted a survey in 1999, the coefficients a and b have values of 0.77 and 0.22, respectively.

2.3.2. Abtew Method (1996)

Abtew (1996) [16] uses a simple method to calculate evapotranspiration based on solar

radiation as follows:

$$ET = K \frac{R_s}{\lambda} \quad (2)$$

Where: ET - the amount of evapotranspiration (mm/day); R_s - solar radiation (MJ/m²/day); λ - latent heat of vaporization (MJ/kg); $K = 0.53$ - Dimensional coefficient.

2.3.3. The Priestley-Taylor Method (1972)

Priestley-Taylor (1972) [17] proposed a method to calculate the amount of evapotranspiration from solar radiation energy as follows:

$$ET = a \frac{\Delta}{\Delta - \gamma} \frac{R_n}{\lambda} + b \quad (3)$$

Where: ET - the amount of evapotranspiration (mm/day); R_n - the daily net radiation (MJ/m²/day); Δ - the saturation vapor pressure curve (kPa/°C); γ - psychrometric constant (kPa/°C); λ - latent heat of vaporization (MJ/kg); a , b are the linear coefficients of the Priestley-Taylor method.

The linear coefficients a , b of the Priestley-Taylor (1972) method used to calculate the amount of evapotranspiration from the topographical surface have the following values: $a = 0.61$ and $b = 0.12$; in 1984, tested in Europe (Switzerland), $a = 0.90$ and $b = 0$ and tested in Asia (Taiwan), 2005, $a = 1.00$ and $b = 0$.

2.3.4. The Hargreaves Samani Method (1982, 1985)

Hargreaves and Samani (1982, 1985) [11] proposed the following formula for evapotranspiration:

$$ET = 0.0135(T + 17.8)R_s/\lambda \quad (4)$$

Where: ET - the amount of evapotranspiration

(mm/day); R_s - solar radiation (MJ/m²/day); λ - latent heat of vaporization (MJ/kg); T - air temperature (°C).

2.3.5. *Statistical analysis, accuracy assessment method*

The regression analysis, basic statistics, deviation, and error calculations in the study were calculated using IBM SPSS Statistics 20 software based on 95% distribution of the series with correlation coefficient calculated in the paper as the Pearson correlation coefficient.

3. Research results

3.1. Results of calculating evapotranspiration from the methods

3.1.1. The Makkink (1957) method of evapotranspiration calculating results

Using formula (1) to calculate the evapotranspiration value according to the Makkink method (1957) with the cases with coefficients a, b respectively, specifically the case ET_Mk1 has

coefficients $a = 0.61$, $b = 0.12$, the ET_Mk2 case has a coefficient $a = 0.9$, $b = 0$, the ET_Mk3 case has a coefficient $a = 1$, $b = 0$, the ET_Mk4 case has a coefficient $a = 0.85$, $b = 0$ and the ET_Mk5 case has a coefficient $a = 0.77$, $b = 0.22$. The results show that the case ET_Mk2 with $a = 0.9$, $b = 0$ gives the best results with the difference between the evapotranspiration from the data calculated by the comparison method with direct observation results at meteorological stations ranging from -1 mm to 2.5 mm and an average of 0.4 mm (Table 2). Thus, the calculated value of evapotranspiration on June 4, 2017 was lowest at Lac Son meteorological station and highest at Hoa Binh meteorological station and Lam Son hydrological station with values of 7.1 mm and 8.6 mm, respectively. The average amount of evapotranspiration at the stations is 8.1 mm. The mean square error between the actual measurement results and the Makkink method (1957) in the case of ET_Mk2 is 1.3 mm.

Table 2. Calculation results of evapotranspiration and evapotranspiration values according to the Makkink (1957) method

No.	Station	The amount of evapotranspiration according to the Makkink method (ET_Mk, mm/day)					Actual evapotran spiration (mm/day)	Difference from actual evapotranspiration (mm/day)				
		ET_Mk1	ET_Mk2	ET_Mk3	ET_Mk4	ET_Mk5		ET_Mk1	ET_Mk2	ET_Mk3	ET_Mk4	ET_Mk5
1	Hoa Binh Meteorology	5.9	8.6	9.5	8.1	7.5	9.6	-3.7	-1.0	-0.1	-1.5	-2.1
2	Mai Chau Meteorology	5.1	7.4	8.2	7.0	6.6	5.7	-0.6	1.7	2.5	1.3	0.9
3	Kim Boi Meteorology	5.4	7.8	8.6	7.3	6.9	7	-1.6	0.8	1.6	0.3	-0.1
4	Chi Ne Meteorology	5.7	8.3	9.2	7.8	7.3	7.8	-2.1	0.5	1.4	0.0	-0.5
5	Lac Son Meteorology	5.0	7.1	7.9	6.7	6.3	4.6	0.4	2.5	3.3	2.1	1.7
6	Hoa Binh Hydrological	5.9	8.5	9.4	8.0	7.5	9.5	-3.6	-1.0	-0.1	-1.5	-2.0
7	Hung Thi Hydrological	5.7	8.2	9.1	7.7	7.2	8	-2.3	0.2	1.1	-0.3	-0.8
8	Lam Son Hydrological	6.0	8.6	9.6	8.2	7.6	9.2	-3.2	-0.6	0.4	-1.0	-1.6
	Mean	5.6	8.1	8.9	7.6	7.1	7.7	-2.1	0.4	1.3	-0.1	-0.6
	Mean square error							2.7	1.3	1.8	1.3	1.5

Note: ET_Mk1 case: $a = 0.61$, $b = 0.12$, ET_Mk2 case: $a = 0.9$, $b = 0$, ET_Mk3 case: $a = 1$, $b = 0$, ET_Mk4 case: $a = 0.85$, $b = 0$, ET_Mk5 case: $a = 0.77$, $b = 0.22$

The correlation between the actual evapotranspiration value and the Makkink evapotranspiration value in 5 cases is shown in Figure 2. The analysis results show that the case ET_Mk2 has the highest correlation with

coefficient of determination $R^2 = 0.969$ and the lowest error ($RMSE = 0.346$). Therefore, Makkink method with coefficients $a = 0.9$, $b = 0$ can be used to calculate evapotranspiration for Hoa Binh area.

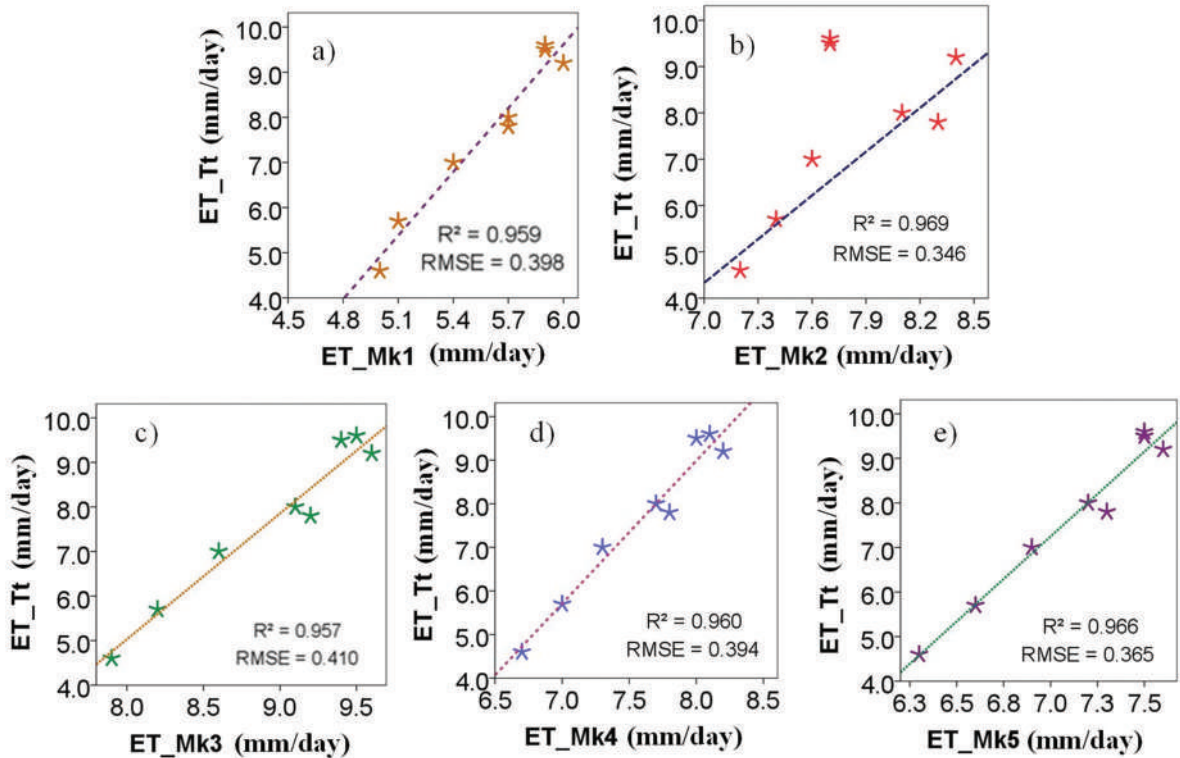


Figure 2. The correlation between actual evapotranspiration (ET_{Act}) and Makkink evapotranspiration (ET_{Mk}) with a) ET_{Mk1} case: $a = 0.61$, $b = 0.12$, b) ET_{Mk2} case: $a = 0.9$, $b = 0$, c) ET_{Mk3} case: $a = 1$, $b = 0$, d) ET_{Mk4} case: $a = 0.85$, $b = 0$ and e) ET_{Mk5} : $a = 0.77$, $b = 0.22$ on 04/06/2017

3.1.2. Abtew (1996) method of evapotranspiration calculating results

Formula (2) is used to calculate the evapotranspiration value according to Abtew (1996) method, the calculation results are shown in Table 3. The results show the difference in evapotranspiration value from the method calculation compared with the results of direct observation at meteorological stations varies from -3.5 mm to 0.6mm and on average of 1.9 mm.

The calculated value of ET according to the Abtew (1996) method on June 4, 2017 shows the lowest evapotranspiration at Le Son meteorological station with a value of 5.2 mm, the highest evapotranspiration at Le Son meteorological station, Hoa Binh meteorological station and Lam Son hydrological station is 6.1 mm. The average amount of evapotranspiration at the stations is 5.8 mm. The mean square error between the actual measurement result and the calculated result from Abtew (1996) method is 2.5 mm.

Table 3. Calculation results of evapotranspiration and evapotranspiration values according to the Abtew (1996) method

No.	Station	The amount of evapotranspiration according to the Abtew method (ET_At, mm/day)	Actual evapotranspiration (mm/day)	Difference from actual evapotranspiration (mm/ day)
1	Hoa Binh Meteorology	6.1	9.6	-3.5
2	Mai Chau Meteorology	5.4	5.7	-0.3
3	Kim Boi Meteorology	5.6	7.0	-1.4
4	Chi Ne Meteorology	5.9	7.8	-1.9
5	Lac Son Meteorology	5.2	4.6	0.6
6	Hoa Binh Hydrological	6.0	9.5	-3.5
7	Hung Thi Hydrological	5.8	8.0	-2.2
8	Lam Son Hydrological	6.1	9.2	-3.1
Mean		5.8	7.7	-1.9
Mean square error				2.5

Figure 3 shows the evapotranspiration calculated by the Abtew method is strongly correlated with the actual evapotranspiration with $R^2 = 0.964$ and $RMSE = 0.372$. However, the results of calculations using the Abtew

method are quite different from the results of direct observations at meteorological stations. Therefore, the Abtew method should not be used to calculate evapotranspiration for Hoa Binh province.

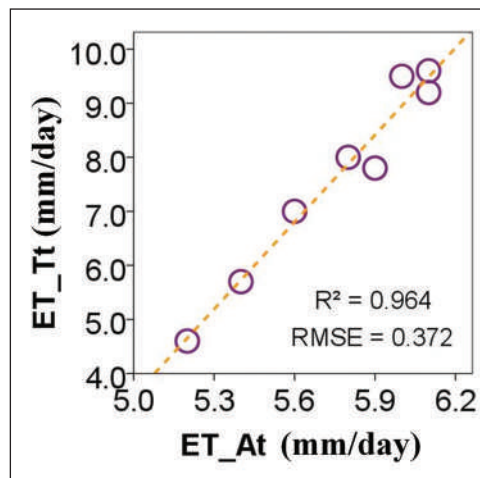


Figure 3. The correlation between actual evapotranspiration (ET_Act) and Abtew evapotranspiration (ET_At) on 04/06/2017

3.1.3. Priestley-Taylor (1972) method of evapotranspiration calculating results

By applying formula (3) to calculate the evapotranspiration value according to the Priestley-Taylor (1972) method for the cases with coefficients a , b respectively, specifically

the case ET_Pt1 with $a = 0.61$, $b = 0.12$, ET_Pt2 case with $a = 0.9$, $b = 0$, ET_Pt3 case with $a = 1$, $b = 0$, and ET_Pt4 case with $a = 0.85$, $b = 0$. The results of above method are shown in Table 4. It can be seen that the ET_Pt4 case with $a = 0.85$, $b = 0$ gives the best results, close to the direct

measurement results from the field. The difference in evapotranspiration from the calculated data compared with the results of direct observations at meteorological stations varies from -1.9 mm to 2.6 mm and is 0.1 mm on average. The calculated result according to Priestley-Taylor (1972) method on 04/06/2017

shows the lowest evapotranspiration at Le Son meteorological station of 7.2 mm, the highest at Lam Son hydrological station with 8.4 mm. The average amount of evapotranspiration at the stations is 7.8 mm. The mean square error between the actual measurement and the Priestley-Taylor (1972) method with ET_Pt4 is 1.6 mm.

Table 4. Calculation results of evapotranspiration and evapotranspiration values according to the Priestley-Taylor (1972) method

No.	Station	The amount of evapotranspiration according to the Abtew method (ET_Pt, mm/day)				Actual evapotranspiration (mm/day)	Difference from actual evapotranspiration (mm/day)			
		ET_Pt1	ET_Pt2	ET_Pt3	ET_Pt4		ET_Pt1	ET_Pt2	ET_Pt3	ET_Pt4
1	Hoa Binh Meteorology	5.6	8.1	9.0	7.7	9.6	-4.0	-1.5	-0.6	-1.9
2	Mai Chau Meteorology	5.4	7.8	8.7	7.4	5.7	-0.3	2.1	3.0	1.7
3	Kim Boi Meteorology	5.6	8.0	8.9	7.6	7	-1.4	1.0	1.9	0.6
4	Chi Ne Meteorology	6.1	8.8	9.7	8.3	7.8	-1.7	1.0	1.9	0.5
5	Lac Son Meteorology	5.3	7.6	8.5	7.2	4.6	0.7	3.0	3.9	2.6
6	Hoa Binh Hydrological	5.7	8.2	9.1	7.7	9.5	-3.8	-1.3	-0.4	-1.8
7	Hung Thi Hydrological	6.0	8.6	9.6	8.1	8	-2.0	0.6	1.6	0.1
8	Lam Son Hydrological	6.2	8.9	9.9	8.4	9.2	-3.0	-0.3	0.7	-0.8
Mean		5.7	8.3	9.2	7.8	7.7	-2.0	0.6	1.5	0.1
Mean square error							2.7	1.7	2.2	1.6

Note: ET_Pt1 case: $a = 0.61, b = 0.12$, ET_Pt2 case: $a = 0.9, b = 0$, ET_Pt3 case: $a = 1, b = 0$, ET_Pt4 case: $a = 0.85, b = 0$

The correlation coefficient between the actual evapotranspiration and the water evaporation calculated by the Priestley-Taylor (1972) method is shown in Figure 4. The calculated results show the value of water evaporation according to the Priestley-Taylor method has a relatively low correlation with actual evapotranspiration, the coefficient of determination R^2 ranges from 0.385 to

0.408 in all 4 cases. But the mean square error between the actual evapotranspiration and the evapotranspiration in the case of ET_Pt4 is 1.6 mm and the average evapotranspiration value at the stations differs barely from the direct measurement results. Therefore, the Priestley-Taylor method with coefficients $a = 0.85$ and $b = 0$ can be used to calculate evapotranspiration for Hoa Binh area.

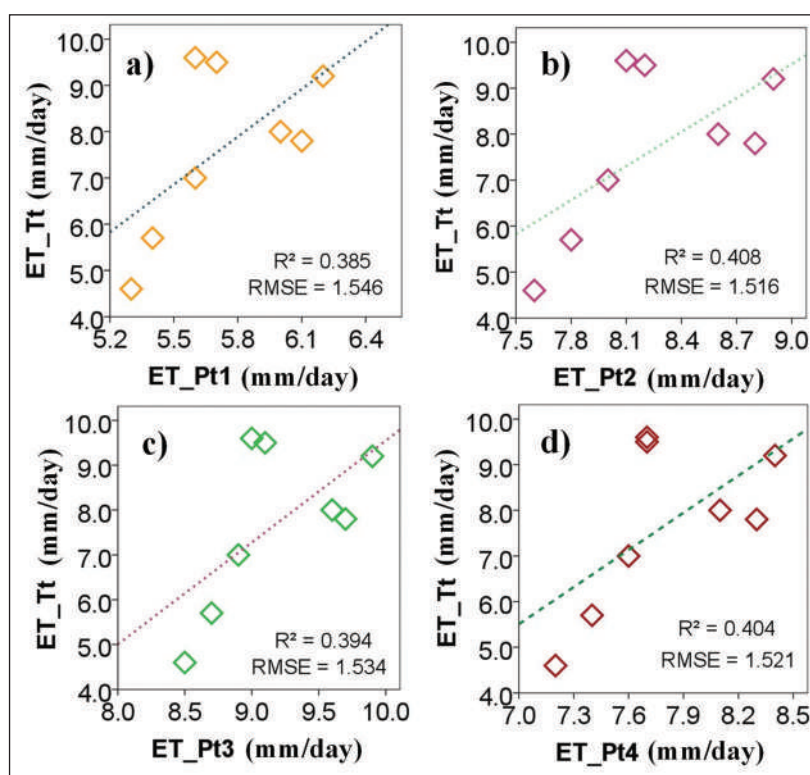


Figure 4. The correlation between actual evapotranspiration (ET_{Tt}) and evapotranspiration calculated by Priestley-Taylor method (ET_{Pt}) with a) ET_{Pt1} case: $a = 0.61$, $b = 0.12$, b) field ET_{Pt2} case: $a = 0.9$, $b = 0$, c) ET_{Pt3} case: $a = 1$, $b = 0$, d) ET_{Pt4} case: $a = 0.85$, $b = 0$ on 04/06/2017

3.1.4. Hargreaves Samani (1982) method of evapotranspiration calculating results

Applying formula (4) to calculate the evapotranspiration value according to the Hargreaves Samani (1982) method, the calculation results are shown in Table 5. The results show the difference in evapotranspiration from calculated data compared with the results of direct observation at meteorological stations has a relatively large variation of unequal values from 0.4 mm to 8.1 mm and an average of 3.6 mm. The calculation value at the time of June 4, 2017 shows that the lowest evapotranspiration at Hoa Binh meteorological station is 10.0 mm, the amount of evapotranspiration at Hoa Binh meteorological station is 10.0 mm. The highest

water vapor at Mai Chau meteorological station is 13.8 mm. The average amount of evapotranspiration at the stations is 11.3 mm. The mean square error between the actual measurement and the Hargreaves Samani method (1982, 1985) is 5.0 mm.

The correlation coefficient between the calculated values of actual evapotranspiration and the value calculated by the Hargreaves Samani (1982, 1985) method is shown in Figure 5. The evapotranspiration according to the Hargreaves Samani method is highly correlated with the actual evapotranspiration. However, the RMSE accuracy is up to 1.110. Thus, the method of calculating evapotranspiration by Hargreaves Samani is not the optimal method for calculating ET in Hoa Binh area.

Table 5. Calculation results of evapotranspiration and evapotranspiration values according to the Hargreaves Samani (1982, 1985) method

No.	Station	The amount of evapotranspiration according to the Abtew method (ET_Hs, mm/day)	Actual evapotranspiration (mm/day)	Difference from actual evapotranspiration (mm/ day)
1	Hoa Binh Meteorology	10.0	9.6	0.4
2	Mai Chau Meteorology	13.8	5.7	8.1
3	Kim Boi Meteorology	12.9	7.0	5.9
4	Chi Ne Meteorology	10.5	7.8	2.7
5	Lac Son Meteorology	12.3	4.6	7.7
6	Hoa Binh Hydrological	10.1	9.5	0.6
7	Hung Thi Hydrological	10.4	8.0	2.4
8	Lam Son Hydrological	10.4	9.2	1.2
Mean		11.3	7.7	3.6
Mean square error				5.0

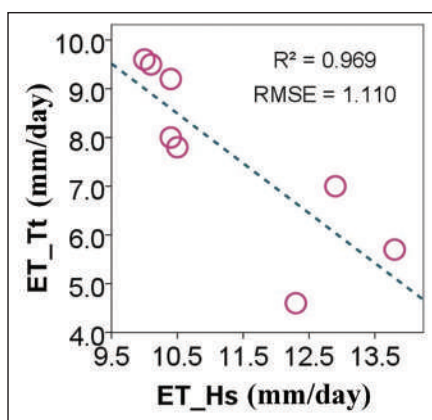


Figure 5. The correlation between actual evapotranspiration (ET_Act) and evapotranspiration calculated by Hargreaves Samani method (ET_Hs) on 04/06/2017

3.2. Comparison of evapotranspiration calculation results from different methods

Figure 6 illustrated that the lowest mean evapotranspiration calculated by the Abtew (1996) method is 5.8 mm, the highest mean evapotranspiration calculated by the Hargreaves Samani method (1982, 1985) is 11.3 mm, the difference from the average evapotranspiration from direct measurement is -1.9 mm and 3.6 mm, respectively. Evaporation at the monitoring stations according to the Priestley-Taylor method (1972) in the case of ET_Pt4 and the Makkink (1957) method in the case of ET_Mk2 with the evapotranspiration close to the directly

measured at meteorological observation stations.

The mean deviation between evapotranspiration according to Abtew method, Hargreaves Samani method and actual evapotranspiration is -1,913 mm and 3,625 mm, respectively, with an error of 24.7% and 46.7%, respectively. Thus, the above two methods should not be used to calculate evapotranspiration in Hoa Binh area. The average deviation of evapotranspiration calculated by Priestley-Taylor method with coefficient $a = 0.85$, $b = 0$ is 0.125, corresponding to the lowest error of 1.3%. Although the evapotranspiration according to this method, has quite low

correlation ($R = 0.635$), but the Priestley-Taylor method ensures the reliability to calculate ETO in Hoa Binh province. Besides, the calculation of evapotranspiration by Makkink (1957) method with the coefficient $a = 0.9$, $b = 0$ has an average difference of 0.4 mm, corresponding to an error of 5.2%. In addition, using the Paired-Sample T-Test for the corresponding pairs of values between the actual evapotranspiration and the

evapotranspiration calculated by the methods (Table 6) shows that the evapotranspiration value of Makkink method has the highest correlation ($R = 0.984$) and the lowest error ($SE = 0.448$) with actual evapotranspiration. The value $\rho = 0.416 > 0.05$ with 95% confidence shows that there is no mean difference between actual evapotranspiration and evapotranspiration value of the Makkink method.

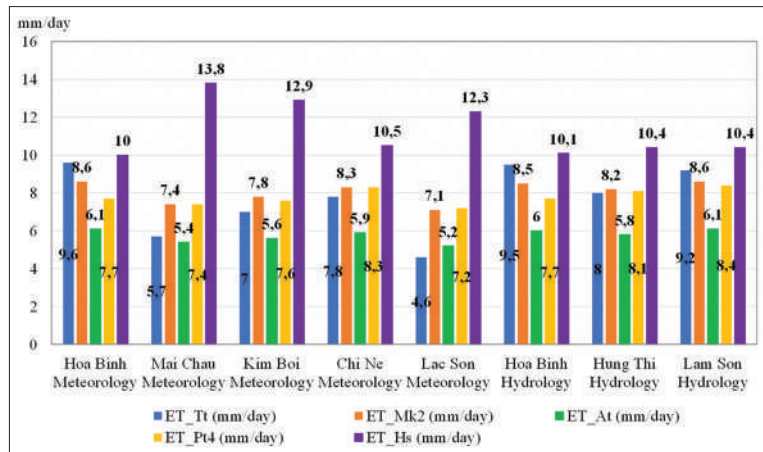


Figure 6. Comparison of evapotranspiration between methods

Note: ET_Mk2: Evaporation by Makkink (1957) method); ET_At: Absorption of water by Abtew (1996); ET_Pt4 Evaporation by Priestley-Taylor method (1972); ET_Hs Hargreaves Samani Evaporation (1982, 1985); ET_Atc Actual evapotranspiration measured

Table 6. Pearson correlation coefficient ($N = 8$) analysis of mean difference between actual evapotranspiration and methods

	M	R	SE	ρ
ET_Mk2 (mm/day)	0,388	0,984	0,448	0,416
ET_At (mm/ day)	-1,913	0,982	0,53	0,009
ET_Pt4 (mm/ day)	0,125	0,635	0,561	0,83
ET_Hs (mm/ day)	3,625	-0,826	1,115	0,014

Note: R (Correlation): pearson correlation, M (mean): mean, SE: Standard Error, value ρ

4. Conclusion

Research results have determined the amount of evaporation by four methods Makkink (1957), Abtew (1996), Priestley & Taylor (1972), Hargreaves & Samani (1982, 1985) from meteorological data on 04/06/2017. The average evapotranspiration according to the Makkink, Abtew, Priestley-Taylor and Hargreaves-Samani methods are 8.1 mm, 5.8 mm, 7.8 mm and 11.3 mm, respectively. Actual evapotranspiration and evapotranspiration according to Makkink,

Abtew, Priestley-Taylor and Hargreaves-Samani methods have correlation and error of $R^2 = 0.969$ with error $RMSE = 0.346$, $R^2 = 0.964$ with error $RMSE = 0.372$, $R^2 = 0.408$ with error $RMSE = 1.516$ and $R^2 = 0.969$ with error $RMSE = 1.110$, respectively. Accordingly, the actual evapotranspiration is highly correlated with the ET calculated by the Makkink, Abtew and Hargreaves-Samani methods. However, the T-Test shows that the evapotranspiration according to the Makkink method has the highest correlation and the

lowest error with the actual evapotranspiration ($R = 0.984$ and $SE = 0.448$).

The Priestley-Taylor method gives the results of the mean deviation and the smallest mean, the evapotranspiration calculated by Priestley-Taylor is the closest to the directly measured evapotranspiration at the meteorological stations. Thus, when calculating evapotranspiration using solar radiation in Hoa Binh province, simple

methods such as Abtew (1996) and Hargreaves Samani method (1982, 1985) should not be used. It is highly recommended to use Priestley-Taylor (1972) method with coefficients $a = 0.85$, $b = 0$ and Makkink (1957) method with coefficients $a = 0.9$, $b = 0$ to calculate evapotranspiration at Hoa Binh due to the result is the closest approximation to the direct evapotranspiration measurement.

References

1. Claude E. BoyD (1987), "Evapotranspiration/Evaporation (E/E_o) ratios for aquatic plants", *Journal of Aquatic Plant Management*, 25:1-3.
2. Kosugi, Y. and M. Katsuyama (2007), "Evapotranspiration over a Japanese cypress forest. 2. Comparison of the eddy covariance and water budget methods", *Journal of Hydrology*, 334, 305-311.
3. Burnash, R. J. C. (1995), *The NWS River forecast system- catchment modeling*. In V. P. Singh (Ed.), *Computer Models of Watershed Hydrology*, 311-366.
4. Landeras, G., A. Ortiz-Barredo and J.J. Lopez (2008), "Comparison of artificial neural network models and empirical and semi-empirical equations for daily reference evapotranspiration estimation in the basque country Northern Spain", *Agric. Water Manage*, 95, 553-565.
5. Trajkovic, S. (2005), "Temperature-based approaches for estimating reference evapotranspiration", *Journal of Irrigation and Drainage Engineering*, 131, 316-323.
6. IPCC (2007), Summary for Policymakers. In M. L. Parry, O. F. Canziani, J. P. Palutikof, P. J. van der Linden, & C. E. Hanson (Eds.), *Climate Change 2007: Impacts, Adaptation and Vulnerability, Contribution of Working Group II to the Fourth Assessment Report of the Intergovernmental Panel on Climate Change*, Cambridge University Press, Cambridge, UK.
7. France, J. and J. Thornley. (1984), *Mathematical Models in Agriculture*, Butterworths, London, ISBN: 10: 085199010X.
8. Penman, H.L. (1948), *Natural evaporation from open water, bare soil, and grass*, *Proceedings of the Royal Society of London. Series A, Mathematical and Physical Sciences*, 193(1032), 120-145.
9. Jensen, M.E., R.D. Burman and R.G. Allen. (1990), *Evapotranspiration and irrigation water requirements*, ASCE Manuals and Reports on Engineering Practice No. 70, New York, 332, ASCE: ISBN: 0872627632.
10. Blaney, H.F. and Criddle, W.D. (1950), *Determining water requirements in irrigated areas from climatological and irrigation data*, USDA Soil Conservation Service Tech, 48.
11. Hargreaves, G. H. and Samani, Z. A. (1985), *Reference crop evapotranspiration from temperature*, *Applied Engineering in Agriculture*, 1(2), 96-99.
12. Thornthwaite, C. W. (1948), "An approach toward a rational classification of climate", *Geographical Review*, 38, 55-94.
13. Van Bavel, C.H.M. (1966), "Potential evaporation: the combination concept and its experimental verification", *Water Resour. Res*, 2, 455-467.
14. Hoa Binh statistics office (2019), *Hoa Binh statistical yearbook 2018*, Statistical publishing house, Ha Noi.
15. Makkink GF. (1957), "Testing the Penman formula by means of lysimeters", *Journal of the Institution of Water Engineers*, 11: 277-288.
16. Abtew, W. (1996), "Evapotranspiration Measurements and Modeling for Three Wetland Systems in South Florida", *Journal of the American Water Resources Association*, 32 (3), 465-473.
17. Priestley CHB, Taylor RJ. (1972), *On the assessment of surface heat fluxes and evaporation using large-scale parameters*, *Monthly Weather Review*.

RADAR EXTRAPOLATION IN VERY SHORT-RANGE RAINFALL FORECASTING IN HO CHI MINH CITY

Truong Ba Kien⁽¹⁾, Tran Duy Thuc⁽¹⁾, Nguyen Quang Trung⁽¹⁾,
Nguyen Binh Phong⁽²⁾, Vu Van Thang⁽¹⁾

⁽¹⁾Viet Nam Institute of Meteorology Hydrology and Climate Change

⁽²⁾Ha Noi University of Natural Resources & Environment

Received: 29 July 2021; Accepted: 18 August 2021

Abstract: This article presents the study results of TITAN and SWIRLS tools for extrapolating radar data to forecast rainfall (1 - 6 hours) in Ho Chi Minh City region. The SWIRLS and TITAN are optional tools to extrapolate radar data. The validation results implemented by comparing with GSMAP data (gridded rainfall data) and observation measured at 219 stations at Southern Viet Nam (SVN). The study results show that TITAN and SWIRLS tools can forecast well the place, direction and speed of rain as well as place of thunderstorm. Especially, the error index calculations showed the better results in SWIRLS than TITAN. However, the better moving trend forecast in the case of Typhoon Usagi is found by TITAN than by SWIRLS.

Keywords: Short-range rainfall forecast, TITAN, SWIRLS, Extrapolation, WRF.

1. Introduction

In Ho Chi Minh City (HCMC), heavy rain is the major phenomena causing the most serious consequences. Heavy rainfall in HCMC has a highly unexpected characteristic, occasional with violent rain (huge amount in a very short time), particularly when combined with high tide to cause local flooding. In recent years, the increase rate of frequency and intensity of un-normal heavy rainfall events are found year by year. Therefore, it is essential to carry out research on improving in extreme heavy rainfall forecasts in HCMC. Currently, the short-range forecast of heavy rainfall in HCMC is still facing many limitations: The use and exploitation of products from weather radar are mainly based on current and past radio-response images to make subjective forecasts for the future; the limitations of numerical models in short-term heavy rainfall forecasting (initial conditions, physics parameterizations...); limited experience in data assimilation,

monitoring data quality; limited facilities (HPC system, software etc.).

In recent years, radar has been being an important equipment in real-time monitoring and forecasting dangerous weather phenomena such as thunderstorms, storms and heavy rain, etc. The advantage of radar is found by providing a large amount of data from surface to altitude levels with a very high spatial and temporal resolution. Currently, there are many methods that suggested in extrapolating radar data for extreme short-term heavy rainfall forecast (1 - 6 hours) over in the world. SWIRLS originally focuses on thunderstorms and forecasting the storm's path, and the system is still being developed and used very effective [1]. The Japan Meteorological Agency (JMA) has been using radar data in extrapolating extreme rainfall short-range forecasts. In the term of the extrapolation process, the development and weakening of the rain system due to the impacts of terrain are also considered. The results show that extrapolated forecasting is more skilled than numerical modeling, but it decreases skills faster over time, so to be more optimal, they apply a combination method between the

Corresponding author: Vu Van Thang
E-mail: vvtang26@gmail.com

extrapolated results of the radar and the numerical model [9]. In Vietnam, there have not been many studies on extrapolating radar data, most recently there has been a study by Cong Thanh and his colleagues who applied Titan software to identify, track, and analyze instantly for thunderstorms in HCMC region. This study has compared the maximum response of CMAX from extrapolation with reality; but has not compared the quantitative rain results of extrapolation and observation [3]. In general, there are many limitations in using tools for extrapolating radar data to improve issues of heavy rainfall in Vietnam. In addition, applications in optimizing results and adjusting tools for a very small region in Vietnam are still very complex and long-term issues, requiring more in-depth studies. Therefore, the purpose of this study is to investigate in applying TITAN and SWIRLS tools to improve short-range rainfall forecast in HCMC based on extrapolating radar data.

1.1. The short-range warning of intense rainstorm in localized systems

SWIRLS (Short-range Warning of Intense Rainstorm in Localized Systems) is an instantaneous precipitation forecasting system developed by the Hong Kong Observatory (HKO) since 1997. The SWIRLS prototype was put to the test during the rainy season in 1998. This test is considered an initial success for the quantitative forecast of rainfall in a few hours. After some minor modifications based on user logs, the SWIRLS system was officially operated in April 1999. Advanced techniques are deployed in SWIRLS to analyze and predict precipitation and convective weather phenomena over the next few hours. SWIRLS is also deployed in various meteorological services or participates in international forecasting projects to support research and development of rainstorm broadcast techniques. The community version of SWIRLS, or com-SWIRLS, was developed to facilitate knowledge exchange and collaborative development of rain broadcast techniques [2]. The main development goal in SWIRLS is to use both radar and rain

gauge data to monitor and predict trends in local precipitation distribution over a few hours. The reanalyzed dataset, based on time-adjusted reflectance precipitation relationships, has proven to be extremely useful in providing real-time precipitation information to forecasters as well. as providing information for the physical process in weather forecasting [1]. Some basic features of SWIRLS are: Quantitative precipitation estimation (QPE) based on radar data, rain gauge or a combination of both; Monitoring storm movements; Extrapolating data using semi-Lagrangian diagram up to 6 - 9 h ahead.

1.2. Thunderstorm Identification, Tracking, Analysis and Nowcasting (TITAN)

TITAN (Thunderstorm Identification, Tracking, Analysis and Nowcasting) is a software that can identify, track, analyze and forecast extremely short thunderstorms and rain from weather radar data, built-in 1990 by M. Dixon and G. Wiener. Model TITAN is constantly developed and perfected by many researchers from NCAR and UCAR (USA) From 1990 - 1992 TITAN was tested on the prototype NEXRAD radar in Denver, Colorado [4]. TITAN uses random methods based on mass tomography data of the thunderstorm and weighted linear extrapolation from the historical dataset to determine the growth of the thunderstorm in the next hours [3]. TITAN can identify, monitor, analyze and forecast extremely short thunderstorms and rain from weather radar data, with main features: Operating in two modes: real-time and historical; Extrapolating of radar data, time step up to 10 minutes; Supporting extrapolation of radar data 10, 20, 30, 40, 50, 60 minutes; Supporting 1, 3, 6, 12, 24 hours cumulative rain forecast; Running multiple radars at the same time; Supporting to export a variety of output formats (xml, mdv, ASCII); and supporting input data quality check.

TITAN software uses a semi-Lagrangian extrapolation diagram with basic functions: Using interpolation of neighboring points to determine cloud drives based on radar

response, and at the same time analyzing basic properties of the cloud do the top condition; Forecasting the displacement of the cloud drive based on linear extrapolation. Based on the predictive information of the responsiveness of the cloud drive, the size of the cloud drive can predict the water content, rainfall intensity and total rainfall accumulated over time by the relationship between the responsiveness Z and the amount of rain R (ZR relationship).

2. Methodology and data

2.1. Radar extrapolation algorithm

Step 1: Determine the TREC vector field: Extremely short-term forecasting is based on radar data with a high update time (5 - 10 minutes) to identify areas of deep convection and clouds with a high probability of precipitation and to estimate displacement (using consecutive data over time using the maximum correlation method for the TREC responsiveness - Tracking Radar Echoes by Correlation) (Figure 1).

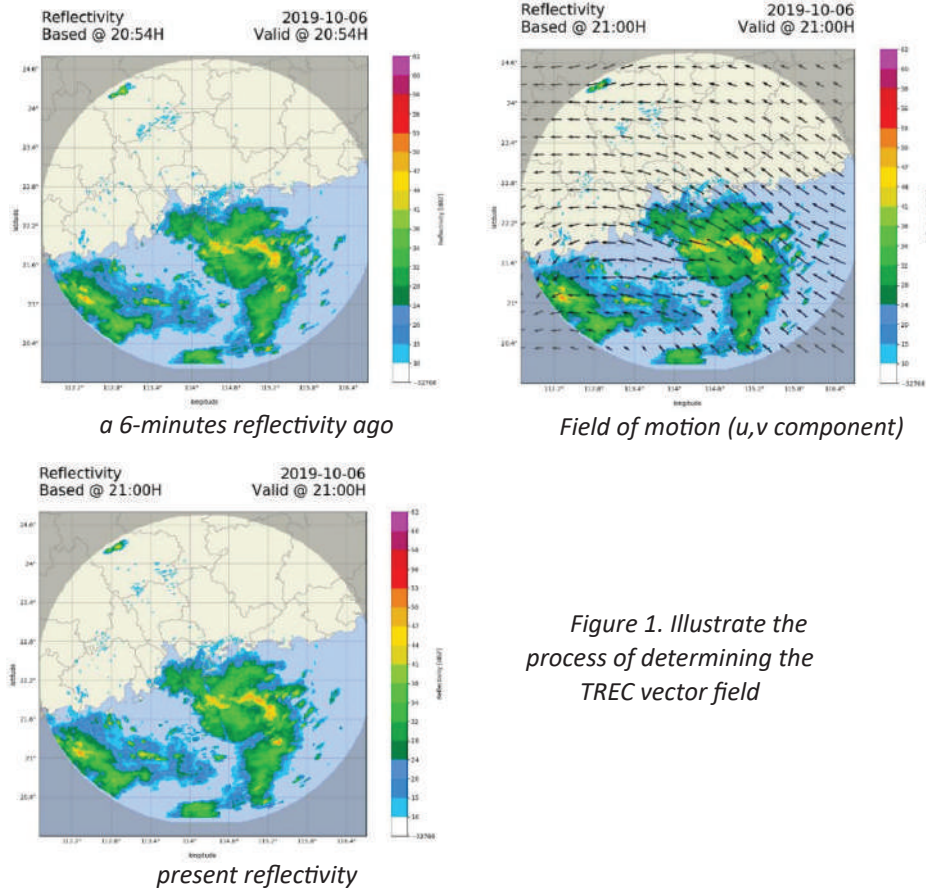


Figure 1. Illustrate the process of determining the TREC vector field

Step 2: Handling deviation vectors: The vector field is then filtered, and the deviation vectors are replaced with the mean of the surrounding vectors.

Step 3: Extrapolation of radar data: After building the direction field and the

displacement speed of the convective drives capability of causing rain, thunderstorms will apply the Lagrangian method to extrapolate the satellite response or radiation over time to determine the region short term effects (Figure 2).

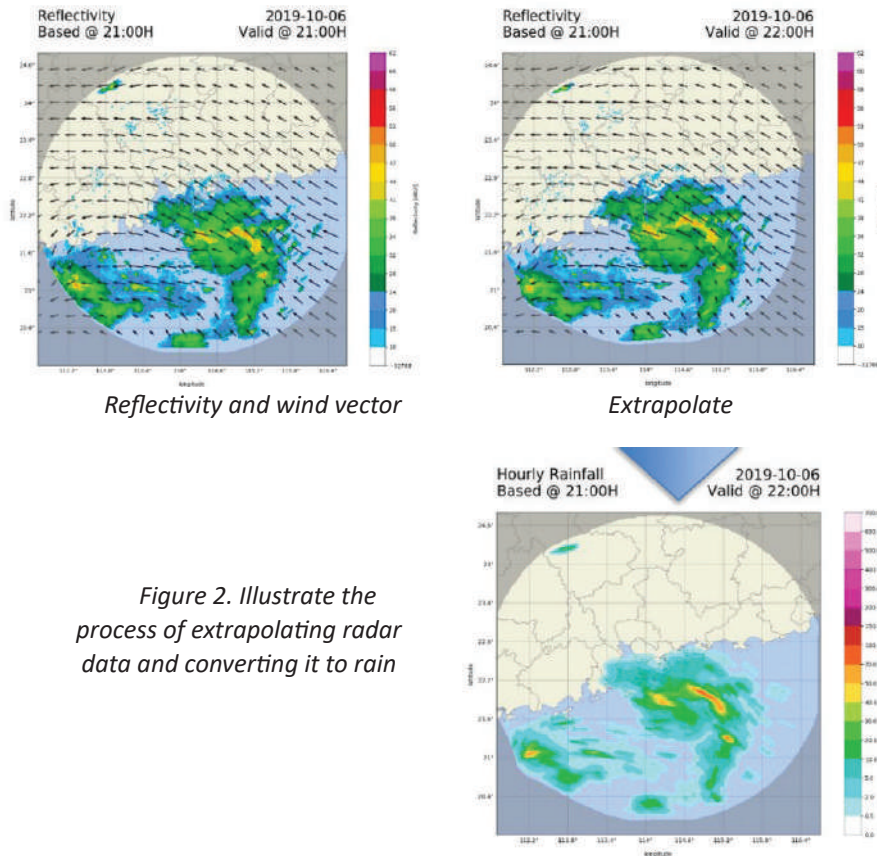


Figure 2. Illustrate the process of extrapolating radar data and converting it to rain

Step 4: Converting reflectivity to rainfall: In the SWIRLS software, the Z-R relationship is adjusted in real-time. This is done by comparing every 5 minutes the reflectivity of the radar with the rainfall at the monitoring station. However, it can also be determined by fixed formulas. After obtaining the radar response monitoring, using the experimental relationship based on the observed response from radar and the rain speed of Marshall-Palmer, we can estimate the rain intensity R (mm/h) from the radio response of the radar target Z (mm^6/m^3) is as follows: $Z = ARB$ where A , B are experimental parameters, typical values are $A = 200$ and $B = 1.6$. Using the relationship between $Z' = 10 \lg Z$ and Z' (dBZ) as the radar response, we have the equation for the rainfall intensity estimate as follows: $R = C10DZ$. The above relationship is usually found with high reliability, a sample set of response and rain data observed over many months or years is needed. In this topic, we have used the formula that proposed by Nguyen Huong Dien

[7]. This formula has been studied with good error for the Southern Vietnam region.

2.2. Handling radar data

In this study, the Nha Be radar ($10^{\circ}39'31''$ N; $106^{\circ}43'42''$ E) data were used with some main technical parameters such as operating frequency: 5500 - 5700 MHz (C wave); antenna blade width: $\leq 1.0^{\circ}$; monitoring radius: 30, 60, 120, 240, 480 m; doppler wind observation radius: 30, 60, 120 km. This radar device has been effective in tracking and monitoring weather phenomena within a radius of about 480 km; warn and forecast dangerous weather phenomena such as storms, tropical depressions, thunderstorms, etc. within a radius of about 240 km; and the phenomenon of rain, heavy rain, etc. within a radius of about 120 km around Ho Chi Minh City. It should also be noted that for Nha Be Radar with a scanning radius greater than 120 km, radial wind speed data should not be used for assimilation because at this time the radial wind will not be good. As mentioned

above, the problem of processing radar data before entering assimilation is one of the important steps, it directly affects the results of 3dvar simulation even if there is too much poor data. It can corrupt the analysis from 3dvar, there are many methods studied to get the best data before it is included in the model.

Regarding quality control, many studies have compared the results of no quality control (QC)

and with QC, the results show that no QC can cause 3dvar to fail to converge or create an analytic field, but bad data propagates to regions other good data and as a result, the original analysis field may deteriorate [8].

For the raw data of Nha Be, there will usually be ground clutter, sea clutter, side beam effects and wind field overlapping noise, therefore, quality testing is necessary [Figure 3].

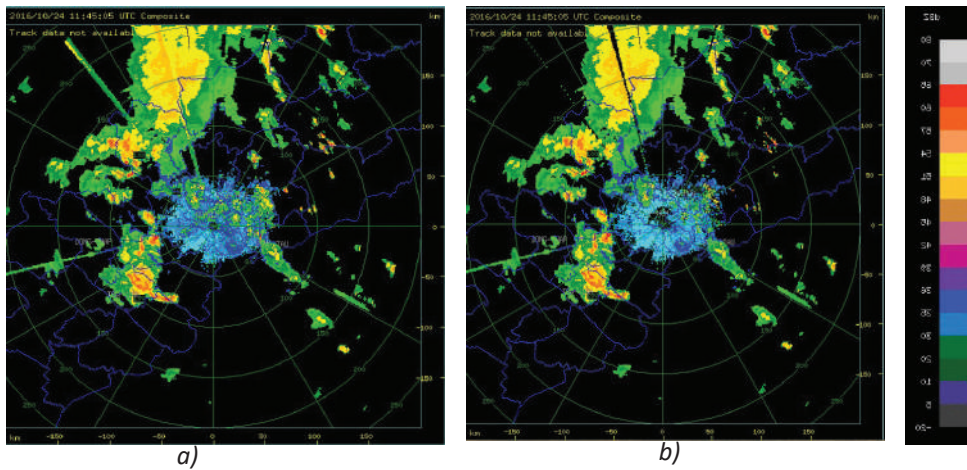


Figure 3. The illustration of non-quality control and quality control for radar data

2.3. Experiment design

To perform the forecast for the next 6 hours, we use 6 radar data files every 10 minutes (for SWIRLS) and all previous 1 - 3 h radar files (for TITAN). Radar data, before being extrapolated, will go through a quality control step before being added to the extrapolation program (TITAN or SWIRLS). The software will automatically extrapolate the response and then convert

it to the corresponding rainfall (Figure 4). In operation the program is run continuously once every hour, providing forecasts and warnings when there is a risk of heavy rain (Figure 5). In this paper, the extrapolation was continuously operated in the cycle from 10:00 am on November 24, 2018 to 9:00 pm on the same day, each extrapolating 1 hour apart and forecasting for the next 6 hours.

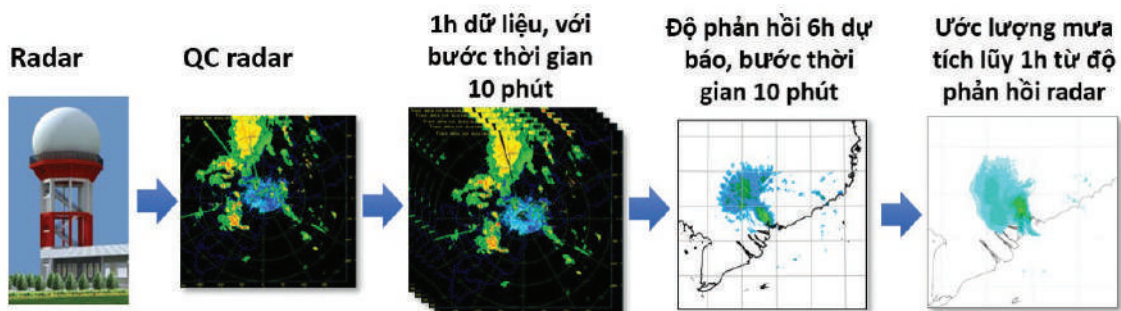


Figure 4. Process of extrapolating radar data

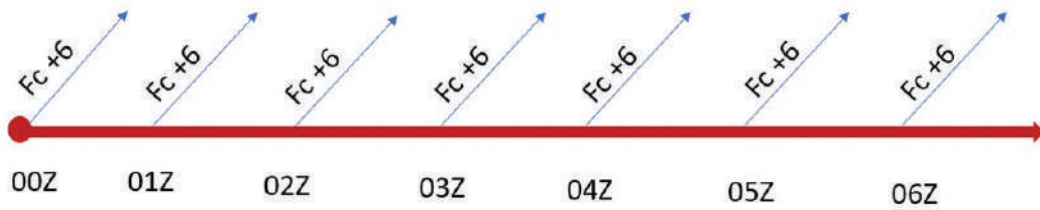


Figure 5. Extrapolation of radar data in real time mode

Data: Monitoring data for simulation evaluation includes rain data of 219 stations around HCMC (Figure 6); Radar data is taken from Nha Be Radar including feedback and radial wind taken every 10 minutes on November 25, 2018; the radar scans 5 - 8

elevation angles and a radius of 120 km during this time.

Evaluation method on station: Using 3 statistical indicators: mean absolute error (MAE), root mean squared error (RMSE) and relative error (RE).

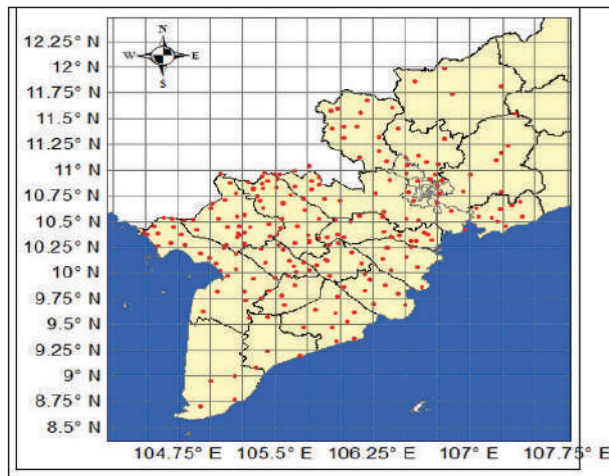


Figure 6. Location of observation stations (red dot)

$$MAE = \frac{1}{n} \sum_{I=1}^n |FI - OI| ; \quad RMSE = \sqrt{\frac{1}{n} \sum_{I=1}^n (FI - OI)^2}$$

FI is the forecast value, OI is the observed value, N is the sample volume

3. Results

3.1. Extrapolation results of radar data

In this section, the simulation results is presented on the grid of SWIRLS, TITAN and compare with the data from GSMAP for the period from 11 - 14 UTC on November 24, 2018.

Figure 7 is the result of extrapolated rainfall accumulated hourly (shaded figure), output from TITAN software, in which the red contour lines are TITAN's forecast for each thunderstorm and the trend of movement and development them in the following hours. Comparing this

result with the actual results from GSMAP data (Figure 9) shows that the TITAN software can capture relatively well the location of heavy rain areas and the movement trend of the USAGI storm (which is gradually entering Ho Chi Minh City). In the period from 11 to 14 UTC on November 24, 2018 this storm tends to move closer to the mainland, making the rainfall in HCMC area increase, the number of thunderstorms in this area also increases and develops more strongly. TITAN software has captured this trend quite well. However, closely monitoring the rain images (after being converted from reflectivity) can see a clear

demarcation within the radius from 100 km onwards from the center of the radar (this does not seem to be reasonable because the rain area must be seamless). In terms of quantitative forecast results, it can be seen that TITAN gives a much higher rainfall than GSMAP. (Although GSMAP is only a reference channel in terms of area, rainfall from this observation is still not good in many cases).

Figure 8 is the extrapolated result from SWIRLS software. About the tendency of rain to

grow stronger, it seems that this software can only catch it in the first 1 hour (at 11 UTC). In the next hours (13 - 14 UTC) rainfall in HCMC area does not increase but even decreases. The software also fails to capture the USAGI storm's tendency to move closer to land. It seems that because SWIRLS only uses simple linear extrapolation, it does not capture as well as TITAN. In terms of rainfall, SWIRLS gives a better forecast of rainfall than TITAN (when compared to GSMAP).

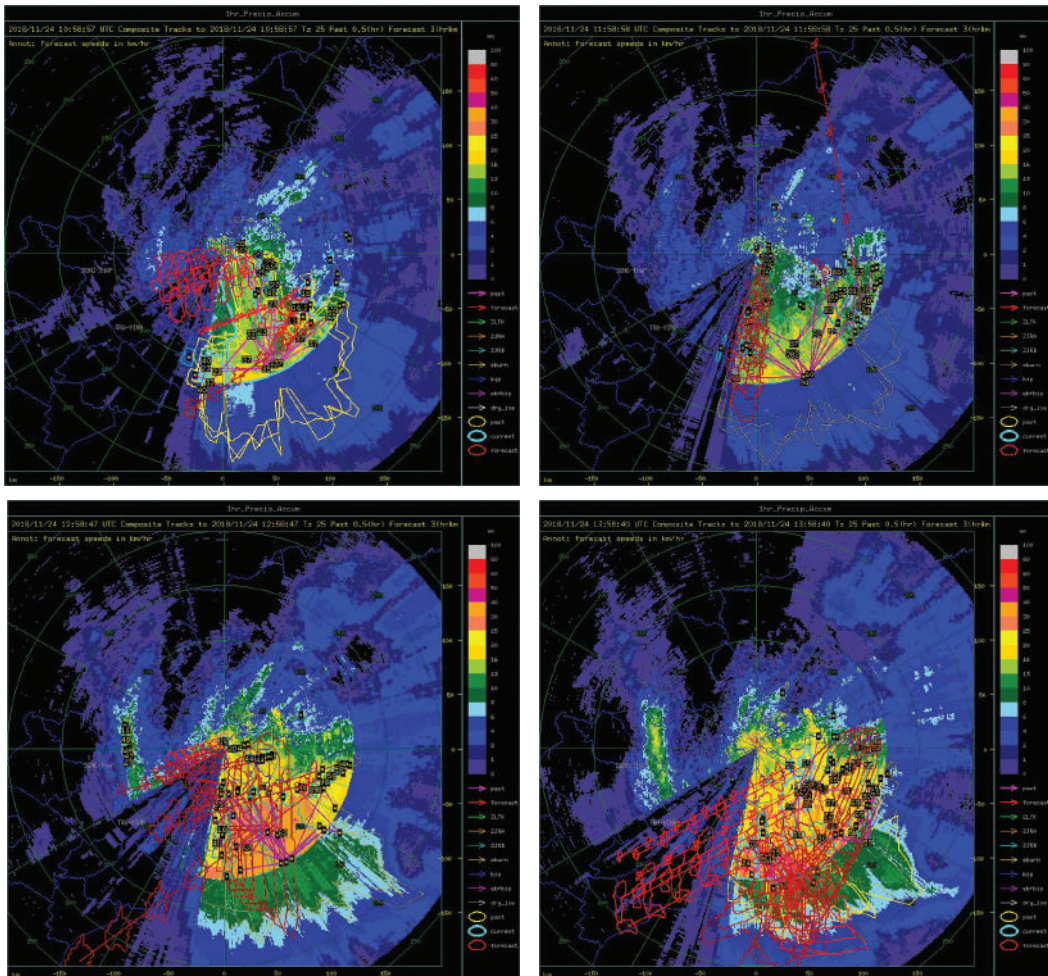


Figure 7. 1 hour cumulative rainfall extrapolated from TITAN software from 11 - 14 UTC on November 24, 2018

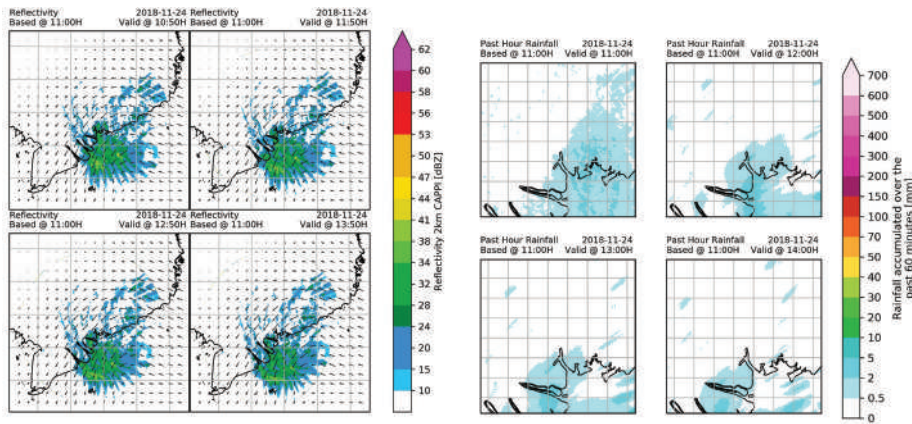


Figure 8. Responsiveness (left) and cumulative precipitation (right) extrapolated from SWIRLS software from 11 - 14 UTC on November 11, 2018

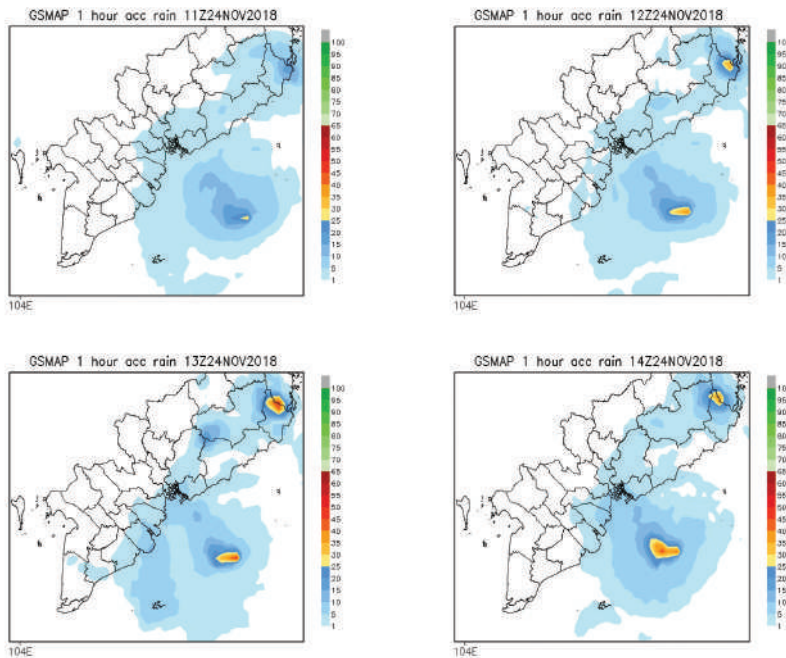


Figure 9. GSMAP data from 11 - 14 UTC on November 24, 2018

3.2. Assess error

The error assessment is based on monitoring data from 219 stations in the Southern region and extrapolated rain data extracted to the corresponding station points for panels from 10 UTC to 21 UTC on November 24, 2018.

Figure 10 is the result of MAE error assessment for each forecast from 10 UTC to 21 UTC on November 24, 2018 with 4 different forecast periods: 1 h - Figure 10a; 2 h - Figure 10b; 3 h - Figure 10c and 6 h - Figure 10d. With the 1h forecast period, the error of MAE of SWIRLS is

quite small at about 0.2 - 0.9, of TITAN is 1 - 4.9. With the 2 h forecast period, the error of MAE of SWIRLS is 0.4 - 1.8, TITAN is 2.5 - 7.3. At the 6 h forecast period, the error of SWIRLS is from 1.1 to 7.8 but that of TITAN is very large from 8.8 to 14.3. Thus, when the forecast period increases, the errors of both software show that the errors also increase gradually (this is quite reasonable compared to previous studies). In general, the results show that the error of SWIRLS is much smaller than that of TITAN at all 4 forecast periods from 1, 2, 3 and 6 hours.

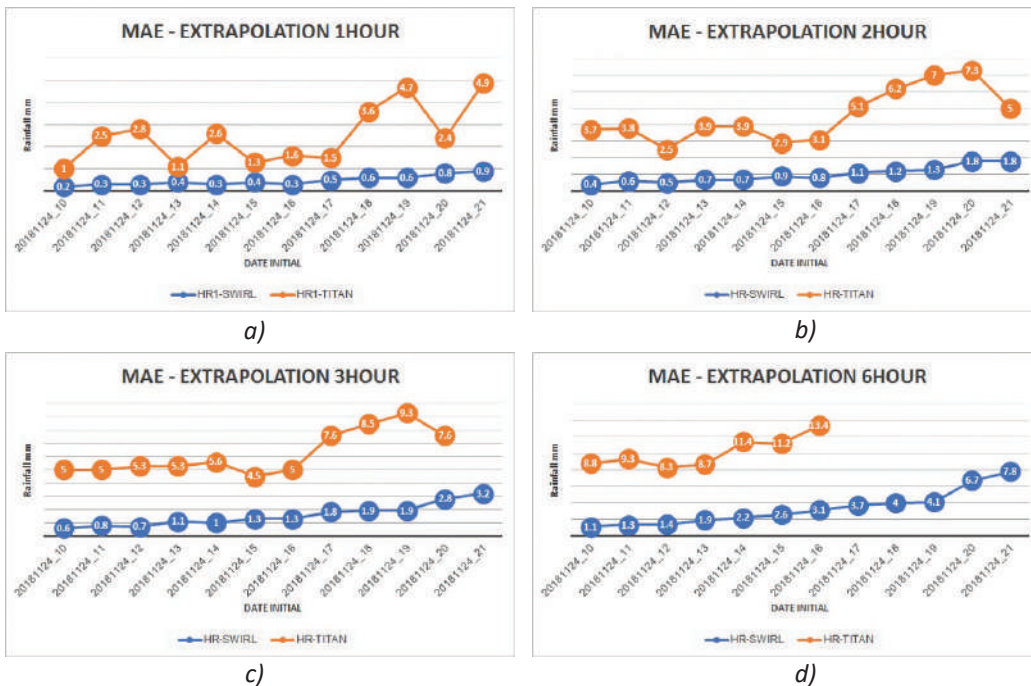


Figure 10. Results of error assessment, comparison between TITAN and SWIRLS

4. Conclusion

This article has studied the application of two software TITAN and SWIRLS to extrapolate radar data for Ho Chi Minh City on November 24, 2018 to provide initial comparisons between these two types of software. The results show that, in terms of area, TITAN software seems to be a better predictor of SWIRL when compared to GSMAP (following the maps Figure 7 - 8 for the forecast period from 1 - 6 h). However, in terms of rainfall, especially when comparing and evaluating the MAE error with 219 stations in the Southern region, the SWIRLS software gives a significantly smaller error.

The study also shows that the error of each compared to actual observations.

Acknowledgment: This research is part of the National Scientific Research Project, code KC.08.14/16-20 "Research on building a professional system to forecast rainfall in the Southern region and warn of the extremely short-term heavy rain for Ho Chi Minh City".

References

1. M.C. Wong, W.K. Wong, & S.T. Lai (2006), *From SWIRLS to RAPIDS: Nowcast Applications Development in Hong Kong*.
2. http://www.typhooncommittee.org/docs/roving_seminar/2019/2019-A1.pdf

3. Cong Thanh, Vo Thi Nguyen, Tran Duy Thuc (2018), *Application of Titan software to identify, track, and analyze thunderstorms immediately for the Ho Chi Minh City*.
4. <https://slideplayer.com/slide/9372394/>
5. <https://ral.ucar.edu/solutions/products/thunderstorm-identification-tracking-analysis-and-nowcasting-titan>
6. "Statistical-interpolation analysis system". *Mon. Wea. Rev.*, 120, 1747-1763.
7. Nguyen Huong Dien, (2015), "The experimental formula for calculating rain intensity from radar response for the Southeast region". *VNU Journal of Science: Natural Sciences and Technology*, Vol 31, No 3S, p.66-70.
8. J. Liu, M. Bray , and D. Han (2012), *A study on WRF Radar data assimilation for hydrological rainfall prediction*.
9. http://www.jma.go.jp/jma/jma-eng/jma-center/nwp/outline2007-nwp/pdf/pdf5/outline5_4.pdf.

THE ABILITY OF RCA4 REGIONAL CLIMATE MODEL TO SIMULATE AND PROJECT SURFACE SOLAR IRRADIATION OVER VIET NAM

Vu Thanh Hang⁽¹⁾, Pham Thi Thanh Nga⁽²⁾, Doan Thi The⁽²⁾, Pham Thanh Ha⁽¹⁾,
Nguyen Thi Phuong Hao⁽³⁾, Nguyen Tien Cong⁽³⁾

⁽¹⁾Ha Noi University of Science

⁽²⁾Viet Nam Institute of Meteorology, Hydrology and Climate change

⁽³⁾Viet Nam National Space Center, Viet Nam Academy of Science and Technology

Received: 09 August 2021; Accepted: 30 August 2021

Abstract: Currently, the application of numerical models in simulating, forecasting, and predicting meteorological factors and features of the atmosphere, including solar radiation combined using satellite data, is widely used. Therefore, comparing the difference between the parameters calculated from the model with the satellite is extremely necessary, thereby evaluating the quality of the model as well as the quality of the satellite products compared to the value of the satellite with monitoring or re-analysis, is the basis for making accurate forecasts/forecasts in the future.

This study aims to assess the regional climate model RCA4 (RCP4.5 and RCP8.5) to simulate surface solar irradiation (SSI) based on estimated radiation data from the Himawari-8 satellite for Viet Nam using statistical indicators.

The results showed that the radiation values estimated from model correlated well with estimates from the satellite, which has been validated very close to the observation at the surface. In the spring and winter, the general correlation trend shows that the radiation at the stations in the North tend to be higher than the stations in the South of Viet Nam. Based on the assessment of the RCA4 model compared to satellites in the period (2016 - 2018), the results of model are used to analyze the progress of solar radiation during the year in 7 climate zones of Viet Nam between different versions. It can be seen that the maximum/minimum values of the month do not change much between versions. Comparing to the period 1976 - 2005, the estimated short-wave radiation at the surface in the period 2020 - 2050 decreases in most of Viet Nam for both scenarios RCP4.5 and RCP8.5. In contrast, the Central Highlands region shows an increase in short-wave radiation.

Keywords: surface solar irradiation, satellite data, RCA4 regional climate model, solar radiation projection.

1. Introduction

The solar radiation reaching ground level is often called surface solar irradiation (SSI). SSI clearly affects temperature and precipitation, drives large-scale atmospheric circulation, and also plays an essential role in some other processes such as global energy balance [24, 29], oceanic heat budget [30], photosynthesis [13], solar energy production [7] and power

productivity [33], etc. SSI shows substantial spatial and temporal variability because it depends on the position of the sun and the cloud cover in the sky [18]. Observations in many regions over the globe indicate a decrease SSI from ~ 1950s to 1980s (“dimming”), followed by an increase SSI during 1990s (“brightening”) in all-sky conditions [12, 23, 32, 34]. There have been a lot of studies focusing on examining SSI using observations, re-analyses, satellite data, or climate models [4, 6, 11, 14] where it is beneficial to use numerical models in simulating

Corresponding author: Pham Thi Thanh Nga
E-mail: phamttnnga@imh.ac.vn

SSI in the past and projecting SSI in the context of climate change according to climate change scenarios.

Brazel et al. (1993) showed that General Circulation Models (GCMs) are able to simulate the annual solar cycle [3]. However, the SSI seems to be underestimated for the southwestern United States. Solar radiation budgets from 20 GCMs are analyzed in the study of Wild (2005) [31]. The results showed that the global mean radiation budgets, especially at the surface, are significantly distinct between GCMs. The models seem to overestimate the land surface isolation of about 9 Wm^{-2} on average compared to surface stations, while the biases of the net solar fluxes at the top of the atmosphere are generally smaller. In the study of Romanou et al. (2007) [20], the ensemble simulations of SSI in the 20th century are analyzed using nine state-of-the-art coupled ocean-atmosphere-land-ice circulation models. The results show that all models estimate a global annual mean decrease in downward SSI of $1 - 4 \text{ Wm}^{-2}$ while the Global temperature increases about $0.4 - 0.7^\circ\text{C}$.

Regional climate models are often used to dynamically downscale global model simulations for specific regions due to higher resolution. Some local features like topography and coastlines are more detailed by Rummukainen, (2010). Alexandri et al. (2015) [1, 21] used the RegCM4 regional climate model to simulate SSI patterns over Europe during the period of 2000 - 2009 and then evaluated against satellite-based observations from Satellite Application Facility on Climate Monitoring (CM SAF). Notably, the SSI bias between the RegCM4 and the CM SAF data depends significantly on the version used. In particular, the SSI bias for MFG (Meteosat First Generation) is +1.5%, while the SSI bias for MSG (Meteosat Second Generation) is +3.3%. Recently, in the study of Tang et al. (2018) [27], the simulations of SSI of 5 Regional Climate Models (RCM, including CCLM4, HIRHAM5, RACMO22T, RCA4, and REMO2009) and ten driving GCMs over Southern Africa are compared to ground-based measurements, satellite-derived products, and reanalyses in the period of 1990 - 2005. The results show that

SSI produced by GCMs over Southern Africa overestimates in term of their multi-model mean by about 1 Wm^{-2} in austral summer and 7.5 Wm^{-2} in austral winter when compare to that of the satellite-derived product SARAH-2. Besides, the RCMs driven by GCMs indicate underestimations of SSI in their multi-model mean in both seasons with mean bias errors of about -30 Wm^{-2} in austral summer and about -14 Wm^{-2} in winter compared to SARAH-2. The discrepancies of the simulated SSI of the RCMs are larger than those of the GCMs over Southern Africa.

Wild et al. (2015) used CMIP5 climate models to project long-term changes in SSI and their influence on energy yields of photovoltaic systems [33]. The RCP8.5 forcing scenarios of 39 GCMs have been implemented to see the decadal changes in all-and clear-sky SSI, cloud amount, and surface temperature projected up to 2050. The SSI of these models agree with the projection of the sign of the changes over almost the entire globe under clear-sky conditions, and still over a significant part of the globe when cloud effects are considered in addition. The statistically significant decreasing trend of clear-sky radiation is projected in most world regions, except for parts of China and Europe.

Viet Nam is a country located in the tropical region where solar energy is abundant. There are so differences in seasonal and annual SSI cycles due to the geographical extension from the North to the South as well as the effects of different weather phenomena. Presently, there are few publications on using climate model to simulated and projected SSI over Viet Nam. This paper aims to examine the ability of the RCA4 regional climate model in doing those above tasks. Section 2 will provide details of data sources and methodology. Section 3 describes results and discussions. Concluding remarks are given in Section 4.

2. Model description and Data

2.1. RCA4 Model

Because of the limitation of the public dataset for SSI, only the experiment of RCA4 RCM is chosen for downscaling to the CORDEX-SEA

domain (89.49 - 146.51 E; 14.81 S - 26.96 N; <http://www.cordex.org>) with the resolution of 25 km. The model is given boundary conditions from the HadGEM2-ES global model from the Met Office Hadley Centre (MOHC). The RCA4 was built on its predecessor, RCA3 [17]. However, some physics parameterizations were improved to cater to simulations outside the European region [22]. For example, a new lake model (FLake) enhanced the land surface model and improved soil processes [22]. The Bechtold-KF scheme was used for cumulus parameterization [2]. Besides, the threshold of relative humidity for cloud formation was adjusted. The representation of the cloud-radiation parameterization was modified following Tiedtke (1996) [28] to account for in-cloud cloud-water heterogeneity [5]. A complete description of RCA4 can be found in Strandberg et al. (2015) [25].

The simulations are performed for i) 1951 - 2005 with historical forcing and ii) for 2006 - 2099 under different Representative Concentration Pathways (RCP) scenarios [19]. In RCA4, the RCP scenarios are expressed as changes in equivalent carbon dioxide concentrations as interpolated from one year to the next. Here, two different RCP scenarios are used, which have been assessed in IPCC (2013) [8] as follow:

- RCP 4.5: Strategies for reducing greenhouse gas emissions cause radiative forcing to stabilize at 4.5 Wm^{-2} before the year 2100.

- RCP 8.5: A scenario of comparatively high greenhouse gas emissions means that radiative forcing will reach 8.5 Wm^{-2} by 2100.

2.2. Satellite data

SSI AMATERASS is the solar irradiation product derived from the Himawari-8 satellite under the Japan Science and Technology Agency (JST) using the EXAM algorithm [26]. The algorithm is based on a fast neural network, accurately reproducing the radiative transfer model, using the Comprehensive Analysis Program for Cloud Optical Measurement (CAPCOM) [10, 15]; algorithm to retrieve cloud optical thickness and cloud-particle effective radius from Himawari-8 observations by a

lookup table (LUT) based approach under a homogeneous plane-parallel and single-layer cloud model. Additional input information included in EXAM, such as water vapor and ozone, was acquired from external data sets (e.g., the Japanese Reanalysis and OMI/Aura satellite), and surface albedo was computed from Himawari-8 observations using a statistical method.

After membership registration, ISS Amaterass data with 30 min temporal resolution and 4 km spatial resolution downloaded from the website: <ftp.amaterass.org>. The AMATERASS data with 30 min time resolution were used to calculate daily data, and converted to a spatial resolution similar to the RCA4 model. The quality of AMATERASS estimation was evaluated with the surface measurement at five stations in Viet Nam with a high correlation (over 0.95) in our previous study [16].

2.3. Method for evaluation

For comparison between RCA4 simulation and satellite estimation, a spatial validation was also performed by calculating the difference between RCA4 and AMATERASS at the grid scale. The indicators used here include: The CORR correlation index, The mean error (ME), the relative mean error (RME), the mean absolute error (MAE) and the relative mean absolute error (RMAE):

$$ME = \frac{1}{n} \sum_{i=1}^n (S_i - G_i) = \bar{S} - \bar{G} \quad (1.1)$$

$$RME = 100\% * \frac{ME}{\bar{O}} \quad (1.2)$$

$$MAE = \frac{1}{N} \sum_{i=1}^N |S_i - G_i| \quad (1.3)$$

$$RMAE = 100\% * \frac{MAE}{\bar{O}} \quad (1.4)$$

$$CORR = \frac{Cov(S, G)}{\sigma_S \sigma_G} \quad (1.5)$$

In which, S is data from satellite, G is ground observation data, N is the number of samples;

$CORR$ is dimensionless, $Cov(S,G)$ is the covariance of the two variables, σ_S and σ_G are standard deviation of S and G , respectively.

Comparisons were carried out separately for seven different climate regions, namely the Northwest (B1), Northeast (B2), North Delta (B3), North Central (B4), South Central (N1), Central Highlands (N2), and the South (N3) and divided by four seasons (winter - DJF, spring - MAM, summer- JJA, and autumn -SON).

3. Results and discussions

3.1. Evaluation of RCA4 simulation against satellite data

Firstly, the relative mean errors RME (%) of SSI in winter (DJF), spring (MAM), summer (JJA), and fall (SON) of RCA4_RCP4.5 and RCA4_RCP8.5 model simulation data compared with AMATERASS satellite data over seven sub-regions in Viet Nam are shown in Figure 1. It can be seen that the two scenarios of the RCA4 model simulation show rather similar RME results. The overestimation of SSI values of the model is almost found in the North part of Viet Nam (B1-B4 sub-regions) during the year in which the most overestimated values are seen

in wintertime and in the B2 sub-region. The underestimated values of RCA4 SSI are often observed in the N2 sub-region during the year. However, some small overestimated values of RCA4 SSI (under 20%) are found in some parts of N2 and N3 sub-regions in summer and autumn.

Figure 2 shows that RCA4's highest RMAE values are found in the B2-B4 subregions in DJF and SON in both RCP scenarios. The smallest RMAE values are observed in the N3 subregion in all seasons.

Monthly RME and RMAE in seven subregions and the whole of Viet Nam during 2016 - 2018 period are shown in Figure 3. It can be seen that RCA4 monthly RME values are normally overestimated in four North subregions (B1-B4) while underestimated in three south subregions (N1-N3) in which the highest values are observed in B2 in January, and the smallest deals are found in N3 in April.

In general, the RMAEs of the two scenario versions are similar and have higher errors in winter and spring. The RMAEs of RCA4 also show better results in the South than in the North of Viet Nam.

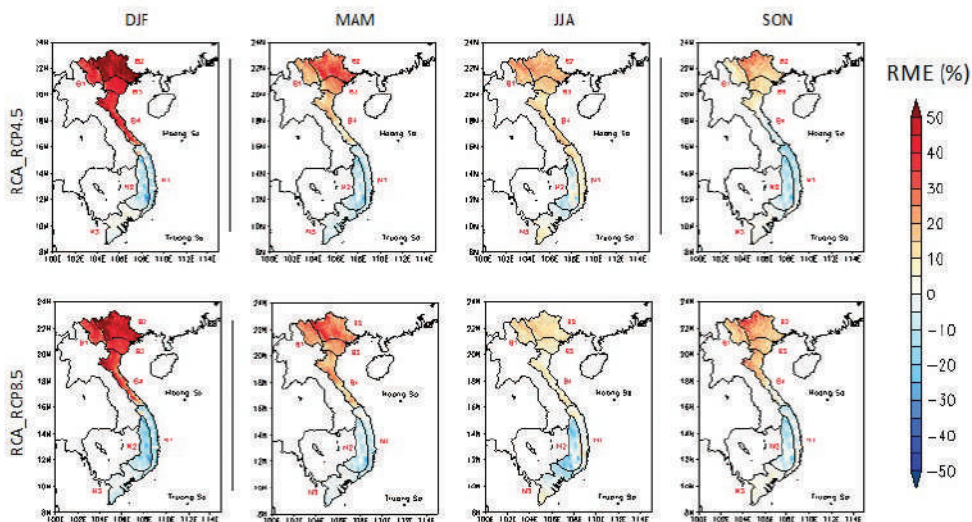


Figure 1. Distribution of relative mean errors RME (%) of SSI in winter (DJF), spring (MAM), summer (JJA) and fall (SON) of RCA4_RCP4.5 (middle) and RCA4_RCP8.5 (lower) compared with AMATERASS over seven sub-regions in Viet Nam during 2016 - 2018 period

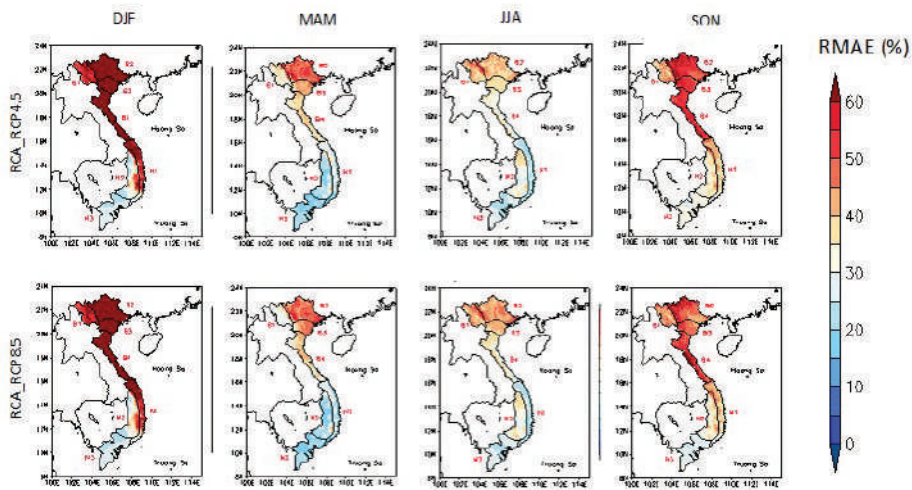


Figure 2. Distribution of relative mean errors RMAE (%) of SSI in winter (DJF), spring (MAM), summer (JJA) and fall (SON) of RCA4_RCP4.5 (middle) and RCA4_RCP8.5 (lower) compared with AMATERASS over seven sub-regions in Viet Nam during 2016 - 2018 period

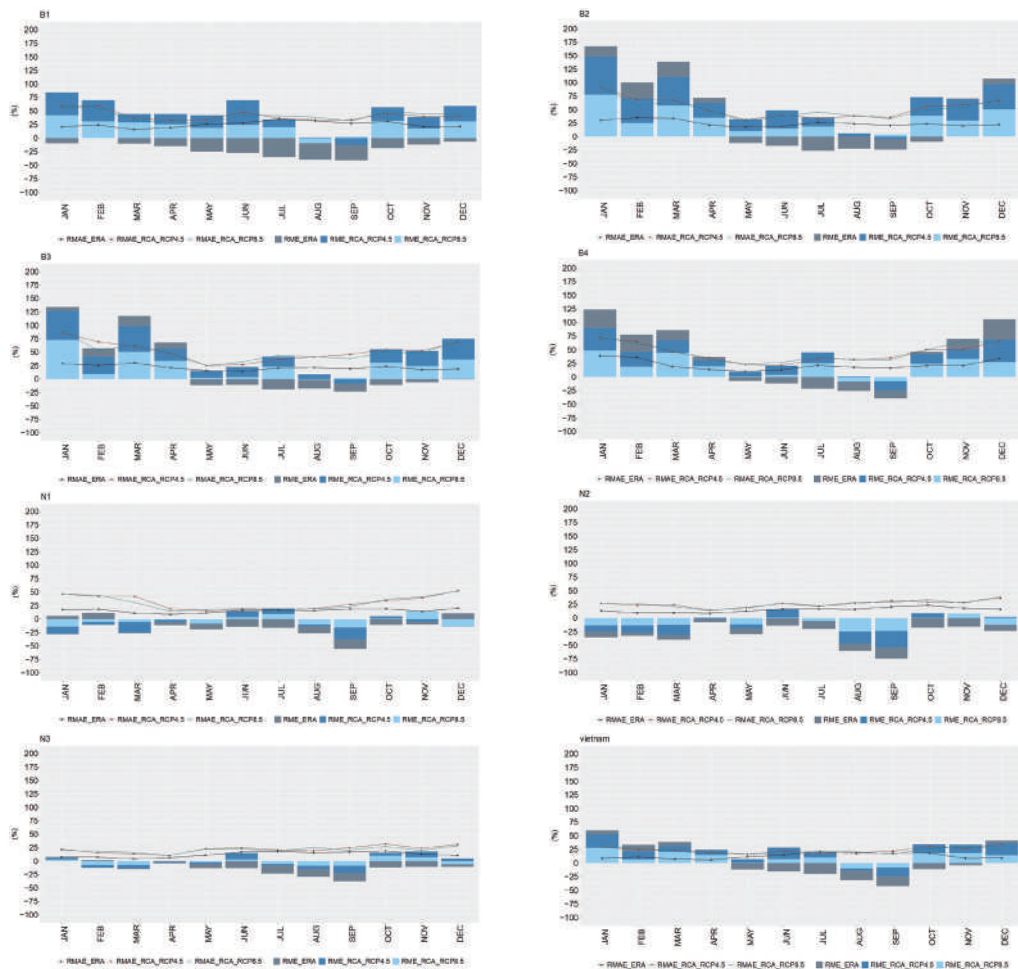


Figure 3. Monthly RME (%), columns and RMAE (%), lines of RCA4_RCP4.5 and RCA4_RCP8.5 compared with AMATERASS in seven subregions and the whole of Viet Nam during 2016 - 2018 period

3.2. RCA4 projection

Based on the comparative agreement between RCA4 and satellite estimations, we used the model projection to investigate the SSI change in the period 2005 - 2016 and the future 2021 - 2050 compared to the period 1976 - 2005 accordingly to climate change scenario RCP4.5 and RCP8.5.

The changes are non-uniformly distributed between 2006 - 2020 (Figure 4) and 2021 - 2050 (Figure 5) of the annual average short-wave radiation at the surface RCP8.5 scenarios. In the period 2006 - 2020, the average yearly short-wave radiation at the surface has an expected increase from 0.3 - 2.0 W/m² in the Northern region, Central Highlands and South Central regions, but the decrease in the North Central, Northern Delta and the Southern regions. In the period 2021 - 2050, the annual average short-wave radiation at the surface increases in the Southern region and Central Highlands regions. But the decrease of 1.0 - 3.0 W/m² in the remaining regions, including the Northern Delta, Central Coast, South Central and Southern regions. Therefore, the short-wave radiation at the surface rises in the Northern region, and in contrast, falls in the Southern region; except for the Central Highlands region that hasn't changed much.

Figure 6 and Figure 7 respectively show changes in the average short-wave radiation at the surface of the scenario RCP8.5 of the periods (2006 - 2020) and (2021 - 2050) compared with the period (1976 - 2005) in 4 seasons.

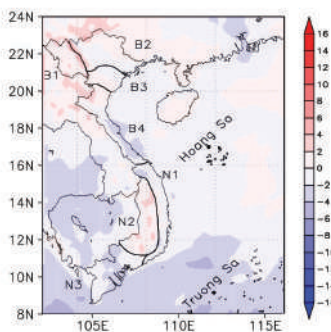


Figure 4. Changes in the annual average short-wave radiation (W/m²) at the surface in the RCP8.5 scenario for 2006 - 2020 compared to 1976 - 2005

According to the RCP4.5 scenario, there are non-uniformly changes between 2006 - 2020 (Figure 8) and 2021 - 2050 (Figure 9) of the annual average short-wave radiation at the surface. In 2006 - 2020, the average yearly short-wave radiation at the surface increased from 1.0 to 5.0 W/m²; high concentration in the Central Highlands, with an increase of 3.0 - 5.0 W/m². Thus, this is the difference between the RCP4.5 scenario and the RCP8.5 scenario for 2006 - 2020. In contrast, in 2021 - 2050, the annual average short-wave radiation at the surface decreases by 1.0 - 5.0 W/m². Except for the provinces bordering China in the Northeast and the high-mountain areas in the Central Highlands, the value increased from 1.0 to 2.0 W/m². Thus, the short-wave radiation at the surface raises in the mountainous regions and decreases in the flat areas, similar to the RCP8.5 scenario.

Figure 10 and Figure 11 respectively show changes in the average short-wave radiation at the surface of the scenario RCP4.5 of the periods (2006 - 2020) and (2021 - 2050) compared with the period (1976 - 2005) in 4 seasons.

The relative mean deviation (RMB) of the short-wave radiation at the surface is negative in most of Viet Nam; apart from that the Central Highlands has a positive value. Thus, the short-wave radiation across Viet Nam decreases, meanwhile in the Central Highlands is increased. The change of short-wave surface radiation under the RCP8.5 scenario is more significant than the RCP4.5 scenario (Figure 12).

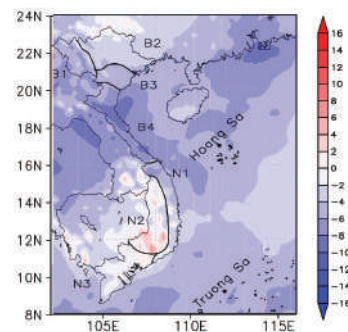
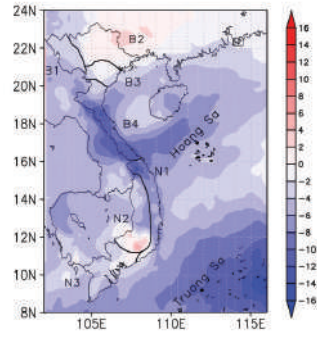
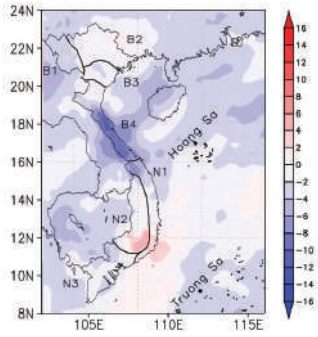
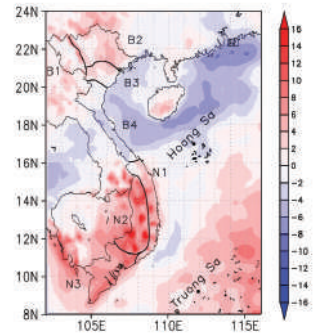
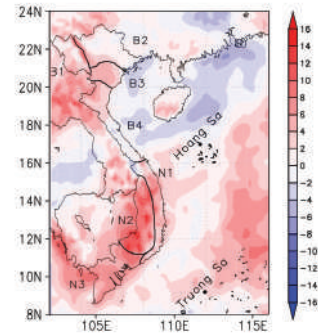


Figure 5. Changes in the annual average short-wave radiation (W/m²) at the surface in the RCP8.5 scenario for 2021 - 2050 compared to 1976 - 2005

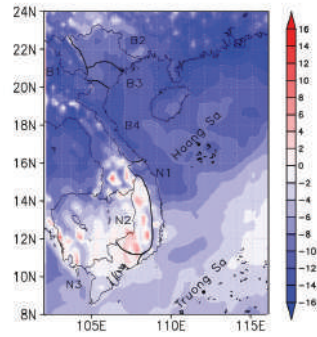
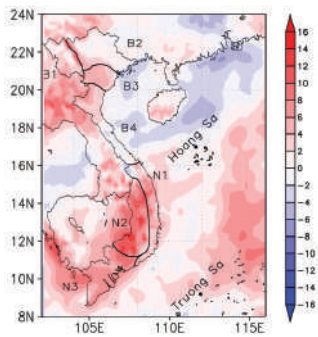
The Winter (DJF)



The Spring (MAM)



The Summer (JJA)



The Autumn (SON)

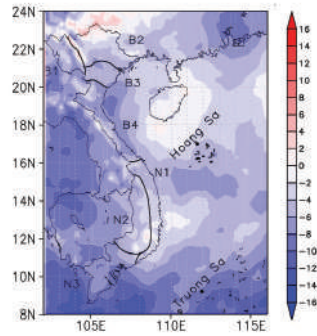
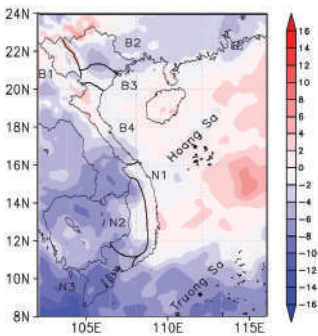


Figure 6. Changes in the average short-wave radiation (W/m^2) at the surface of the RCP8.5 scenario of 2006 - 2020 compared to 1976 - 2005 in 4 seasons

Figure 7. Changes in average short-wave radiation (W/m^2) at the surface of the RCP8.5 scenario of 2021 - 2050 compared to 1976 - 2005 in 4 seasons

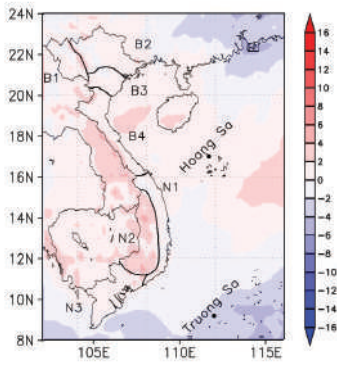


Figure 8. Changes in the annual average short-wave radiation (W/m^2) at the surface in the RCP4.5 scenario for 2006 - 2020 compared to 1976 - 2005

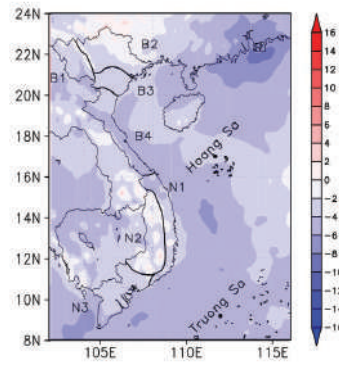


Figure 9. Changes in the annual average short-wave radiation (W/m^2) at the surface in the RCP4.5 scenario for 2021 - 2050 compared to 1976 - 2005.

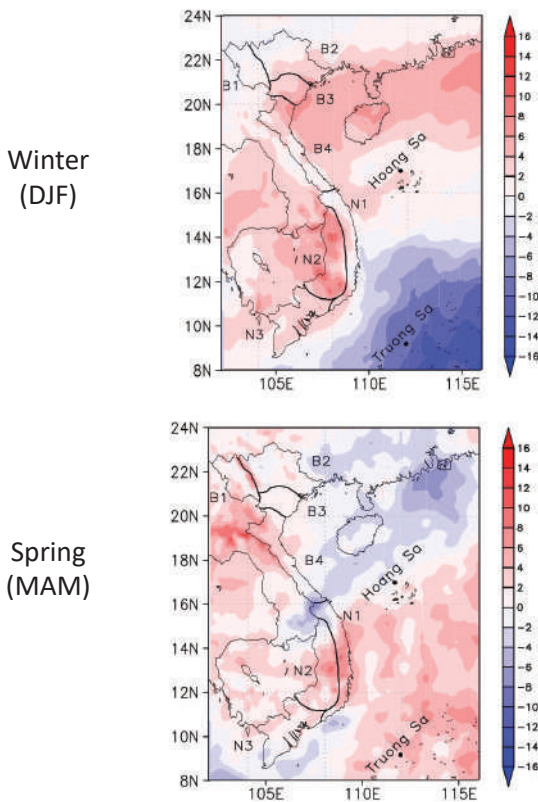


Figure 10. Changes in the average short-wave radiation (W/m^2) at the surface of the RCP4.5 scenario of 2006 - 2020 compared to 1976 - 2005 in Winter (DJF) and Spring (MAM)

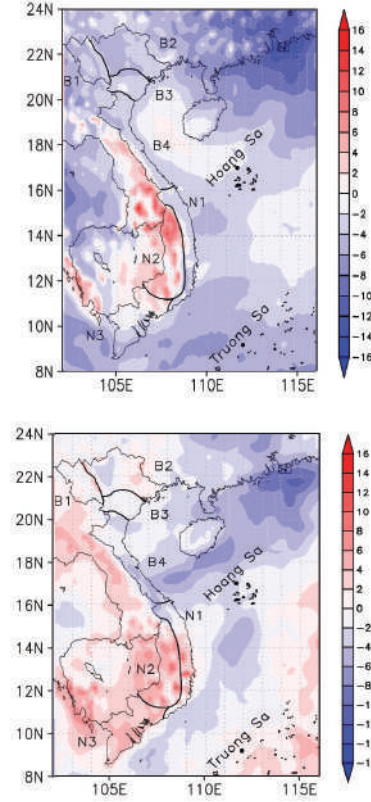
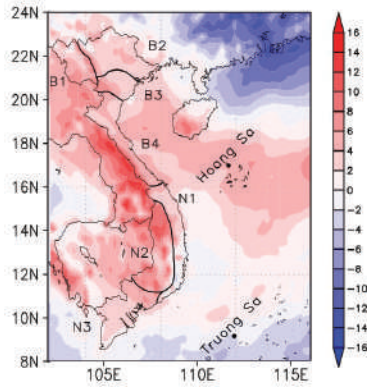


Figure 11. Changes in the average short-wave radiation (W/m^2) at the surface of the RCP4.5 scenario of 2021 - 2050 compared to 1976 - 2005 in Winter (DJF) and Spring (MAM)

Summer
(JJA)



Autumn
(SON)

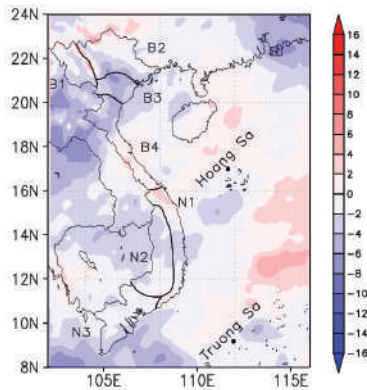


Figure 10. Changes in the average short-wave radiation (W/m^2) at the surface of the RCP4.5 scenario of 2006 - 2020 compared to 1976 - 2005 in Summer (JJA) and Autumn (SON)

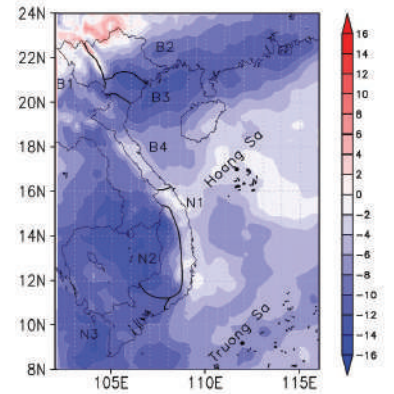
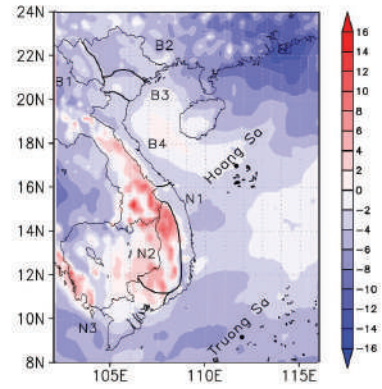


Figure 11. Changes in the average short-wave radiation (W/m^2) at the surface of the RCP4.5 scenario of 2021 - 2050 compared to 1976 - 2005 in Summer (JJA) and Autumn (SON)

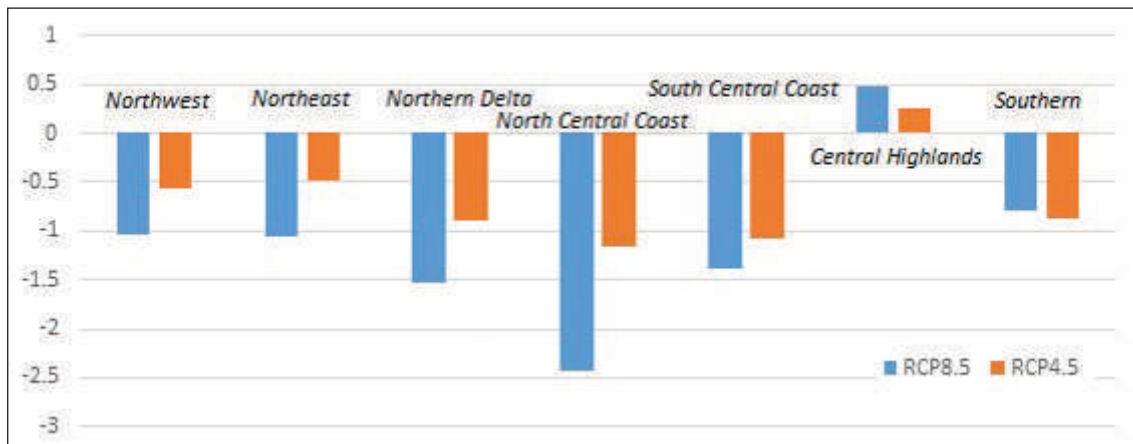


Figure 12. The relative mean bias RMB (%) of the short-wave radiation at the surface in Viet Nam

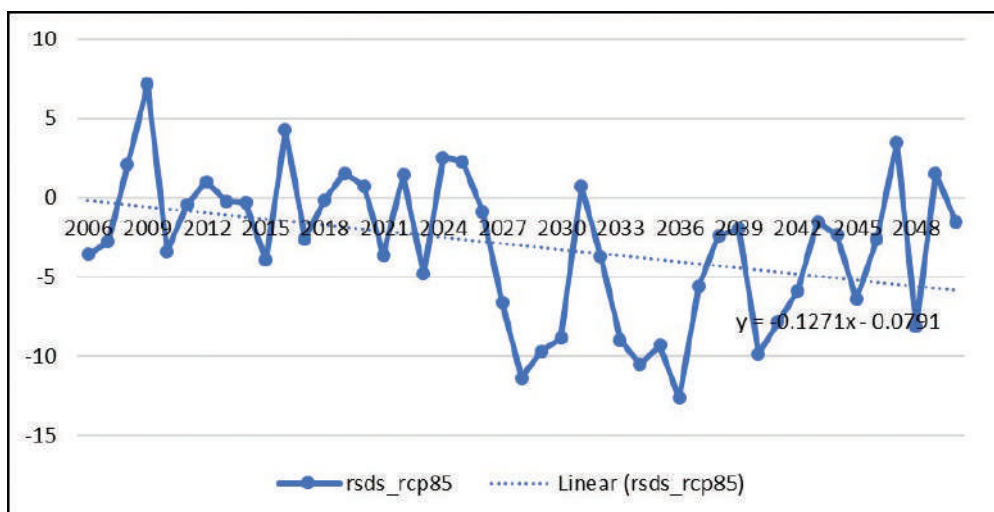


Figure 13. Future changes in annual short-wave radiation (W/m^2) at the surface in Viet Nam in the RCP8.5 scenario for 2006 - 2050 compared to 1976 - 2005.

In general, the annual average surface short-wave radiation decreases in the future under both the RCP4.5 and RCP8.5 scenarios (Figure 13 and Figure 14). In the RCP8.5 scenario, the annual average shortwave radiation at the surface tends to fluctuate steadily around 0 for the period from 2006 to 2026, and negative during the period of 2027 to 2047, then the

trend fluctuates slightly around 0 in the last 3 years. Meanwhile, in the RCP4.5 scenario, there is a decrease around the value of 0 in the 2006 - 2032 period and, it is a negative bias in the 2033 - 2050 period. The annual average short-wave radiation surface changes in the RCP 8.5 scenario are approximately in the RCP 4.5 scenario.

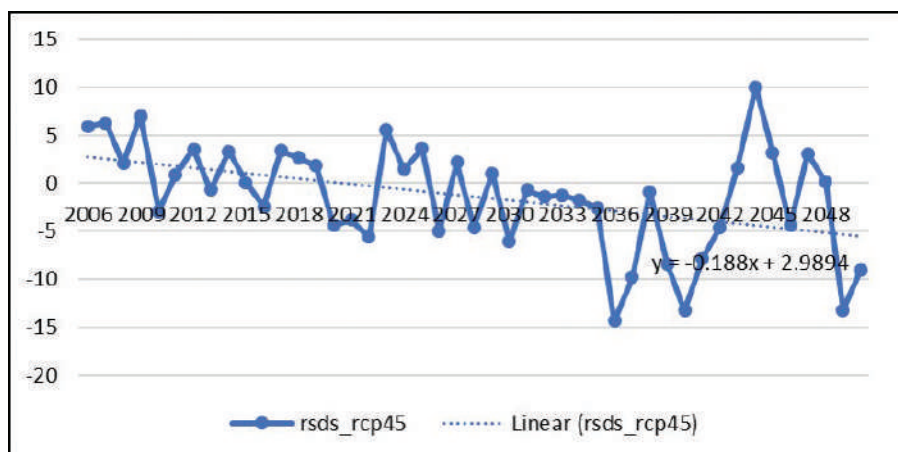


Figure 14. Future changes in annual short-wave radiation (W/m^2) at the surface in Viet Nam in the RCP4.5 scenario for 2006 - 2050 compared to 1976 - 2005.

4. Conclusions

This study focuses on assessing the variation of solar radiation at the surface (SSI) in Viet Nam for the period 2006 - 2020 and the future period 2021 - 2050 compared with the period 1976 - 2005 using the regional climate forecasting

model RCA4 RCM under high emission scenarios (RCP8.5) and medium emission scenarios (RCP4.5) [9]. Based on the evaluation of the error of the SSI from the model compared with the estimated data from the Himawari-8 satellite for the period 2016 - 2018, it shows the relative

agreement of the model and satellite estimates to use model for assessing future volatility.

In general, in the spring, satellite data compared with model data for two scenarios shows that there is a markedly higher bias for RCP8.5 than RCP4.5. During the summer, the model estimation is more consistent with the satellite data in case of the RCP4.5 than the RCP8.5 scenario. The solar irradiance value in the RCP4.5 is higher than that in the RCP8.5. These high values are concentrated mainly in June and July. In the autumn, solar radiation has decreased markedly compared to the summer, and there is little difference between

North and South Viet Nam. During the winter, solar radiation reduced significantly, especially in the Northern area affected by the strong Northeast monsoon during this time.

The relative mean bias (RMB) of short-wave surface radiation for the RCP8.5 scenario in the North Central region and the North is lower than in the RCP4.5 scenario. It is approximately equal from the South Central Coast region to the Southern. Compared to the period 1976 - 2005 (in both scenarios), the short-wave radiation at the surface in the period 2020 - 2050 decreases in most of Viet Nam, except for Central Highlands.

Acknowledgement: This study was conducted under the National Space Technology Program of 2016-2020 period (Grant number: VT-CB.14/18-20).

References

1. Alexandri G., G.A.K., Zanis P., Katragkou E., Tsikerdekis A., Kourtidis K., and Meleti C., (2015). "On the ability of RegCM4 regional climate model to simulate surface solar radiation patterns over Europe: an assessment using satellite-based observations". *Atmos. Chem. Phys.*, 15, 13195-13216. doi:10.5194/acp-15-13195-2015.
2. Bechtold., a.e.a., (2001). "A mass flux convection scheme for regional and global models". *Q. J. R. Meteorol. Soc.*, 127, 869–886,
3. Brazel A. J., M.G.J., Jr, Verville H. J., (1993). "Incident solar radiation simulated by general circulation models for the southwestern United States". *Clim. Res.*, 2, 177-181.
4. Chiacchio M., S.F., Giorgi F., Stackhouse P., and Wild M., (2015). "Evaluation of the radiation budget with a regional climate model over Europe and inspection of dimming and brightening", . *J. Geophys. Res.*, 120, 1951-1971, .doi:10.1002/2014JD022497.
5. Fredolin Tangang., J.X.C., and et al., (2019). "Projected future changes in rainfall in Southeast Asia based on CORDEX–SEA multi-model simulations". *Climate Dynamics*.<https://doi.org/10.1007/s00382-020-05322-2>.
6. Guettler I., B.C., Srncic L., and Patarcic M., (2014). "The impact of boundary forcing on RegCM4.2 surface energy budget, *Climatic Change*". *Climatic Change*, 125, 67-78.doi:10.1007/s10584-013-0995-x.
7. Hammer A., H.D., Hoyer C. R. K., Lorenz E., Mueller R., and Beyer H., (2003). "Solar energy assessment using remote sensing technologies", . *Remote Sens. Environ.*, 86, 423-432.doi:10.1016/S0034-4257(03)00083-X.
8. IPCC, (2013). *Climate change 2013: The Physical Science Basis. Contribution of Working Group I to the Fifth Assessment Report of the Intergovernmental Panel on Climate change Cambridge, United Kingdom and New York, NY, USA.*
9. IPCC, (2019). *Special Report on climate change, desertification, land degradation, sustainable land management, food security, and greenhouse gas fluxes in terrestrial ecosystems (SRCCL).*
10. Kawamoto, K., Teruyuki Nakajima, and Takashi Y. Nakajima, (2001). "A global determination of cloud microphysics with AVHRR remote sensing". *Journal of Climate*, 14 (9) (2001): 2054-2068
11. Kothe S., D.A., Beck A., and Ahrens B., (2011). "The radiation budget in a regional climate model", . *Clim. Dynam.*, 36, 1023-1036.doi:10.1007/s00382-009-0733-2.

12. Liepert B. G., (2002). "Observed reductions of surface solar radiation at sites in the United State and worldwide from 1961 to 1990". *Geophys. Res. Lett.*, 29 (10), 1421.doi:10.1029/2002GL014910.
13. Mercado L. M., B.N., Sitch S., Boucher O., Huntingford C., Wild M., and Cox P. M., (2009). "Impact of changes in diffuse radiation on the global land carbon sink", *Nature*, 458, 1014-1017,. doi:10.1038/nature07949.
14. Mueller R., M.C., Gratzki A., Hollman R., and Behr H., (2009). "The CM-SAF operational scheme for the satellite based retrieval of solar surface irradiation-a LUT based eigenvector hybrid approach", *Remote Sens. Environ.*, 113, 1012-1022, .doi:10.1016/j.rse.2009.01.012.
15. Nakajima, T.Y., and Teruyuki Nakajima. , (1995). "Wide-area determination of cloud microphysical properties from NOAA AVHRR measurements for FIRE and ASTEX regions". *Journal of the Atmospheric Sciences*, , 52 (23) (1995): 4043-4059.
16. Nga, P.T.T., Hao, N. T. P., Cong, N. T., Hang, V. T., Ha, P. T., Hoa, P. V., ... & Hong, P. V. , (2020). "Comparative Assessment of Solar Radiation by Satellite-Based and Reanalysis Products Over Viet Nam Regions". In *IGARSS 2020-2020 IEEE International Geoscience and Remote Sensing Symposium* (pp. 6702-6705). IEEE.],
17. Patrick SamuelssonColin G. Jones, e.a., . (2011). *The Rossby Centre Regional Climate model RCA3: model description and performance*. January 2011Tellus.DOI: 10.3402/tellusa.v63i1.15770
18. Perez R., H.T., (2013). "Solar resource variability solar energy forecasting and resource assessment", *Elsevier, Philadelphia*,, 133-148.
19. Richard Moss, R.M., and et al, (2010). "The Next Generation of Scenarios for Climate Change Research and Assessment". *Nature*, 463(7282):747-56.DOI: 10.1038/nature08823
20. Romanou A., L.B., Schmidt G. A., Rossow W. B., Ruedy R. A., Zhang Y., , (2007). "20th century changes in surface solar irradiance in simulations and observations", *Geophys. Res. Lett.*, 34, L05713, .doi:10.1029/2006GL028356.
21. Rummukainen M., (2010). "State-of-the-art with regional climate models", *Wiley Interdiscip. Rev. Clim. Chang.*,, 1, 82-96, .doi:10.1002/wcc.8
22. Samuelsson, P., Kourzeneva, E., and Mironov, D.: , (2010). "The impact of lakes on the European climate as simulated by a regional climate model", *Boreal Environ. Res.*, 15, 113–129, 2010
23. Stanhill G. and Cohen S., (2001). "Global dimming: A review of the evidence for a widespread and significant reduction in global radiation with discussion of its probable causes and possible agriculture consequences", *Agric. For. Meteorol.*, , 107, 255-278.
24. Stephens G. L., L.J., Wild M., Clayson C. A., Loeb N., Kato S., L'Ecuyer T., Stackhouse P. W., Lebsock M., and Andrews T., (2012). "An update on Earth's energy balance in light of the latest global observations", *Nat. Geosci.*, 5, 691-696, .doi:10.1038/ngeo1580.
25. Strandberg, G., Barring, L., Hansson, U., Jansson, C., Jones, C., Kjellström, E., Kolax, M., Kupiainen, M., Nikulin, G., Samuelsson, P., Ullerstig, A., and Wang, S., (2015). *CORDEX scenarios for Europe from the Rossby Centre Regional Climate Model RCA4*. Available at: <http://www.diva-portal.org/smash/get/diva2:948136/FULLTEXT01.pdf> [Accessed 11th February 2017].
26. Takenaka, H., Takashi Y. Nakajima, Akiko Higurashi, Atsushi Higuchi, Tamio Takamura, Rachiel T. Pinker, and Teruyuki Nakajima., (2011). "Estimation of solar radiation using a neural network based on radiative transfer". *Journal of Geophysical Research: Atmospheres* 8 (2011): 64.
27. Tang C., M.B., Wild M., Pohl B., Abiodun B., Bessafi M., (2018). "Numerical simulation of surface solar radiation over Southern Africa", *Climate Dynamics*,, 52, 457-477.doi:10.1007/s00382-018-4143-1.
28. Tiedtke, M., (1996). "The representation of the cloud - radiation parameterization was modified following Tiedtke(1996)". *Monthly Weather Review*, 124(4), 745-750.[https://doi.org/10.1175/1520-0493\(1996\)124<0745:AEOCRP>2.0.CO;2](https://doi.org/10.1175/1520-0493(1996)124<0745:AEOCRP>2.0.CO;2)
29. Trenberth K. E., F.J.T., and Kiehl J., (2009). "Earth's global energy budget", *B. Am. Meteorol. Soc.*,

90, 311-323.doi:10.1175/2008bams2634.1.

30. Webster P. J., C.C.A., and Curry J. A., (1996). "Clouds, radiation, and the diurnal cycle of sea surface temperature in the Tropical Western Pacific". *J. Climate.*, 9, 1712-1730.doi:10.1175/1520-0442(1996)009<1712:CRATDC>2.0.CO;2.
31. Wild M., (2005). "Solar radiation budgets in atmospheric model intercomparisons from a surface perspective", *Geophys. Res. Lett.*, 32, L07704.doi:10.1029/2005GL022421.
32. Wild M., (2009a). "Global dimming and brightening: A review", . *J. Geophys. Res.*,, 114, D00D16. doi:10.1029/2008JD011470
33. Wild M., F.D., Henschel F., Muller B., (2015). "Projections of long term changes in solar radiation based on CMIP5 climate models and their influence on energy yeilds of photovoltaic systems". *Solar Energy*, 116, 12-24.
34. Wild M., G.H., Roesch A., Ohmura A., Long C. N., Dutton E. G., Forgan B., Kallis A., Russak V., and Tsvetkov A.,, (2005). "From dimming to brightening: Decadal changes in solar radiation at Earth's surface". *Science*, 308, 847-850.

DEVELOPING TROPICAL CYCLONE RISK WARNING SYSTEM FOR NORTH CENTRAL VIET NAM

Nguyen Xuan Hien⁽¹⁾, Nguyen Thi Thanh⁽²⁾, Ngo Thi Thuy⁽²⁾, Du Duc Tien⁽³⁾

⁽¹⁾Centre for Oceanography, Viet Nam Administration of Sea and Islands

⁽²⁾Viet Nam Institute of Meteorology Hydrology and Climate change

⁽³⁾National Centre for Hydro-Meteorological Forecasting

Received: 10 September 2021; Accepted: 30 September 2021

Abstract: Viet Nam is one of the most impacted countries by climate natural disasters especially tropical cyclone and tropical depression. Under climate change context, the natural disasters in prone areas have becoming more extreme. With the supporting of advance technology, warning systems are considered as effective measures to prevent and mitigate damages of natural disasters, in particular, tropical cyclone and tropical depression. Locating in the middle of Viet Nam and Gulf of Tonkin, the North Central region is directly affected by one to two tropical cyclones every year, one of the most tropical cyclone - impacted regions in Viet Nam. Developing an effective tropical cyclone risk warning system would be helpful to protect local people in tropical cyclone seasons. This paper proposes a methodology to assess tropical cyclone risk and introduce a practical risk warning system to apply to local hydrometeorological stations.

Keywords: tropical cyclone, risk assessment, warning system, North Central region.

1. Introduction

Viet Nam is located in the Western Pacific region, the area with the most active tropical cyclones (TCs) in the world. Every year, on average about 5 - 7 TCs and tropical depressions make landfall or directly impact on Viet Nam, causing heavy damage to people, economic, social and environmental. For example, Typhoon Doksuri in 2017 killed 6 people, injured 37 people, collapsed more than 800 houses, damaged 190,000 houses and damaged 2,855 power poles. Total damage was estimated at over VND 11,000 billion [12]. In recent years, due to the effects of climate change, TC and tropical depression activity in the East Sea have been abnormal, causing more serious consequences [11]. Therefore, assessing the risks caused by TC is one of the necessary tasks for disaster prevention, control and response [1, 9].

The assessment of disaster risk in general and risk due to TC in particular is carried out

in two approaches: Risk assessment based on consequences of natural disasters and risk assessment based on constituent elements. The approach to risk assessment based on the consequences of natural disasters is expressed through the assessment of the probability of occurrence of a disaster and its consequences [6]. Applying this approach, a TC risk assessment was carried out in Queensland (Australia), in which the consequences of the TC were determined to include damage to power lines, communications, houses, infrastructure and transport infrastructure [10]. This approach does not require complicated calculations and can be used to assess risk for disaster impact zoning. However, the assessment of consequences requires observations and historical records, so this approach can hardly be applied in disaster risk forecasting and warning.

Many studies in the direction of risk assessment approach based on constituent factors have been carried out to assess TC risk. Hurricane risk for coastal areas in the United States is assessed through the Hurricane Risk Index (HDRI) [2]. The

Corresponding author: Nguyen Xuan Hien
E-mail: nguyensexuanhien79@gmail.com

HDRI index is built as the criteria of factors H, E, V, in which V includes two components: sensitivity level (S) and adaptive capacity (AC). The criteria for expressing H include wind, storm surge and rain. Expression criteria E includes population, buildings and power lines. For S, research focuses on population, housing and economic criteria. The area's AC is mainly the criteria of connectivity, shelter, communication and other resources. Similar approaches have also been taken in the coastal areas of China [25, 26] and in Bangladesh [17].

In order to build a real-time TC risk warning system for the North Central region to serve natural disaster prevention and control, the article conducts a pilot study on risk warning for tropical storm Sinlaku occurring in 2020. For the calculation of factor H for real-time risk warning, wind and rain forecast data will be established from the TC forecast bulletins of the National Center for Hydro - Meteorological Forecasting (NCHMF) combined with results of the numerical weather prediction (NWP) models. The study is limited to the scope of the Hydro - Meteorological Station in the North Central region [16], including three provinces: Thanh Hoa, Nghe An, and Ha Tinh.

2. Study area and Methodology

2.1. Study area

The study is pilot conducted in the North Central region of Viet Nam including Thanh Hoa, Nghe An and Ha Tinh. These coastal provinces were formed by Ma and Ca rivers that flowing from scattered rocky mountains to Tonkin Gulf. The North Central region is a populated and large region that occupies 7.8% of total population and 10.1% of area. The North Central region has an important location of Viet Nam with the Tonkin Gulf in the east, Lao PDR in the west, Red River Delta in the North and Mid Central region in the south. Locating at an inner corner of the S-shape of Viet Nam map, North Central is one of the most TC - impacted regions. Every year, the region is directly affected by one to two tropical cyclones with the maximum sustainable wind reaching upto Category 14.

In 2020, tropical storm Sinlaku began as a

tropical depression on July 31 in the East Sea. The Sinlaku strengthened into a tropical storm the following day. On August 2nd, the center of the Sinlaku was at 19.4°N and 106.4°E, on the coastal areas of Ninh Binh - Nghe An province. The maximum sustainable wind reached Category 8 (60 - 75 km/h) with gust wind reaching Category 10. The Sinlaku made landfall on Ninh Binh - Thanh Hoa province at 13:00 on August 2nd, then rapidly weakened and dissipated on August 3rd, 2020 [4].

2.2. Data

Data sources (primary and secondary) used in disaster risk warning due to TC for the North Central region include:

- Data on economy and society of 3 provinces Thanh Hoa, Nghe An, Ha Tinh detailed to district level are collected from statistical yearbooks at provincial and district level [18, 19, 20].

- Data on communication, disaster prevention works, number of coastal resorts are collected through field surveys in localities.

- Data of the 10 m wind speed, 24-hour accumulative rainfall and the forecast confident interval are taken from existing NWP products at NCHMF combined with the NCHMF's TC forecast bulletin.

2.3. Method

The TC risk warning system is conducted using indicator-based risk assessment. In which, risk is assessed from three components hazard, exposure and vulnerability [8]. Hazard is defined as a danger potentially causing damages in human, property, society, economy, and environment [23]. The hazard refers to the magnitude, frequency, and extent of disasters. Exposure indicates the presence of properties in the adversely affected area of hazards. Vulnerability (V) refers to the tendency of hazards, such as people, their lives, and their assets, to be adversely affected by hazards [23]. The following will introduce the detailed estimation of each component of risk.

2.3.1. Determination of TC hazard from meteorological forecasting reports

According to [14] the TC hazard is composed by criteria of intensity and probability of

occurrence. In which, the hazard intensity is characterized by the TC maximum 10 m sustainable wind and the amount of rainfall due to TC. In this paper, the 10 m wind speed (V_{max}) and 24-hour accumulative rainfall (R24) corresponding to forecast lead times are calculated of each district for determination of the hazard intensity. For the forecast lead time less than 24 hours, R24 is considered the accumulative rainfall in the first 24 hours of the forecast. The probability of TC occurrence is assumed to be equivalent to the confident interval (CI) of TC forecast. In order to calculate and warning the TC hazard nearly real time, it is necessary to forecast CI corresponding to forecast lead times for each district.

a. Determination of the 10 m wind speed

At each forecast lead time, V_{max} for each district is calculated based on two information sources with including the NCHMF's TC forecast bulletin and results of the NWP model. For districts located inside the forecasted strong wind radius affected by TC, V_{max} is assigned by the wind speed corresponding to the determined TC wind category. It is worth noting that the NCHMF's TC forecast bulletin only has information about the forecasted TC location and strong wind radius corresponding to the basic TC wind categories (Beaufort category of 6 and 10). Using the TC wind distribution profiles depending on the intensity and the strong wind radius corresponding to the basic TC wind categories, it is able to interpolate strong wind radius corresponding to the other TC wind categories.

b. Determination of the 24-hour accumulative rainfall

The 24-hour accumulative rainfall at each forecast lead time is taken from the NWP model similar to determining V_{max} (in case the district location is outside the forecasted strong wind radius affected by TC).

c. Determination of the confident interval of TC forecast

In order to determine the confident interval of TC forecast, it is necessary to carefully analyze the method of determining this indicator. For a set of operational TC forecast data long enough, it is able to determine forecast error and CI. The CI could be determined by the high percentile (90%, 95%) or error intervals of approximately 1 - 3 times the standard deviation [24] or statistical empirical formulas [15] or using the method of random sampling with a large number of tests to ensure the level of statistical limitation for each specific sample set [5]. On the other hand, according to Tien et al [21], increasing the forecast quality of the TC track is also increase the forecast quality of the TC intensity, although this increase rate not really linear. Therefore, this paper approaches in a different way to determine CI assumed that the TC intensity forecast is considered as a conditional forecast for the TC track forecast.

This study uses the NCHMF's TC forecast data from April 2008 to September 2020 to calculate the Direct Position Error (DPE). The DPE of the models running in the NCHMF's is also evaluated to provide a basis for data addition with locations where the NCHMF's TC forecast bulletin is missing. Details of the DPE calculation are given in [22] and [13].

2.3.2. Assessing exposure and vulnerability

In this study the TC exposure is estimated based on indicators of people (E1), agriculture (E2), economy (E3) and infrastructure (E4). The sub-indicators of them are collected from statistic books or field survey. The estimation method is extracted from [7].

The V factor is made up of two components of sensitivity (S) representing characteristics of the exposure elements that increase the risk of natural disasters and adaptive capacity (AC) denoting the region's capacity in terms of technical, information, economic and educational capacities to enhance disaster resilience [23]. The list of indicators of exposure and vulnerability is summarized in Table 1.

Table 1. List of exposure and vulnerability indicators

Factor	Indicator	Sub-indicator
Exposure	People (E1)	Population
	Agriculture (E2)	Agricultural area
		Number of livestock and poultry
		Number of ships and boats with marine fishing engines
		Aquacultural area
	Trade and services (E3)	Number of businesses and economic establishments operating in the area
		Number of coastal tourist areas
	Infrastructure (E4)	Number of kilometers of roads, including national highways, provincial roads, and district roads
		Number of key projects (headquarters, schools, medical stations)
		Residential land area
Sensitivity	Socio-economy (S1)	Value of products obtained per hectare of cultivated land
		Value of products obtained per hectare of aquaculture water surface
		Percentage of poor and near-poor households
	Environment (S2)	Percentage of households that do not use hygienic latrines
		Percentage of households that do not use clean water
Adaptive capacity	Education (AC1)	Percentage of people graduating from high school and above/ Total population
	Economy (AC2)	Per capita income
	Social groups (AC3)	Percentage of people participating in health insurance
		Percentage of people participating in social insurance
	Health (AC4)	Number of health facilities/commune number
		Number of hospital beds/1000 people
		Number of medical staff/1000 people
	Information Communication (AC5)	Percentage of households using the internet
		Percentage of phone users
	Disaster prevention (AC6)	Traffic density
Total capacity of mooring area		

2.3.3. Classification of TC risk level

The factors H, E, V of TC are classified into five levels (very low, low, moderate, high, very high) and formed into 3 matrices of size 5 x 1 correspondingly. The risk level of TC is identified by a combination of these matrices. In this study, risk value is a product of hazard, exposure and vulnerability levels. More specifically, a value in grids of Figure 1 is equal to hazard level (vertical

axis) multiply with exposure and vulnerability level (up and down horizontal axes). The maximum value is $5 \times 5 \times 5 = 125$ and the minimum value is 1. These risk values are then classified into five levels corresponding to magnitude of storm risk in the study area (1 = very low, 5 = very high). Figure 1 is conducted to visualize the three-dimensional matrix of risk.

Hazard level	Exposure level																								
	1	2	3	4	5	1	2	3	4	5	1	2	3	4	5	1	2	3	4	5					
1	1	2	3	4	5	2	4	6	8	10	3	6	9	12	15	4	8	12	16	20	5	10	15	20	25
2	2	4	6	8	10	4	8	12	16	20	6	12	18	24	30	8	16	24	32	40	10	20	30	40	50
3	3	6	9	12	15	6	12	18	24	30	9	18	27	36	45	12	24	36	48	60	15	30	45	60	75
4	4	8	12	16	20	8	16	24	32	40	12	24	36	48	60	16	32	48	64	80	20	40	60	80	100
5	5	10	15	20	25	10	20	30	40	50	15	30	45	60	75	20	40	60	80	100	25	50	75	100	125

Vulnerability level

1 2 3 4 5

Very low
 Low
 Moderate
 High
 Very high

Figure 1. The combination of hazard, exposure and vulnerability

In which, risk value of 60 is product of hazard level 4 with exposure level 5 and vulnerability level 3 ($4 \times 5 \times 3 = 60$). TC risk levels are determined using professional knowledge of experts based on practical analysis. In this approach, the experts stated that the E and V are relatively static factors while H is considered as a dynamic factor (changes according to the TC forecast reports) in the risk warning system. The H factor dominates the exposure and vulnerability and the risk level increases as the level of $E \times V$ increases. Risk level of 5 is product of hazard level at least 4 and hazard level of 1 and 2 only product to risk level of 1 and 2 correspondingly. If hazard is at level 5, the consequently risk is at least level 3.

2.3.4. Developing TC risk warning system

The proposed warning system of TC risk consists of four elements: (1) Input data, (2) Risk knowledge; (3) Risk warning and (4) Risk information. The diagram of proposed warning system is presented in Figure 2.

The input data includes static data that is periodically updated such as socio-economic and meteorological data and dynamic inputs that is real-time updated during the TC event. The risk knowledge component refers to risk assessment and mapping. The third element is warning in terms of hazard and risk of the TC. The fourth element is to translate the risk warning into levels indicated in Decision No. 18/2021/QD-TTg [3].

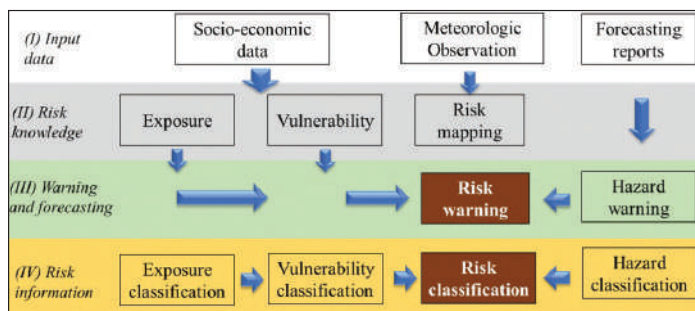


Figure 2. Diagram of TC risk warning system

The steps to develop the TC risk warning report in a TC is summarized following:

Step 1: Prepare risk knowledge before TC events.

This step can be conducted before TC events using historical observation and survey. The information of exposure, vulnerability and risk maps is provided.

Step 2: Calculate hazard indicators of TC

from the NCHMF's TC forecast bulletin and the NWP model.

The third component is implemented once TC forecast bulletins are provided by NCHMF. The assessment is automatically updated following the real-time TC forecast (Figure 3).

Step 3: Transfer the risk assessment to risk level by a combination of matrix as Figure 1.

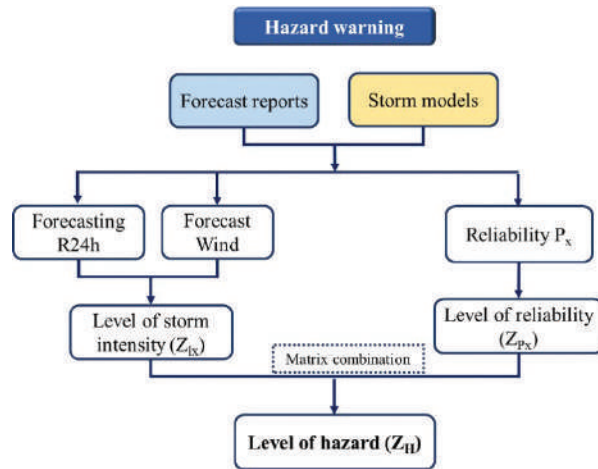


Figure 3. Method of hazard level estimation

3. Results and Discussion

3.1. Assessing exposure and vulnerability in North Central region

The map of TC exposure and vulnerability of the North Central region is shown in Figure 4. Accordingly, the exposure to TCs in coastal districts, towns and cities is usually at very high and high levels while in mountainous districts it is at low and very low levels. This is quite consistent with the actual nature of socio-economic and

human characteristics. The TC vulnerability of the North Central region shows the highest vulnerability in mountainous and midland areas with underdeveloped economic conditions, high rates of poor and near-poor households such as Tuong Duong, Quy Chau districts (Nghe An province) or lowland areas where income is mainly based on farming and aquatic products such as Vinh Loc, Quang Xuong (Thanh Hoa province), Dien Chau (Nghe An province), Nghi Loc (Ha Tinh province) districts.

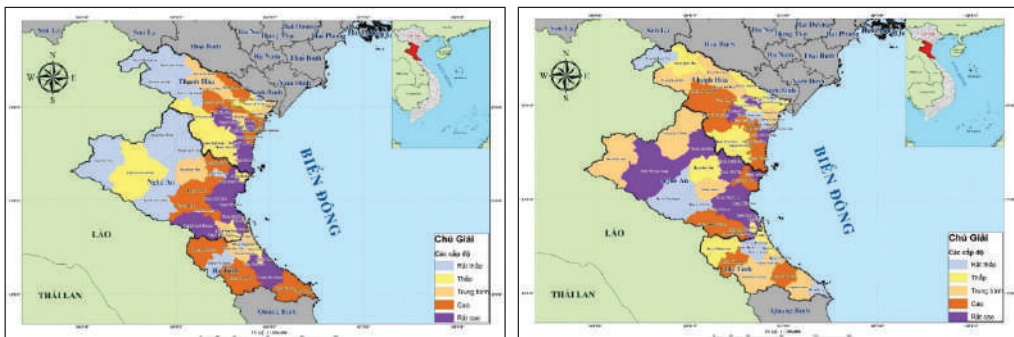


Figure 4. Maps of exposure (left) and vulnerability (right) in the North Central region

3.2. Pilot application of TC risk warning system in North Central region

The results of risk warning in tropical storm Sinlaku at the forecast lead time of 6, 12, 18 and 24 hour from 12 UTC on August 1, 2020 are shown in Figure 5. In general, risk caused by tropical storm Sinlaku is very low and low at the 6, 18, and 24 hour forecast lead times. The Sinlaku risk in North Central region reaches moderate (Level 3 categorized in Decision No.

18/2021/QĐ-TTg) at 12 hour forecast. The evaluation of risk warning shows an acceptable consistency with the actual impacts of Sinlaku on the North Central region. More specifically, at 7 am August 2, 2020 (Viet Nam time zone) the tropical storm approached the coast of Nghe An and Thanh Hoa provinces before landing in the coastal areas of Thanh Hoa - Ninh Binh provinces, then rapidly weakening on August 2, 2020.

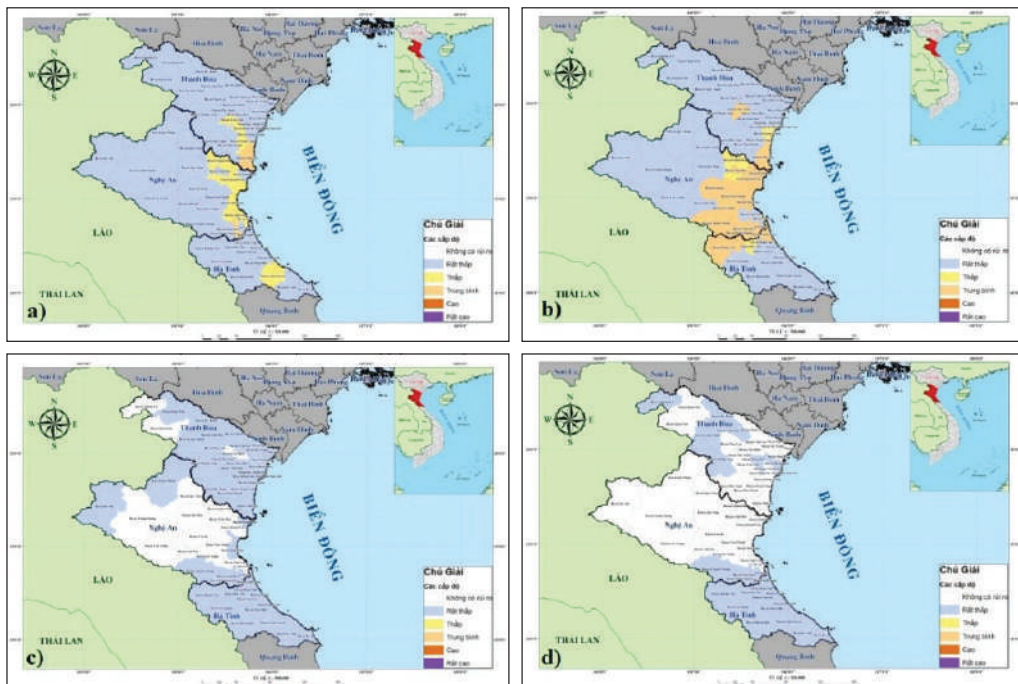


Figure 5. Warning maps of tropical storm Sinlaku at the forecast lead time of 6, 12, 18 and 24 hours from 12 UTC on August 1, 2020

4. Conclusion

The paper introduced a method to estimate TC risk using indicator-based approach. The proposed method is then adopted to develop the TC risk early warning system for North Central region. The estimation of TC risk demonstrates that risk level is different at provincial and district scales depending on local hazard, exposure and vulnerability. Even the Decision

No. 18/2021/QĐ-TTg provide a classification of TC risk from the Beaufort based TC wind category and for provincial resolution, it is valuable to identify TC risk at district level in a combination of hazardous factor, natural and social characteristics and resilience of the local areas. The evaluation in the pilot case study shows promising applicability of the proposed warning system in other areas.

Acknowledgement: This study is results of the state-level science and technology research project “Developing risk level warning system of tropical cyclone using formal forecasting reports, case study in North Central region”, code number KC.08.36/16-20.

References

1. Ahmed, B.; Kelman, I.; Fehr, H.; Saha, M. (2016). *Community resilience to cyclone disasters in coastal Bangladesh*. Sustainability, 8, 805.
2. Davidson, R.A.; Lambert, K.B. (2001). *Comparing the hurricane disaster risk of U.S. coastal counties*. Nat. Hazard. Rev., 2, pp-pp.
3. *Decision No. 18/2021/QĐ-TTg on detailed regulations on natural disaster risk levels*.
4. *Digital Typhoon: Typhoon Images and Information*. Available online: <http://agora.ex.nii.ac.jp/digital-typhoon/>.
5. Efron, B. (1987). “Better Bootstrap Confidence Intervals”, *J. Am. Stat. Assoc.*, 82, 171–185.
6. Einstein, H. (1988). “Landslide risk assessment procedure”, *Proceedings Fifth International Symposium on Landslides, Lausanne (Balkema)*, 2, 1075-1090.

7. Huong, H.T.L.; Hien, N.X.; Thuy, N.T.; Hang, V.T. (2020). "Pre-disaster assessment of flood risk for mid Central Viet Nam", *International Journal of Disaster Resilience in the Built Environment*. 1759-5908 DOI 10.1108/IJDRBE-06-2020-0065.
8. IPCC (2012). "Managing the risks of extreme events and disasters to Advance climate change adaptation". A special report of working groups I and II of the Int' governmental Panel on climate change. In: Field, C.B., Barros, et al, Cambridge University Press, Cambridge, UK, and New York, NY, USA, p. 582.
9. Joyce, K.E.; Belliss, S.E.; Samsonov, S.V.; McNeill, S.J.; Glassey, P.J. (2009). "A review of the status of satellite remote sensing and image processing techniques for mapping natural hazards and disasters". *Prog. Phys. Geogr.*, 33, 1-25.
10. Middelmann, M.H. (Eds) (2007). *Natural Hazards in Australia. Identifying Risk Analysis Requirements*, Geoscience Australia, Canberra.
11. MONRE (2016). *Scenarios of Climate change and sea level rise*. Viet Nam Publishing house of Natural Resources, Environment and Cartograph.
12. NCHMF National Centre for Hydro-Meteorological Forecasting (2018). *Characteristics of Viet Nam hydro-meteorology (in Viet Nameese)*.
13. Nang, T.Q.; Tien, T.T. (2020). "Evaluation of the tropical cyclone track forecasting skills of the combinatorial model system", *Viet Nam Journal of Hydro - Meteorology*, 717, 11-19 (Viet Nameese).
14. Hien, N.X. (2020). *Research the scientific basis for classifying risk levels for natural disasters in Viet Nam*, Final report of the scientific and technological research project at ministerial level, code number TNMT.2017.05.04, Viet Nam institute of Meteorology, Hydrology and Climate Change (Viet Nameese).
15. North, G.R.; Bell, T.L.; Cahalan, R.F.; Moeng, F.J. (1982). "Sampling errors in the estimation of empirical orthogonal functions", *Mon. Weather Rev.*, 110, 699-706.
16. North Central Hydro-Meteorological Station, Viet Nam Hydro-Meteorological Administration. <http://dkvbtb.gov.vn/>.
17. Quader, M.A.; Khan, A.U.; Kervyn, M. (2017). "Assessing Risks from Cyclones for Human Lives and Livelihoods in the Coastal Region of Bangladesh". *Int. J. Environ. Res. Public Health*, 14, 831.
18. *Statistic book of Thanh Hoa province (2018)*. Thanh Hoa Statistics Office (Viet Nameese).
19. *Statistic book of Nghe An province (2018)*. Nghe An Statistics Office (Viet Nameese).
20. *Statistic book of Ha Tinh province (2018)*. Ha Tinh Statistics Office (Viet Nameese).
21. Tien, D.D.; Thanh, N.D.; Mai H.T. (2013). "A study of the connection between tropical cyclone track and intensity errors in the WRF model", *Meteorol. Atmos. Phys.*, 122, 55-64.
22. Tien, D.D.; Thanh, N.D.; Chanh, K.Q.; Hang, N.T. (2016). "Surveying forecasting error and skill of the tropical cyclone track and intensity of forecasting centers and NWP models in the East Sea", *Viet Nam Journal of Hydro - Meteorology*, 661, 17-23 (Viet Nameese).
23. UNISDR (2009). *Terminology on disaster risk reduction*. <https://www.undrr.org/publication/2009-unisdr-terminology-disaster-risk-reduction>.
24. Wilks, D.S. (2006). *Statistical Methods in the Atmospheric Sciences*, Academic Press, pp. 704.
25. Yin, J.; Yin, Z.; Xu, S. (2013). "Composite risk assessment of typhoon-induced disaster for China's coastal area". *Nat. Hazards*, 69, 1423-1434.
26. Zhang, J.; Chen, Y. (2017). *Risk assessment of flood disaster induced by typhoon rainstorms in Guangdong province, China*. *Sustainability*, 11, 2738.

ASSESSING CLIMATE CHANGE RISK AND VULNERABILITY FOR AGRICULTURAL SECTOR IN HOA BINH PROVINCE

Le Ngoc Cau, Pham Van Sy, Ngo Thi Van Anh,
Le Van Quy, Mai Trong Hoang

Viet Nam Institute of Meteorology, Hydrology and Climate change

Received: 02 August 2021; Accepted: 24 August 2021

Abstract: *Hoa Binh is the Northern mountainous province of Viet Nam, with the economy still depends on agriculture. Hoa Binh province in general and the province's agricultural sector in particular have been affected by climate change. Under the climate change scenario, 2016, temperature and precipitation are increasing. This will put more pressure on the province's agricultural sector. This study, using climate change scenario information and documents and local data, assesses the vulnerability and risks of the provincial agricultural sector to climate change to 2030. The results show that some poor mountainous districts, dependent on agriculture, have high sensitivity and high risk, such as Luong Son, Lac Son, and Kimboi district. While Hoa Binh city has low vulnerability and low level of risk because of its small area of agricultural land, small proportion of agriculture in the economy, and high adaptability. In addition, the study also proposes some major solutions on planning, technology, capacity building and economy to minimize the impacts of climate change on districts with high vulnerability and risk.*

Keywords: *Hoa Binh province, climate change, vulnerability, risk.*

1. Introduction

Hoa Binh is the Northern mountainous province of Viet Nam, located at geographical coordinates from 20°39' to 21°08' North latitude; 104°48' to 104°51' East longitude, still facing many difficulties with low starting point in economic development. At present and in the coming years, agricultural production and rural economy of Hoa Binh will still occupy a very important position and make great contributions to the socio-economic development of Hoa Binh province. The province has branded agricultural products that are reaching far to meet the needs of domestic and international customers. According to the report of the Provincial Statistics Office, the province's gross domestic product (GRDP) (at 2010 constant prices) was estimated at 29,423.07 billion VND, an increase of 3.80% compared to 2019. In which, the agriculture,

forestry and fishery sector reached VND 6,387.23 billion, up 4.33%. The economic structure continues to shift in the right direction, with the proportion of agriculture, forestry and fishery 22.95%. The province's livestock industry is also gradually shifting towards large-scale production, the form of farms, concentrated farms, using high-yield breeds, changing husbandry methods, and ensuring disease safety [1, 2].

Recently, due to the impact of climate change, high mountainous areas are frequently affected by flash floods, landslides, forest fires, and droughts, causing adverse impacts on the environment, water resources, health, food security, especially the agricultural sector (crop, livestock) of the province. Specifically, the mountainous districts such as Da Bac, Mai Chau, and Cao Phong are often affected by flash floods and landslides, causing heavy damage to crops. In addition, Yen Thuy, Lac Son, and Tan Lac districts, which are in low mountainous terrain, also are affected by climate change. Climate change has been increasing drought, causing

Corresponding author: Le Ngoc Cau
E-mail: caukttv@gmail.com

water shortage for production and daily life, reducing crop and livestock productivity [3].

According to the scenario of climate change and sea level rise, 2016, by the middle of the century, the average annual temperature of Hoa Binh province will increase by 1.6 to 2.2 degrees for the RCP4.5 and RCP8.5 scenarios. Temperature increases at the end of century, century with levels from 2.3 to 3.9 degrees for scenarios RCP4.5 and RCP8.5. Similarly, rainfall will increase from about 12% to 21% in the middle and end of the century for both RCP4.5 and RCP8.5 scenarios. In addition, natural disasters such as storms, prolonged heat and drought are expected to increase in the province [4]. This will impact and huge risks for Hoa Binh province in general and agriculture in particular, therefore, this study conducted assessment of vulnerability and risk from the impact of Climate change, in particular temperature change and rainfall change, affects the agricultural sector of Hoa Binh province. In addition, the study also proposes some solutions to minimize the

impacts of climate change on districts with high vulnerability and risk. The research results will be a useful scientific basis for local authorities to take appropriate mitigation measures to reduce risks caused by climate change impacts.

2. Methodology

2.1. Vulnerability and risk assessment approach

Risk assessment is the starting point for climate change adaptation and disaster risk reduction and sharing. According to IPCC (2012) and SREX (2015) [5, 6, 7, 8] risk is composed of 3 elements (Figure 1):

- (1) Hazard (H: Hazard).
- (2) Exposure to hazards (E: Exposure).
- (3) Vulnerability (V: Vulnerability).

If one of the three elements is missing, there is no natural disaster risk. The formula for calculating disaster risk is expressed in the following expression:

$$R = f(H, E, V)$$

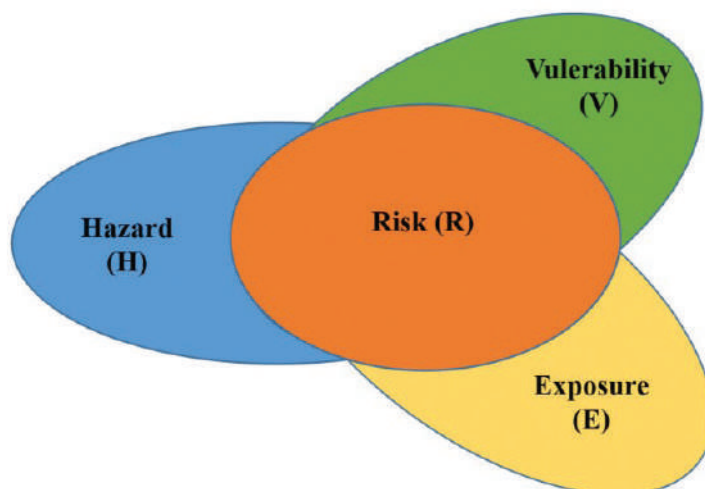


Figure 1. IPCC's approach to risk identification

Vulnerability (V) is expressed mathematically as follows:

$$V = f(S, AC)$$

In which: *S* is sensitivity; and *AC* is adaptive capacity.

2.2. Selection of indicators for vulnerability and risk assessment for the agricultural sector

The change in temperature, precipitation due to climate change has a big impact on growth, productivity, seasonality of crops, increases the risk of disease outbreaks and greatly affects the reproduction and growth of aquatic species.

Within the framework of the study, the vulnerability and risk assessment method is based on calculating the vulnerability index (V) from the vulnerability indicators as sensitivity (S) and adaptive capacity (AC), hazard (H) and exposure (E) via component indicators. Therefore, the development of a set of vulnerability and risk indicators is very important, it must characterize the sensitivity and adaptive capacity of the assessed object, and the characteristics of the hazard affecting that object. This is a method of assessing disaster risk and quantitative risk, comparing localities (districts) in the province with each other to determine which localities are more vulnerable to climate change.

The selection of the vulnerability and risk indicators is based on consideration of climate change scenarios, documents and secondary socio-economic situation information available at the provincial and district levels (such as Yearbook, statistics, general reports of the industry...) and combined with the analysis of primary survey information in the locality (direct interview by questionnaire, expert consultation...), especially information on the capacity of localities to adapt to climate change.

By synthesizing and evaluating the collected data, the study has selected a set of indicators to assess the climate change vulnerability and risk due to temperature and rainfall changes for the agricultural sector up to 2030 as presented in Appendix A1 - A4.

3. Results

3.1. Assessment of Vulnerability to climate change of the agricultural sector of Hoa Binh province

Sensitivity: the agricultural sector of Hoa Binh province is characterized by a relatively high proportion of the province's economy (about 13 - 22%), however the value of agricultural production is not high due to high productivity and production level is still low. The crop sector plays a major role in the structure of the agricultural sector. However, in recent years and in the coming time, the agricultural sector of this province has gradually changed its structure towards improving the value and efficiency of

production, transforming from small-scale farming to concentrated industrial crops and fruit trees, gradually increasing the proportion of livestock and aquaculture in the structure of the agricultural sector. The agricultural sector is inherently very sensitive to the impacts of climate change such as temperature changes, rainfall changes, floods, landslides... In which, cultivation is the most sensitive field due to farming; Plant growth is highly dependent on natural conditions. Moreover, Hoa Binh province has a high altitude and steep slope, so it is more difficult for agricultural cultivation to supply water for irrigation, to prevent drought and soil erosion. Due to limited capital combined with difficult mountainous terrain conditions, investment in infrastructure for the agricultural sector in this area such as irrigation canals has not met the demand. In general, the agricultural production value of Hoa Binh province has not developed commensurate with its potential, and the production efficiency is not high. However, agriculture is still the main source of income for the people and makes an important contribution to the economy of the province. Thus, the agricultural sector of Hoa Binh province is sensitive to climate change because the province's economy and people's income depend heavily on agriculture. Specifically, districts with high agricultural sensitivity to climate change are Luong Son, Tan Lac and Lac Son districts (Table 1 & 2).

Adaptive capacity: In general, the city and some districts have been selected by the state and international NGOs to implement a number of adaptation-related projects and programs. Climate change, the awareness as well as actions of people and local authorities on climate change adaptation is better. In addition, the ability to adapt to climate change is also reflected in the economic conditions of the people. Besides, in the field of agriculture, it is very important to change the needs of crops, livestock and crops to suit changing climate conditions. In the context of climate change like today, with the trend of average temperature increasing, the frequency of occurrence of severe heat waves and even severe cold spells has also increased,

the rainy season and rainfall in each region are also increasing. The change leads to the unsuitability of the previous traditional crop, livestock and crop structure. Faced with this problem, the agricultural sector of each locality needs to study the specific conditions of their locality in order to take specific actions to adapt to the climate change situation. For example, research on changing plant structure, choosing to replace with drought-tolerant and flood-tolerant varieties. Or research on changing crops, farming techniques such as 3 decrease 3 increase, alternate wet-dry irrigation, fruit tree planting model, industrial plants for export, etc. to increase production efficiency and adapt to climate change (Table 1 & 2).

Vulnerability: The results of vulnerability assessment pointed out that the Hoa Binh city

has low agricultural vulnerability to Climate Change. Due to Hoa Binh city has a low level of agricultural sensitivity (small agricultural land area, agriculture only accounts for a small proportion of the economy) and at the same time, has high adaptability, so the combined vulnerability to climate change is only at low level. Meanwhile, the poor and remote districts with large agricultural land, their economy dependent on agriculture and poor irrigation such as Luong Son, Tan Lac, Lac Son, Lac Thuy districts are sensitive. At the same time, the adaptive capacity is low (low income, ability to change crop structure, low crop, limited awareness of climate change) leading to a high degree of vulnerability to climate change. The remaining districts have moderate agricultural vulnerability to climate change (Figure 2 and Table 1).

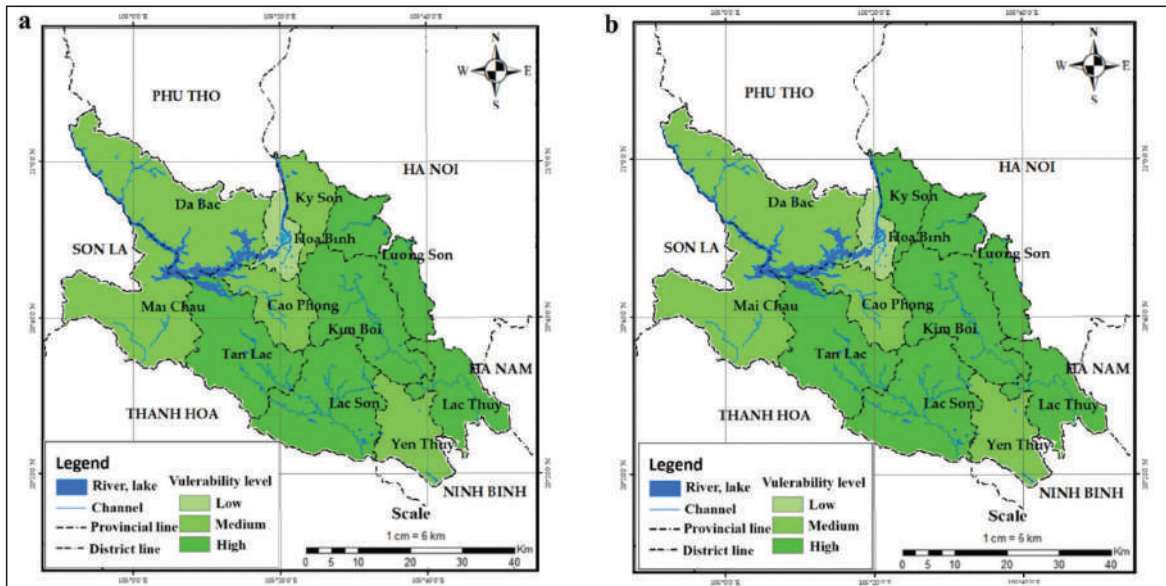


Figure 2. Map of agricultural vulnerability to climate change for year 2030. (a) due to the change of temperature and (b) due to the change of rainfall

3.2. Assessment of Risk to climate change of the agricultural sector of Hoa Binh province

Hazard: According to the climate change scenarios for the RCP 4.5 scenario, by 2030, it is shown that Ky Son, Luong Son and Da Bac districts have a high degree of danger due to temperature change from high to very high due to the changing trend. Annual average and extreme temperature changes are higher than in other

districts, Ky Son, Kim Boi and Luong Son districts have a high level of danger due to the change in rainfall from high to very high due to the trend of changing annual rainfall, the maximum 1- and 5-day rainfall changes increase (Table 1 & 2).

Exposure: Lac Son district has an area of agricultural land is very high (13127 ha), the area of aquaculture large (501 ha) and the large number of cattle and poultry, so the level of

exposure of the district is facing a very high level of hazard. Next is the Luong Son district which has a high level of hazard. The remaining districts mostly level from moderate to very low (Table 1 & 2).

Risk: The results show that, for temperature change, Hoa Binh province has 2 districts with high risk including Luong Son and Lac Son, because Luong Son district has a very high risk due to temperature change, and both exposure and vulnerability are high. For Lac Son district, although the hazard level is only moderate, the vulnerability is high and the exposure level is very high (a large area of agricultural and aquaculture land, a large number of cattle and poultry are abundant and the canal system is poor). Hoa Binh city has a very low level of risk because the city has the least agricultural land area (2191 ha) and the number of livestock and poultry is not much. In addition, as a mountainous district with a small area of aquaculture, the number of livestock and poultry is not much, the level of danger to temperature changes is not high, so the risk level is low. The remaining districts have a moderate level of risk due to

temperature change (Figure 3 and Table 1 & 2).

For rainfall change: Luong Son district has a high level of risk, due to its high tendency to change rainfall, along with high exposure and vulnerability (Luong Son district is one of the poorest districts in the world). In remote areas, large agricultural land, poor irrigation system, Kim Boi and Lac Son districts also have a high level of risk due to changes in rainfall. For Kim Boi district, the level of risk is high. This is because it is also a poor district, with a high degree of sensitivity and low adaptability, and a high level of danger. As for Lac Son district, although it has a low level of hazard due to changes in rainfall but this is a poor district with poor adaptability, a purely agricultural district with a large area of agricultural land, aquaculture and livestock and poultry raising, so exposure is very high to hazards. Hoa Binh city and Mai Chau district are two areas with low risk from rainfall variability because the level of hazard, exposure and vulnerability is only low to moderate. Ky Son, Lacthuy districts, etc. have a medium level of risk due to changes in rainfall (Figure 3 and Table 1 & 2).

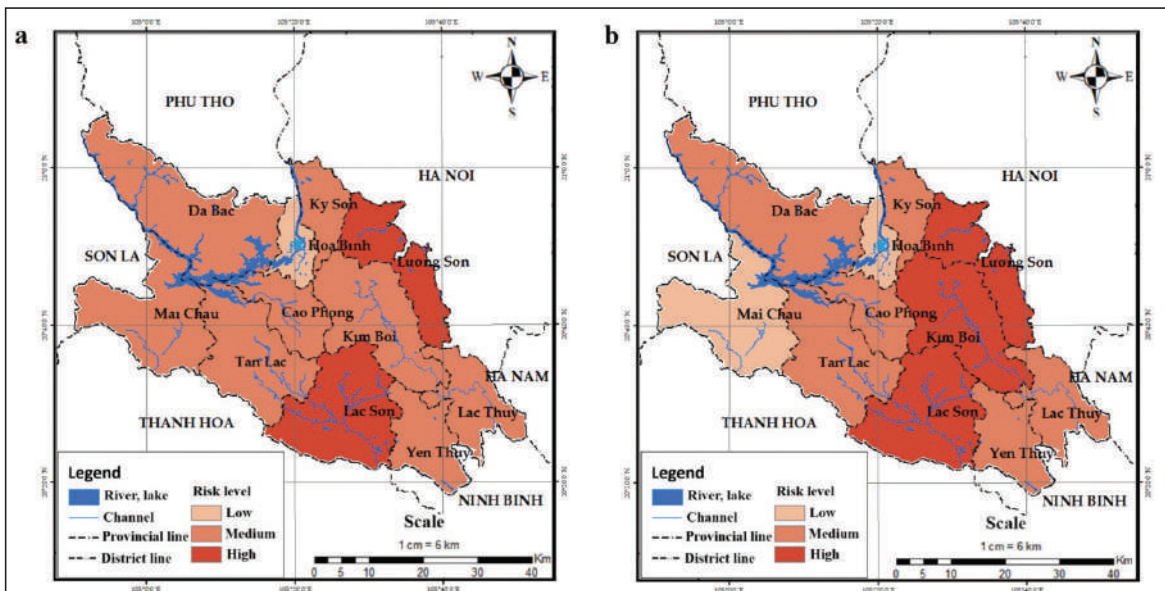


Figure 3. Map of agricultural risk to climate change for year 2030. (a) due to the change of temperature and (b) due to the change of rainfall

Table 1. Levels of agricultural sensitivity, adaptive capacity, vulnerability, hazard, exposure and risk due to temperature change of the districts in Hoa Binh province

District	S	Level (S)	AC	Level (AC)	V	Level (V)	H	Level (H)	E	Level E	R	Level (R)
Hoa Binh city	0.25	L	0.33	H	0.29	L	0.40	L	0.02	VL	0.24	L
Da Bac	0.48	M	0.58	M	0.53	M	0.81	H	0.24	L	0.53	M
Ky Son	0.35	L	0.85	VL	0.60	M	0.77	H	0.06	VL	0.48	M
Luong Son	0.56	M	0.78	L	0.67	H	0.88	H	0.70	H	0.75	H
Kim Boi	0.59	M	0.70	L	0.65	H	0.54	M	0.50	M	0.56	M
Cao Phong	0.42	M	0.54	M	0.48	M	0.44	M	0.25	L	0.39	L
Tan Lac	0.66	H	0.65	L	0.66	H	0.48	M	0.52	M	0.55	M
Mai Chau	0.37	L	0.69	L	0.53	M	0.35	L	0.36	L	0.41	M
Lac Son	0.70	H	0.72	L	0.71	H	0.58	M	0.94	H	0.74	H
Yen Thuy	0.41	M	0.52	M	0.47	M	0.37	L	0.43	M	0.42	M
Lac Thuy	0.58	M	0.68	L	0.63	H	0.36	L	0.57	M	0.52	M

Note: VL is very low; L is low; M is medium; H is high and VH is very high

Table 2. Levels of agricultural sensitivity, adaptive capacity, vulnerability, hazard, exposure and risk due to rainfall change of the districts in Hoa Binh province

District	S	Level (S)	AC	Level (AC)	V	Level (V)	H	Level (H)	E	Level E	R	Level (R)
Hoa Binh city	0.30	L	0.36	H	0.33	L	0.55	M	0.03	VL	0.30	L
Da Bac	0.42	M	0.67	L	0.54	M	0.49	M	0.23	L	0.42	M
Ky Son	0.40	M	0.90	VL	0.65	H	0.77	H	0.05	VL	0.49	M
Luong Son	0.62	H	0.87	VL	0.74	H	0.97	H	0.69	H	0.79	H
Kim Boi	0.62	H	0.72	L	0.67	H	0.73	H	0.49	M	0.63	H
Cao Phong	0.42	M	0.61	L	0.51	M	0.53	M	0.24	L	0.43	M
Tan Lac	0.66	H	0.71	L	0.69	H	0.52	M	0.50	M	0.57	M
Mai Chau	0.26	L	0.70	L	0.48	M	0.31	L	0.34	L	0.38	L
Lac Son	0.71	H	0.79	L	0.75	H	0.31	L	0.90	H	0.66	H
Yen Thuy	0.47	M	0.59	M	0.53	M	0.39	L	0.46	M	0.46	M
Lac Thuy	0.68	H	0.72	L	0.70	H	0.37	L	0.53	M	0.53	M

Note: VL is very low; L is low; M is medium; H is high and VH is very high

3.3. Some solutions applied to districts with high vulnerability and high risk due to climate change

According to the results of the vulnerability and risk assessment, the districts with a high level of vulnerability and risk due to climate change in agriculture in Hoa Binh province include Luong Son, Tan Lac, Lac Son, Lac Thuy and Kim Boi districts. Therefore, these districts

need to implement some solutions to improve the adaptive capacity and reduce the effect of climate change. Based on the guidelines on building application solutions with climate change, a number of application solutions can be considered and applied to districts with high vulnerability and high-risk levels in Hoa Binh province, which are:

- Solutions on planning and technology

(Transformation of structure and services of susceptible crops; Researching and creating new plant varieties and livestock to adapt to weather changes, disease sensing; Application of crops with advanced, modern and high-tech production models; agricultural model 4.0);

- Solutions for capacity building (Communication, training, technical guidance for farmers; Training and capacity building for sector managers; Upgrading the forecasting and warning system early, preventing risks and losses);

- Economic solutions (diversification of capital sources for climate change adaptation (ODA, international funding, private sector, enterprises); applying financial policies (price stabilization, agricultural insurance, etc.) Districts need to consider and consider criteria when choosing adaptation solutions, depending on the priorities, strategies, orientations of each district and the sharing of responsibilities of the stakeholders. Solutions need to ensure feasibility, be suitable with available resources, characteristics of each locality, ensure flexibility, be able to adjust when there are changes in climate factors; integrated and linked with existing local agricultural development plans, plans and policies and related fields.

4. Conclusions

Hoa Binh is a province that has been affected by climate change. Under the scenarios of climate change and sea level rise, 2016, temperature and rainfall tend to increase in the mid and end of the century, will be a great influence with the province in general and agriculture, in particular. Based on local data, climate change scenarios, vulnerability and risk

assessment approaches, the main results of the study are as follows:

1. The poor, remote districts have high vulnerability due to large agricultural land area, economy dependent on agriculture and weak irrigation system such as Luong Son, Tan Lac, Lac Son, Lac Thuy district. Their sensitivity is moderate to high, while their adaptive capacity is low. Meanwhile, Hoa Binh city has a low level of vulnerability due to low agricultural sensitivity because of the small area of agricultural land, agriculture accounts for only a small proportion of the economy, and at the same time, has high adaptability.

2. The districts of Luong Son and Lac Son and Kim Boi are at high risk because they are agriculturally dependent, have high exposure to hazards, and are highly vulnerable. Meanwhile, Hoa Binh city and Mai Chau district 2 area with the level of risk due to climate change at a low level by the level of hazard, exposure and vulnerability only at low to medium. The remaining districts such as Da Bac, Ky Son, Lac Thuy, etc. have medium level of risk.

3. Districts with high level and high risk due to climate change in agriculture in Hoa Binh province include: Luong Son, Tan Lac, Lac Son, Lac Thuy and Kim Boi need to take some measures such as: Researching and creating new plant varieties and livestock to adapt to weather changes, disease sensing; Upgrading the forecasting and warning system early, preventing risks and losses; Districts need to consider and consider criteria when choosing adaptation solutions, depending on the priorities, strategies, orientations of each district and the sharing of responsibilities of the stakeholders.

References

1. Trung Long (2020), *"Hoa Binh: Create strong and comprehensive changes in the field of agriculture"*, <http://consosukien.vn>.
2. Trung Han Dat (2018), *"Hoa Binh accelerates the restructuring of the agricultural sector"*, <https://nhandan.vn>.
3. Thuy An (2020), *"Press conference to announce socio-economic statistics for 2020"*, [http://Hoa Binh.gov.vn](http://HoaBinh.gov.vn).
4. Ministry of Natural Resources and Environment (2016), *Climate change scenario, sea level rise for*

- Viet Nam*, Viet Nam Publishing House of Natural Resources, Environment and Cartography, Ha Noi.
5. IPCC (2007), *AR4 Climate Change 2007: Synthesis Report. Contribution of Working Groups I, II and III to the Fourth Assessment Report of the Intergovernmental Panel on Climate Change Core Writing Team*, Cambridge University Press, Cambridge, UK, and New York, USA.
 6. IPCC (2014), *AR5 Climate change 2014: Impact, Adaptation and Vulnerability*. Working group II- IPCC, Cambridge University Press, Cambridge, UK, and New York, USA.
 7. IPCC (2012), *"Managing the Risks of Extreme Events and Disasters to Advance Climate Change Adaptation". A Special Report of Working Groups I and II of the Intergovernmental Panel on Climate Change*, Cambridge University Press, Cambridge, UK, and New York, USA.
 8. IMHEN and UNDP (2015), *SREX: Viet Nam Special Report on Managing the Risks of Extreme Events and Disasters to Advance Climate Change Adaptation*, Viet Nam Publishing House of Natural Resources, Environment and Cartography, Ha Noi.

Table A1. Data on sensitivity indicators for agricultural sector of districts in Hoa Binh province

VULNERABILITY INDICATORS		SENSITIVITY									
Component indicators	District	S1	S2	S3	S4	S5	S6	S7	S8	S9	S10
No	Province	Average area of agricultural land per capita (m ² /person)	Rice yield (ton/ha)	Production of grain crops (tons)	Aquacultural production (tons)	Pork production output (tons)	Total value of agricultural production (billion VND)	GDP contribution of agriculture sector (%)	Number of non-agricultural individual economic establishments	Ratio of solidified canal length (%)	Average terrain elevation (m)
1	Hoa Binh	167	51	8259	948	2012	299	4.38	8240	76	171
2	Hoa Binh	739	49	36045	1180	2368	824	25.68	1556	72	476
3	Hoa Binh	565	52	18070	179	3917	460	29.62	1417	70	173
4	Hoa Binh	305	55	29045	1111	11962	1993	13.75	3756	112	185
5	Hoa Binh	564	54	53540	506	9837	1351	40.81	3924	50	238
6	Hoa Binh	1427	54	15987	612	2898	881	47.97	1598	70	349
7	Hoa Binh	917	54	47720	1155	7530	2322	35.07	4068	26	341
8	Hoa Binh	1335	47	31217	242	2480	856	41.76	2313	77	607
9	Hoa Binh	631	55	75539	702	12554	1808	46.82	5015	45	262
10	Hoa Binh	850	51	31377	622	6316	822	38.86	2764	69	139

Table A2. Data on adaptive capacity indicators for agricultural sector of districts in Hoa Binh province

RISK INDICATORS		ADAPTIVE CAPACITY					
Component indicators		AC1	AC2	AC3	AC4	AC5	AC6
No	Province District	Average income per capita/year (million dong)	Ability to change the structure of crops, livestock and crops to adapt to climate change (% of area)	Number of agricultural staffs and veterinary trained on climate change	High school graduation rate (%)	Community's awareness about climate change (%)	Awareness and actions of the local government to respond to climate change
1	Hoa Binh Hoa Binh city	70	0	8	98.5	97.26	8.51
2	Hoa Binh Da Bac	27.2	3.1	5	94.9	82.05	3.70
3	Hoa Binh Ky Son	52	3.2	3	73.9	98.15	15.14
4	Hoa Binh Luong Son	47.5	1.5	4	90.6	93.19	15.17
5	Hoa Binh Kim Boi	32.5	2.1	6	98.7	93.40	14.70
6	Hoa Binh Cao Phong	48	3.6	7	99.7	93.86	11.90
7	Hoa Binh Tan Lac	34.21	1.9	8	97.79	92.39	6.65
8	Hoa Binh Mai Chau	27	0.94	10	97.19	89.43	8.33
9	Hoa Binh Lac Son	38.8	2.8	4	95.5	90.32	7.10
10	Hoa Binh Yen Thuy	32.4	12.0	5	96.7	94.61	14.32

Table A3. Data on Hazard indicators for agricultural sector of districts in Hoa Binh province (2030)

RISK INDICATORS		HAZARD								
		Temperature change			Rainfall change					
No	Province	District	H1	H2	H3	H1	H2	H3		
			annual temperature change (degrees/year)	Minimum temperature change (degrees/feet)	Maximum temperature change (degrees/grips)	Change in average annual rainfall (mm/year)	Maximum 1-day rainfall change (mm/year)	The largest 5-day rainfall change (mm/year)		
1	Hoa Binh	Hoa Binh city	1.02	0.93	1.30	7.23	29.27	26.33		
2	Hoa Binh	Da Bac	1.05	0.96	1.31	7.21	28.21	26.24		
3	Hoa Binh	Ky Son	1.05	0.96	1.30	8.04	30.69	28.82		
4	Hoa Binh	Luong Son	1.05	0.99	1.29	8.58	32.39	30.72		
5	Hoa Binh	Kim Boi	1.01	0.97	1.29	7.11	33.13	27.10		
6	Hoa Binh	Cao Phong	1.01	0.94	1.30	7.17	29.85	25.59		
7	Hoa Binh	Tan Lac	1.01	0.96	1.30	7.48	29.29	25.11		
8	Hoa Binh	Mai Chau	1.01	0.92	1.30	7.37	25.11	24.61		
9	Hoa Binh	Lac Son	1.00	0.99	1.29	6.47	29.14	22.40		
10	Hoa Binh	Yen Thuy	1.00	0.99	1.25	5.20	31.47	24.51		

Table A4. Data on Exposure indicators for agricultural sector of districts in Hoa Binh province (2030)

RISK INDICATORS			EXPOSURE			
Component indicators			E1	E2	E3	E4
No	Province	District	Area of agricultural land (ha)	Aquaculture area (ha)	Number of cattle	Number of poultry
1	Hoa Binh	Hoa Binh city	2191	171	14254	230511
2	Hoa Binh	Da Bac	6485	108	47333	347987
3	Hoa Binh	Ky Son	2782	105	34103	309844
4	Hoa Binh	Luong Son	7200	400	96800	1500000
5	Hoa Binh	Kim Boi	9254	211	94354	860552
6	Hoa Binh	Cao Phong	8588	80	31811	255235
7	Hoa Binh	Tan Lac	10940	154	82431	704200
8	Hoa Binh	Mai Chau	10229	82	43998	276681
9	Hoa Binh	Lac Son	13127	541	138010	988029
10	Hoa Binh	Yen Thuy	7742	468	62177	763685

REVIEW OF ASSESSMENT OF AGRICULTURAL METEOROLOGY IN VIET NAM CROPS 2020

Doan Thi The⁽¹⁾, Duong Hai Yen⁽¹⁾, Nguyen Van Son⁽¹⁾, Le Thi Thu⁽²⁾,
Nguyen Hong Son⁽¹⁾, Le Thi Thu Ha⁽¹⁾

⁽¹⁾Viet Nam Institute of Meteorology, Hydrology and Climate change

⁽²⁾Tokyo University, Japan

Received: 12 September 2021; Accepted: 29 September 2021

Abstract: Assessment of the agricultural meteorology has a critical role in agriculture production, especially in Viet Nam, where the agricultural products play a majority part in its economy. In addition to that, more frequent and intense changes in climate patterns as a result of the global warming have been recently increasing. This study therefore attempts to provide an assessment as an input for sustainable solutions to cultivation, improvement and protection of climate resources that facilitate the crop production.

The climatic impacts on each cropping pattern vary by the growth cycles of different crops. In this study, the authors generally review agricultural meteorology in Viet Nam by applying the comprehensive methodology of the seasonal characteristics of climate factors, based on the meteorological and statistical data of the General Department of Meteorology and Hydrology of Viet Nam (MONRE), in order to determine the changes and characteristics. The characteristics of climate factors according to each season throughout the territory of Viet Nam in 2020, are the basis for assessing the agro-climate for the next production crops.

Keywords: Agricultural meteorology, Viet Nam crops 2020, crops season, climate factors.

1. Introduction

Agriculture is an important sector of the Viet Nam economy [6, 10, 13]. The share of agriculture, forestry, and fishery sector in 2020 GDP preliminarily reached 14.85% [10]. Generally, in 2016 - 2020, the production of cereals reached 240.7 million tons. The gross output per hectare of arable land witnessed 102.8 million VND per hectare in 2020 [10]. Agriculture, forestry, and fishery production in 2020 faced many difficulties due to the impact of drought, saline intrusion, and floods; the complicated and unpredictable developments of the COVID-19 pandemic that caused effecting to the export, import actives of agricultural products [10]. Agricultural production depends greatly on climate conditions, so the direct and long-term challenge to agricultural production is the impact of climate change - Viet Nam is

considered as one of the countries most affected by climate change [3, 7]. Climate change has created challenges for the agricultural sector - and will continue to do so. Climate change-induced increases in temperatures, rainfall variation, and the frequency and intensity of extreme weather events are adding to pressures on global agricultural and food systems. Climate change is expected to negatively affect crop and livestock production systems in most regions, although some countries may benefit from the changing conditions. The changing climate is also adding to resource problems, such as water scarcity, pollution, and soil degradation [1, 5, 13]. Therefore, studying the characteristics of agro-climate is necessary to develop agriculture in harmony with the specific natural conditions of each region and adapt to abnormal changes due to the impact of climate change [1, 4, 5].

In 2020, The effects of climate change had appeared in most of Viet Nam, most often in the Central Coast zone with the weather and climate

Corresponding author: Doan Thi The
E-mail: doanthe00@gmail.com

extremes events such as heavy rains, floods, flash floods, landslides and tornadoes, hail. The Northern in Viet Nam, was the record-breaking heat-wave in the past 27 years and rare hailstorms. According to Viet Nam Disaster Management Authority, Ministry of Agriculture and Rural Development in 2020 and General Statistics Office of Viet Nam, natural disasters consecutively and complicated occurred including 14 storms; 265 thunderstorms, whirlwinds, heavy rains; 120 floods, flash floods, landslides and droughts, saltwater intrusion caused 379 deaths and missing, 1,060 injuries; 4.3 thousand houses collapsed and swept away; 594.9 thousand houses were damaged; nearly 269 thousand hectares of rice and 134.9 thousand hectares of arable crop were damaged; 38.6 thousand cattle and 4.1 million poultry died. Total property loss was estimated at 39.1 trillion VND, of which damage caused by the storms and flood was 32.3 trillion VND (accounting for 82.8% of total loss) [8, 10]. In the socio-economic situation in the fourth quarter and the whole year 2020 by Viet Nam General Statistics Office[9], rice production was estimated at 42.69 million tons, down 806.6 thousand tons over the previous year. In comparison with the crop of 2019, the country's winter-spring paddy production reached 19.9 million tons, a drop of 593.5 thousand tons; the cultivated area this year was at 3,024.1 thousand hectares, a decrease of 100.3 thousand hectares; the summer-autumn paddy crop yield in 2020 reached higher results, but due to the effects of drought, salinity, and change of use purposes on rice land, the area of cultivation decreased, resulting in total output reduced. This year, the country cultivated 1,945.1 thousand hectares of summer-autumn paddy, a decrease of 64.5 thousand hectares compared to 2019; the yield reached 55.2 quintal/hectare, an increase of 0.7 quintal/hectare; the total production reached 10.74 million tons, a drop of 205.4 thousand tons. Of which, production of the Mekong River Delta reached 8.46 million tons, a fall of 219.1 thousand tons; The results of winter rice production in 2020 increased in yield, but due to the cultivated decreased, the

total output of whole crop declined. The whole country's winter rice cultivated area reached 1,584.6 thousand hectares, a fall of 27 thousand hectares compared to the crop in 2019; the yield reached 51 quintal/ha, increased by 0.7 quintal/ha; the production reached 8.08 million tons, down 20.7 thousand tons; Results of production of crops and some annual crops: maize output reached 4.59 million tons, a decrease of 140.3 thousand tons compared to 2019; sweet potato reached 1.37 million tons, down 57.5 thousand tons; sugarcane reached 11.88 million tons, down 3.44 million tons; cassava reached 10.49 million tons, an increase of 313 thousand tons; groundnut reached 425.5 thousand tons, down 17.1 thousand tons; soybean reached 65.7 thousand tons, down 11.6 thousand tons; the output of vegetables of all kinds reached 18.33 million tons, an increase of 339.1 thousand tons [9, 10].

The influence of weather and climate on the growth, development, and yield of crops is very obvious. According to the list of agro-climate and agro-ecological indicators developed by FAO for the tropical monsoon climate area of Southeast Asia, a specific example. Rice in the sprouting stage, with a suitable temperature from 22 - 18°C, a suitable temperature from 14 - 18°C, an unsuitable temperature below 7°C. For the growth stage, the most suitable temperature for rice to develop is 32 - 30°C; at the harvest stage, it is 33°C. Rainfall is suitable from 200 - 400 mm. The humidity in the germination stage is from 60 - 75°C, in the development stage from 37 - 65%. With the characteristics of climate factors outside this threshold, rice plants may be slow to grow, yield low, or die.

In general, agricultural production recommendations in Viet Nam are based on agro-climatic information on a large scale, such as regional or provincial levels [11, 12]. At this scale, the recommendations provide specific climatic factors both in time and space. In terms of time, advice on planting season is often based on multi-year average meteorological data. Therefore, recommendations are being built based on short-term (weather) and medium

-term (month, season, crop) forecast information. In terms of space, recommending agricultural production based on administrative boundaries is a method that is easily accessible to farmers because of the habits in receiving information in Viet Nam. In this article, the authors have synthesized, evaluated, and analyzed the agricultural climate conditions of Viet Nam in 2020 for crops. The data and methods of analysis are presented in section 2. The analysis by month and production season is presented in section 3 of this paper.

2. Data and Methods

2.1. Data

To assess meteorological conditions, monthly and yearly meteorological data at Viet Nam's meteorological stations were collected from 1961 to 2020, including mean temperature (Tmean), maximum temperature (Tmax), minimum temperature (Tmin), average air humidity (Umean), number of hours of sunshine (SH), precipitation (P). Data was provided by the Ministry of Natural Resources and Environment by 150 measuring stations [2] (Figure 1).

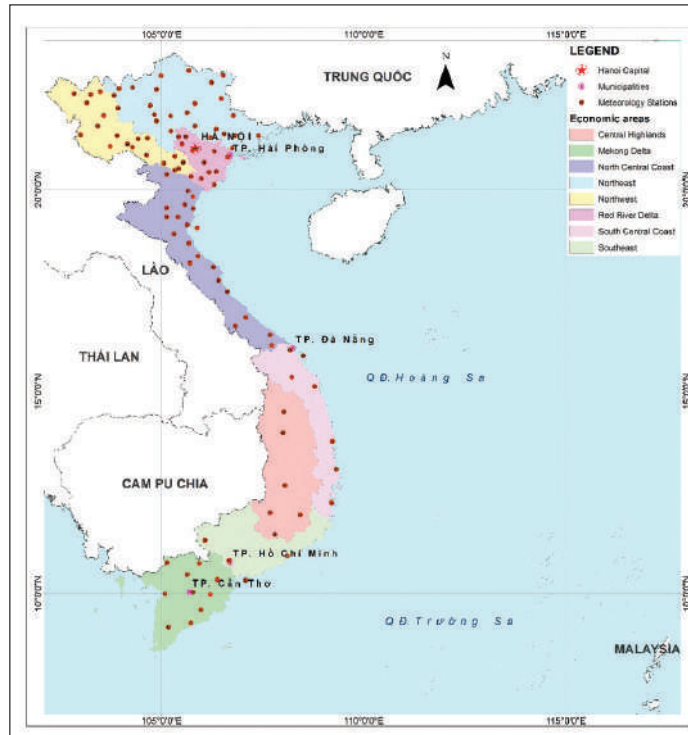


Figure 1. Meteorological Stations in Viet Nam

2.2. Method for assessment

The authors use basic formulas used in hydrometeorology to assess climate conditions, including:

- The average value for many years:

$$\bar{x} = a_1 = \frac{1}{n} \sum_{t=1}^n x_t \quad (1)$$

- The differences in meteorological characteristics (temperature, precipitation,...) compared to the average of many years:

$$v_a = \frac{1}{n} \sum_{t=1}^n |x_t - \bar{x}| \quad (2)$$

- Maximum value (Max):

$$Maxx_t = Max (x_1, x_2, \dots, x_n) \quad (3)$$

- Minimum value (Min):

$$Minx_t = Min (x_1, x_2, \dots, x_n) \quad (4)$$

In which:

x_t is the the time series value (actual data) at period t .

t is time series ($t= 1, 2, \dots, n-1, n$);

- The linear regression method is used to determine the trend and degree of variation of climate extremes:

$$X = a_0 + a_1 t \quad (5)$$

In which:

x is the the time series value (actual data) at period t .

t is time ($t= 1, 2, \dots, n-1, n$);

The slope of the line is a_1 , and a_0 is the intercept. If $a_1 > 0$ then the series tends to increase, if $a_1 < 0$ then the series tends to decrease.

To assess climate conditions base on 7 different regions, namely the Northwest (B1), Northeast (B2), North Delta (B3), North Central (B4), South Central (N1), Central Highlands (N2), and the South and Mekong Delta (N3) (Figure 1) and divided by 2 seasons of crops are the winter-spring cropping season and Main season (summer-autumn cropping season) in 2020.

3. Results and Discussions

In response to Viet Nam's tropical climate zone characteristics, the crops are produced

in two main seasons called winter-spring and main cropping (summer-autumn season). Rice is the major crop grown in both Red River (RRD) and Mekong Deltas (MKD) of Viet Nam, which occupies two-thirds of the total field area and presents up to 70 percent of the rice production nationwide.

3.1. Assessment of agrometeorological conditions in winter-spring 2020

3.1.1. Detailed evolution of meteorological conditions

The winter-spring season is the most important cropping among others around the year (starting from November to April of the following year), responsible for more than 40% of the whole year's growing area, giving the highest yield in all cropping seasons and presenting roughly 45% - 47% of the total yearly production output [10]. For the above reasons, it is critical to assess the detailed evolution of meteorological conditions in the winter-spring crop and provide practical information for proper production management and implementation of the annual agricultural produce in general and rice yield in particular.

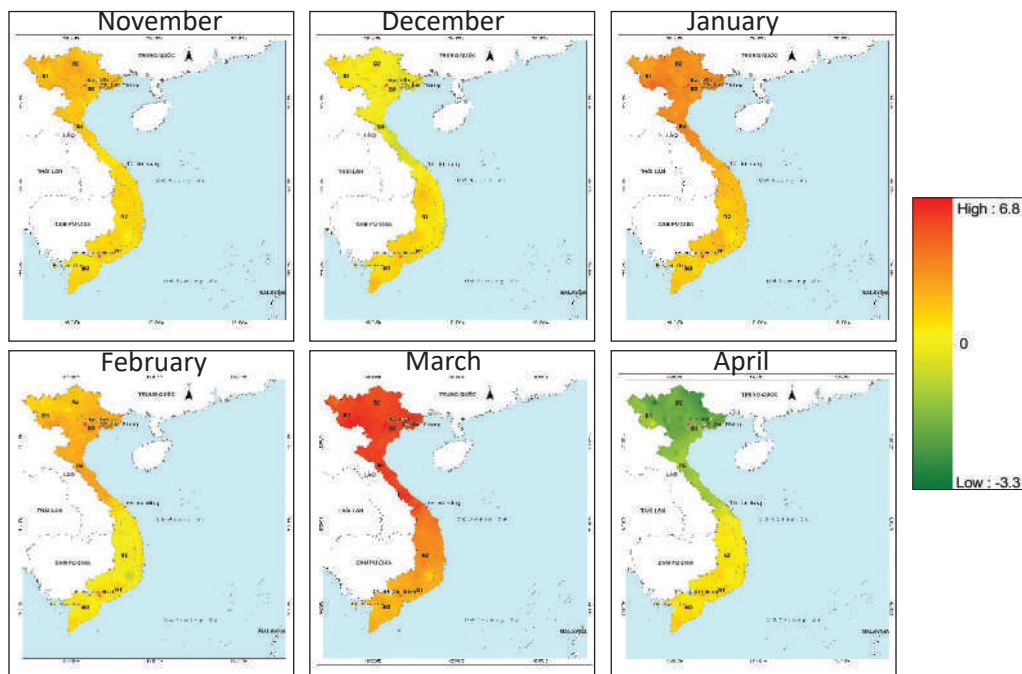


Figure 2. Temperature mapping relative to the average temperatures over many years in the winter-spring season 2020

Figure 2 shows the Temperature difference in the winter-spring season months in 2020 with an average of many years. The average temperature observed during the first month of the crop (from December 2019 to January 2020) was always (approximately between 0.2°C and 4.8°C) higher than the average temperatures recorded over recent years. Starting February 2020, the overall surface temperature across the country continued fluctuating around the average temperatures recorded over many recent years between -0.9°C and 3.3°C. In the middle and late periods of the crop, the temperature continued to increase and is higher than the average temperatures recorded over many recent years

(from 0.2°C to 5.7°C).

Figure 3 illustrates the difference in precipitation in winter-spring season months in 2020 with an average of many years. In some mountainous regions and Northern midlands, the high daily rainfall often varies between 3 mm and 25 mm; the highest of 39 mm occurs on February 3 in Bac Can. The number of rainy days of one month is commonly from 3 to 21 days. The number of consecutive rainy days happens from 1 to 14 days. The number of consecutive days without rain is common from 3 to 18 days. In some Southern regions, monthly rainfall ranges from 6 mm to roughly 51 mm, while there is no rain in some provinces such as Phan Thiet and Phan Rang.

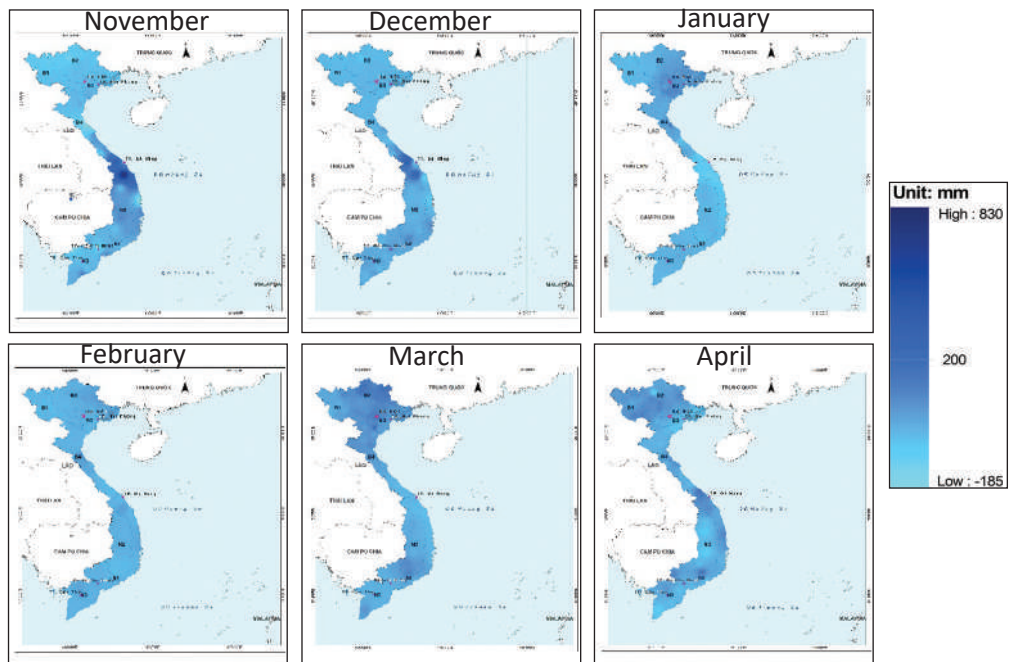


Figure 3. The difference of precipitation in winter-spring season months in 2020 with the average of many years

Most of the regions in Viet Nam normally get the total number of sunshine hours in the early months of the cropping season relative to the sunshine duration averages recorded over many recent years (from -77.9 hours to 77.3 hours) (in figure 4). The average monthly air humidity in most localities in the country has a common value that is approximately or fluctuates around

the average value (from -16% to 9%). In the mid-crop period and at the end of the season, the total monthly sunshine hours fluctuated around the average value (from -55.2 hours to 110.5 hours). The average monthly atmospheric humidity in most of the regions around the annual averages recorded over recent years (ranging from -15% to 10%).

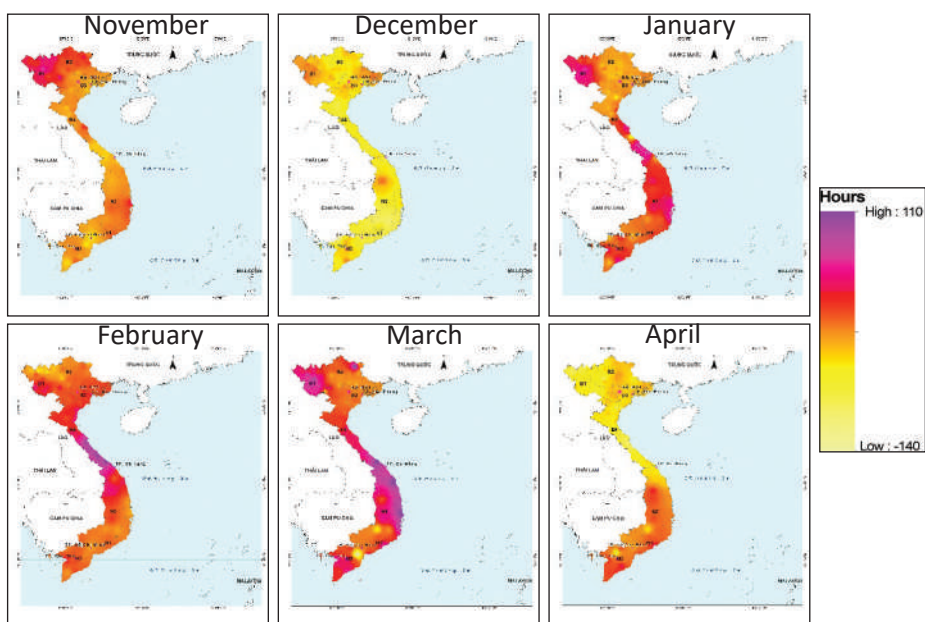


Figure 4. The difference of sunshine of the winter-spring crop season 2020 with the the average of many years

Extreme weather events [8, 10]:

During the early months of the season, the Northern midlands and mountains often experience thunderstorms for 1 to 3 days. In the central and Southern regions, thunderstorms usually last longer, from 1 to 10 days. Drizzle also occurs earlier than usual in the Central region, and later also in February in the Northern midlands and mountains.

In the mid-crop months, hot and dry westerly winds from Laos are becoming more common, especially more extreme in the southern region. This kind of wind occurs from 3 to 27 days, of which six days, typically intense in Dong Phu, other places also Ayunpa and Kon Tum. Thunderstorms also appear more than they used to during this period, primarily in the Central Highlands for a duration of 1 - 12 days.

At the end of the season, thunderstorms appear in most areas from 4 to 16 days in the South. Hot and dry weather occurs in the Southeast region (Bien Hoa, Xuan Loc, Tan Son Nhat, Dong Phu, and Phuoc Long), lasting from 9 to 27 days where it intensifies for 3 - 11 days. This weather pattern is also seen in the Southwest region including Soc Trang, Can Tho, and Cang Long lasting for 16 - 21 days while other regions experience a shorter occurrence between 2 - 7

days at a mild intensity.

3.1.2. Observed meteorological conditions influencing agricultural productivity in the winter-spring season

At the beginning months of crop growth period (December 2019 to January 2020), agricultural, forestry and fishery production activities at the end of 2019 face multiple stresses, in particular prolonged droughts and severe heat affect crop yields and productivities. Besides, African swine fever spreads across the country causing serious losses to the livestock industry and also consumers. In January 2020 the unfavourable weather conditions interrupted agricultural production in most provinces. The surface monthly average temperature of these regions was primarily higher than the annual averages recorded over many recent years, but cold air waves in the beginning and middle of the month and the number of hours of sunshine decreases much lower than the the annual averages recorded over many recent years, which affected the harvest activities of winter crops and preparing land field for next winter-spring rice production.

Mid-season period:

Natural disasters happened in February,

mainly hail, heavy rain, landslides and salinity intrusion in some areas, damaging an extensive amount of roughly 15,000 hectares of rice and 878 hectares of crops. Some provinces suffered significant losses, for instance the hail and thunderstorms in Lao Cai affect 17.1 hectares of agricultural production area, and more than 1,000 poultries. In Yen Bai, there were more than 5 hectares of crops, ruining forestry trees and harm to 58 fish cages in Yen Binh district.

In March 2020, the main natural disasters such as hail, heavy rain, thunderstorms, salinity intrusion and land subsidence ruined nearly 24.3 thousand hectares of rice paddies and more than 6 thousand hectares of vegetable crops. In the South Central region and the Highlands, the prolonged drought also greatly affected agricultural production. Rainfall in the South Central provinces and the Highlands has decreased significantly due to the lower rainfall than the average recorded over many years. Therefore, water reserves in irrigation reservoirs are currently very low. At the end of February 2020, the amount of water in reservoirs in the South Central region only reached around 31 - 87% of the design capacity, 22% lower than the same period in 2019; in the Highlands, only reached 59 - 73%, it means 6% lower than the same period in 2019. In the South Central Coast and Highlands a total of approximately 1,392 hectares of agricultural production (1,157 hectares of rice paddies and 235 hectares of coffee) are suffering from water shortages.

End-season period:

During this time, the most common natural disasters were hail, heavy rain, landslides and salinity intrusion in some areas causing a failure of 29.4 thousand hectares of rice paddies and 9.2 thousand hectares of crops. Total economic loss caused by such natural disasters is VND 1,577.4 billion. Currently, the drought event still intensifies in the Central and Highland provinces.

Agro-meteorological conditions in May 2020 in most Northern regions are relatively favorable for crop planting and growth. During this time there was an increase in the number of days with thunderstorms and heavy thunderstorms in some areas. In particular, hot and dry westerly winds appeared in places while hot

and dry weather waves with strong intensity occurred in Northwest, North Central, South Central, Highlands, and the South, which had strong impacts on agricultural production. Natural disasters in May were mainly hail, heavy rain, landslides and salinity intrusion in some areas, damaging 32.2 thousand hectares of rice paddies and 10.3 thousand hectares of vegetable crops. Particularly, drought and salinity intrusion occurred in 6 provinces: Kon Tum, Gia Lai, Tien Giang, Ben Tre, Tra Vinh, Soc Trang, which caused damage to more than 8.7 thousand hectares of rice paddies and 917 hectares of vegetable crops.

3.2. Assessment of agrometeorological conditions in main season in 2020

3.2.1. Detailed changes of meteorological conditions

The 2020 crop started from May to November. The average atmospheric temperature in the early months of the season in 2020 across all parts of the country was generally higher than the annual averages recorded over many recent years (between 0.1°C and 3.2°C higher) (Figure 5).

Other areas, including Son La, Hoa Binh, Phu Tho, Lang Son, North and Central North regions, Northwest part of the Mekong Delta, experienced the lower temperature than the annual averages recorded over many recent years (0°C - 2.6°C). The absolute highest temperature of 35.3°C occurred on October 1, 2020 in Song Ma and the absolute lowest temperature of 7°C occurred on October 11, 2020 in SaPa. During the last months of the season, the monthly atmospheric temperature was commonly (0.1°C to 3.2°C) higher than the averages recorded over recent years. The absolute highest temperature of 35.3°C occurred on November 17, 2020 in Bien Hoa, and the absolute lowest temperature of 7.3°C occurred on November 11, 2020 in Sin Ho.

The monthly rainfall in most of the areas was higher than the annual averages recorded over many recent years (from 0 to 2450 mm). The exception occurred in some areas of the Northwest and Northeast, Tay Ninh, where the rainfall was 0mm -167 mm lower than the averages recorded over many recent years. The

highest total rainfall per month was 3449 mm in A Luoi, and the lowest is 21 mm in Tuan Giao.

The highest rainfall per day of 756 mm occurred on October 19, 2020 in Ba Don (Figure 6).

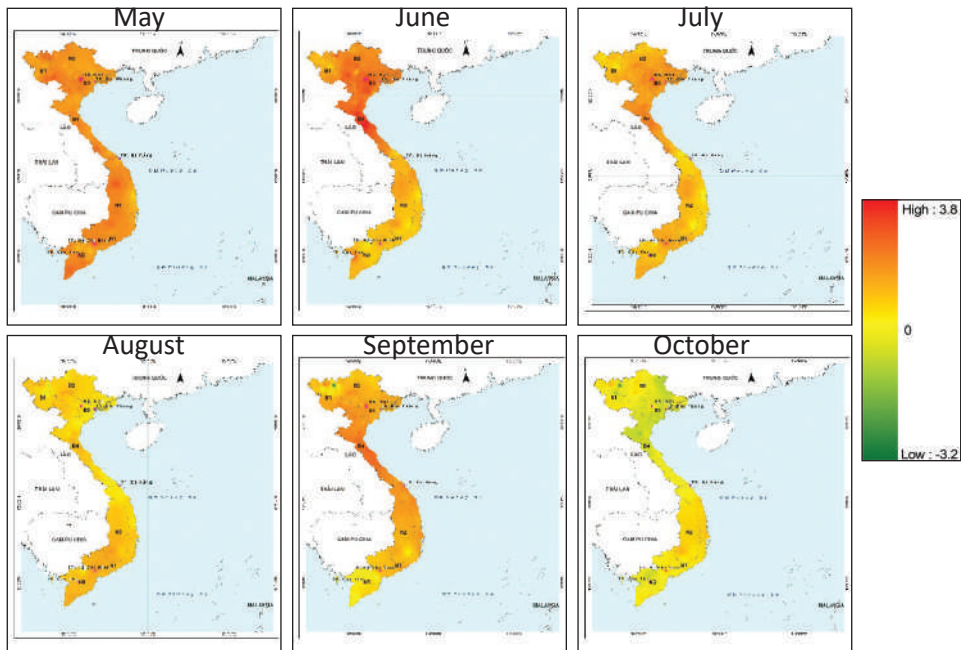


Figure 5. Temperature mapping relative to the average temperatures over many years in the main season 2020

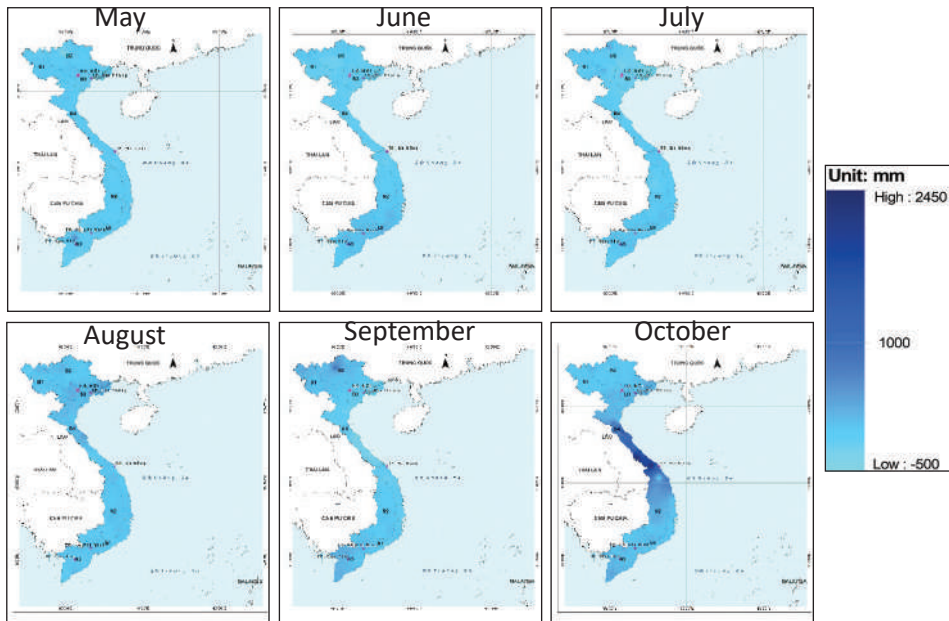


Figure 6. The difference of precipitation in main season months in 2020 with the average of many years

The monthly rainfall in most region was lower than the annual averages recorded over many recent years (from 0 to 181.7 mm), except for some areas of Quang Binh and Quang Ngai, the Central Highlands it was recorded higher than

the averages recorded over many recent years from 0mm to 830.5 mm. The highest total rainfall per month was 1746 mm in Tra My, the lowest was 1 mm in That Khe. The highest daily rainfall of 463 mm occurred on 11/11/2020 in A Luoi.

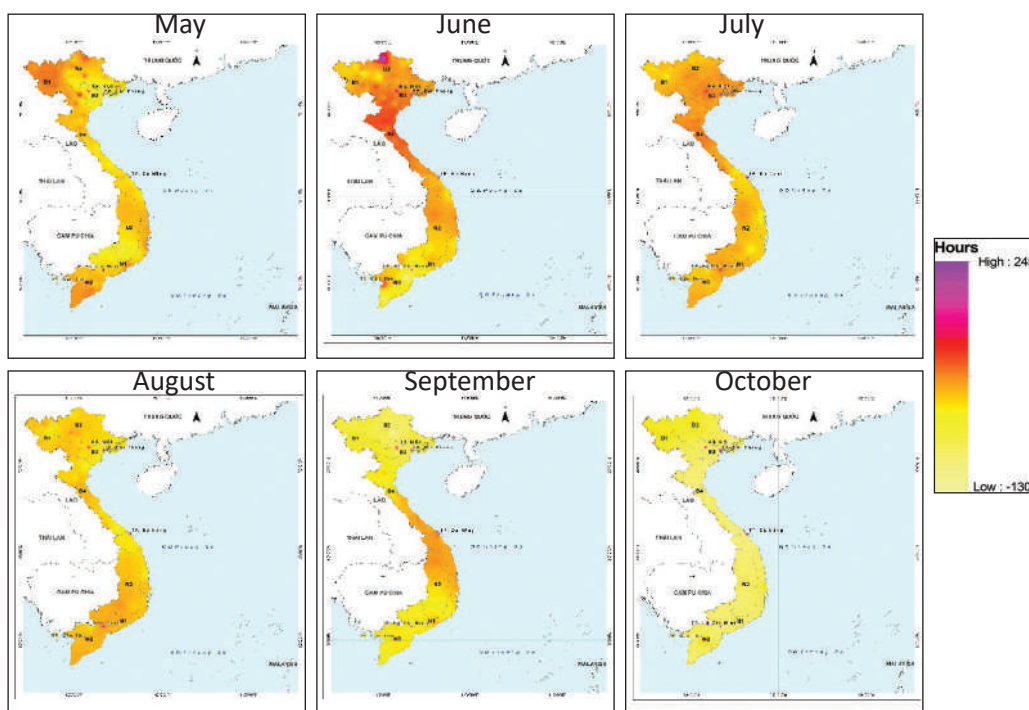


Figure 7. The difference of sunshine of the main crop season 2020 with the the average of many years

The total number of monthly sunshine hours in most of regions was (from 0 to 111 hours) lower than the averages recorded over many recent years, other areas such as Lai Chau, Quynh Nhai and Ha Giang experienced from 0 to 54 hours higher than the averages recorded over many recent years. The average atmospheric humidity per month in most parts of the country was 0 - 7% higher than the averages recorded over many recent years, except for the Northern Midlands and Mountains, the Northern Delta, and the Northern Midlands. Thanh Hoa and Nghe An which experienced 0% to 12% lower than the averages recorded over many recent years.

Extreme weather events:

The situation was recorded relatively similar to those of the winter-spring season, during the early months there were often thunderstorms, dry and hot weather events in the Northern mountain and midland areas. In the Northern and Northern-central and southern regions, the hot and dry phenomenon happened with stronger intensity for 18 days. During the middle and late months, there was mild drought in the Northern mountainous and midland areas. No extreme

weather event occurred in the Central and Southern regions.

3.2.2. Observed meteorological conditions influencing agricultural productivity in the main crop season 2020

Early season period

Agro-meteorological conditions observed in July 2020 in most parts of the North were relatively favorable for crop planting and growth. However, there was hot dry westerly wind in the Central region resulting in hot, more evaporation than rainfall, leading to a shortage of water for agricultural production. Natural disasters in July were mainly hail, heavy rain, landslides and salinity intrusion in some areas, causing damage of 11.9 thousand hectares of rice paddies and 24.7 thousand hectares of vegetable crops. In July, agricultural production activities primarily included starting new rice paddies, cultivating summer-autumn cropping and harvesting summer-autumn rice early, ensuring planting and harvesting in the best practices. However, the prolonged heat caused drought in some areas, and affected the progress of rice cultivation.

As effects of the tropical storm No. 2, excessive rainfall was generated in the provinces

of the Northern Delta, the North Central Coast, and some other places of the Northern Midlands and Mountains, causing significant loss in people and economy. Further than that, the hot and dry westerly wind remained strongly active in the Central region, resulting in low local water shortage for agricultural production. In the Mekong Delta, floods and high tides also affected agricultural production. Natural disasters mostly storms, heavy rains, landslides, tornadoes occurred in July 2020, that ruined 7 thousand hectares of rice paddies and 2.9 thousand hectares of vegetable crops.

Mid season period

In August 2020, such weather events as significant rainfall, several rainy days occurring in different times of a month, and good temperature and sunshine hours, sharply decrease in extreme hot and dry winds days compared to previous months supported crop growth and development.

Similar weather conditions remained till September with significant rainfall, more frequent rainy days together with good sunshine hours, less hot dry westerly wind compared to the previous months. These contributed to the proper growth and development of crops. However, there was a storm No. 5 at the beginning of the month and heavy rain in the central provinces, causing loss in human and economy. In addition, the hot dry westerly wind remained strongly active in the Central region, it resulted in shortage of water for agricultural production in some locations. In the Mekong Delta, floods and high tides also affected cropping activities. Some natural disasters in September including mainly storms, floods, heavy rains, cyclones and landslides ruined 4.4 thousand hectares of rice paddies and 3.7 thousand hectares of crops.

End-season period

Natural disasters occurring in October were mainly storms, heavy rains, landslides, tornadoes, particularly consecutive storms No. 6 (Oct 12), No. 7 (Oct 14), No. 8 (Oct 25), No. 9 (Oct 29) hit in the Central region, causing heavy rain, significant losses to agricultural production in some provinces of Northern Midlands and Highlands, where thousand cattles and 600.5

thousand poultrys died; 45 thousand hectares of rice and 22.3 thousand hectares of crops were ruined.

In November 2020, natural disasters primarily included storms, floods and landslides, causing excessive losses of 5.6 thousand cattles and 1.5 million poultrys; 66.7 thousand hectares of rice and 35.4 thousand hectares of crops. In particular, the damage caused by storm No. 11 in Nghe An, as a result of heavy rain and flood after the storm, the water level in the fields of some deltas increased, thus 100% of the remaining rice area and all winter crops were completely damaged.

4. Conclusion

This study aims to review agro-meteorological conditions in Viet Nam 2020. Based on such information, they can make better decisions on agricultural production activities which help improve yield and productivity in following years, and adapt to expected adverse weather events. The initial assessment shows that in 2020, natural disasters occurred continuously and had complicated developments. It greatly affects agricultural production activities in Viet Nam, especially rice and crop production.

The assessment of agro-meteorological conditions in the winter-spring crop of 2020 shows that the temperature in the first and last months of the crop is higher than the average value of many years from 0.2 to 5.7°C. The change in rainfall tends to increase more in the central region in the starting months of the crop. In the last months of the crop, rainfall changes tend to be more in the North and North Central. As for the change of sunshine hours, there is a strong change and an increasing trend in the mid-crop months (January, February and March). Extremely weather such as heavy rain, hail; drought and hot weather have greatly affected rice and crop production; Thunderstorms are quite frequent in the winter-spring crop, however, reports indicate no damage to crops;

The assessment of agro-meteorological conditions in the main crop of 2020 shows that the temperature in 2020 will be 0.1 - 3.6°C higher than the average value of many years. Monthly rainfall in most areas is lower than the average

value of many years (from 0 to 181.7 mm), except for some areas from Quang Binh to Quang Ngai, the Central Highlands is higher than the average for many years from 0mm to 830.5 mm. The total number of monthly sunshine hours in most areas is lower than the average number of years from 0 to 111

hours; Lai Chau, Quynh Nhai and Ha Giang areas are higher than the average for many years from 0 to 54 hours. The crop of 2020 agricultural production is strongly affected by storms, heavy rains, landslides, floods, landslides and cyclones, especially in the central coastal provinces.

References

1. Food and Agriculture Organization of the United Nations, (2016). *Activity Manual - World Food Day 2016*. <http://www.fao.org/publications/card/en/c/I5685VI/>.
2. General Department of Meteorology and Hydrology, M.o.N.R.a.E., (2020). *Statistical meteorological data in 2020*.
3. IMHEN and UNDP, (2015), *Viet Nam Special Report on managing the risks of Extreme Events and Disasters to Advance Climate Change Adaptation* [Tran Thuc, Koos Neefjes, Ta Thi Thanh Huong, Nguyen Van Thang, Mai Trong Nhuan, Le Quang Tri, Le Dinh Thanh, Huynh Thi Lan Huong, Vo Thanh Son, Nguyen Thi Hien Thuan, Le Nguyen Tuong]. Viet Nam Publishing House of Natural Resources, Environment and Cartography, Ha Noi, Viet Nam.
4. IPCC, (2007), *Climate Change 2007: Mitigation. Contribution of Working Group III to the Fourth Assessment Report of the Intergovernmental Panel on Climate Change*, B. Metz, O. Davidson, P. Bosch, R. Dave and L. Meyer, Eds., . Cambridge University Press, Cambridge, UK.
5. Nelson, G.C., et al., *Climate change: Impact on agriculture and costs of adaptation*. Food Policy Report (21), ed. D.C. Washington. 2009: International Food Policy Research Institute (IFPRI). <http://dx.doi.org/10.2499/0896295354>
6. OECD, (2015). *Agricultural Policies in Viet Nam 2015, OECD Food and Agricultural Reviews*, . OECD Publishing, Paris, <https://doi.org/10.1787/9789264235151-en>,
7. Sönke Kreft, D.E.a.I.M. (2016), *GLOBAL CLIMATE RISK INDEX 2017. Who Suffers Most From Extreme Weather Events? Weather-related Loss Events in 2015 and 1996 to 2015*, ed. D.B. Joanne Chapman-Rose. 2016, Kaiserstr. 201 Stresemannstr. 72 D-53113 Bonn D-10963 Berlin Germanwatch e.V.
8. The National General Administration of Natural Disaster Prevention and Control Viet Nam, (2020). *Report on the situation of natural disasters in 2020*.
9. Viet Nam General Statistic Office., (2020). *Report of Socio-economic Situation In The Fourth Quarter And The Whole Year 2020*. <https://www.gso.gov.vn/en/data-and-statistics/2021/01/socio-economic-situation-in-the-fourth-quarter-and-the-whole-year-2020/>
10. Viet Nam General Statistic Office. (2021), *Statistical yearbook of Viet Nam 2020*. Ha Noi, Viet Nam: Viet Nam General Statistic House.
11. Viet Nam Institute of Science Hydrology and Climate Change, (2020). *The Agricultural Meteorological Notice*. <http://www.imh.ac.vn/nghiep-vu/cat54/Thong-bao-khi-tuong-nong-nghiep>.
12. Viet Nam Meteorological and Hydrological Administration, (2020). *Announcement of Agricultural Meteorology*. <http://vnmma.gov.vn/thong-bao-can-h-bao-ktnn-140>.
13. World Bank, (2011). *Climate-Resilient Development in Viet Nam: Strategic Directions for the World Bank*. 105p.

CHANGES IN AIR QUALITY DURING COVID-19 SOCIAL DISTANCING IN HA NOI CITY

Ngo Thi Thuy⁽¹⁾, Tran Van Tra⁽²⁾, Cung Hong Viet⁽¹⁾, Nguyen Dinh Hoang⁽¹⁾

⁽¹⁾Viet Nam Institute of Meteorology Hydrology and Climate Change

⁽²⁾Water Resources Institute

Received: 15 July 2021; Accepted: 11 August 2021

Abstract: *The COVID-19 pandemic has changed people's lives in many ways. Under the impact of COVID-19, the economy and society face challenges to recover. To control the spread of the COVID-19 epidemic, Viet Nam and countries around the world have restricted unnecessary travelling and transportations. The regulations on social distancing have significantly changed people's habits, activities, living and working styles. Many studies have shown that social distancing has significantly changed air quality. This study was conducted to assess the change of air quality in Ha Noi during the social distancing period. The evaluation is built based on measurements at air monitoring stations in the period before and after social distancing in 2021. The results show a significant improvement of air quality compared to its situation before social distancing at most of the air monitoring stations. The average daily VN_AQI index at Nguyen Van Cu station (Long Bien district), Kim Lien (Dong Da district), Tan Mai (Hoang Mai district) and Tay Mo (Nam Tu Liem district) and Minh Khai (Bac Tu Liem district) in the first 8 months of 2021 dropped from 97 (near unhealthy grade for sensitive groups) to 52 (near good) in averaged. The concentration of other pollutants (PM_{10} , $PM_{2.5}$) at other stations also show a significant decrease compared to the previous time.*

Keywords: *Air quality, monitoring stations, COVID-19, social distancing.*

1. Introduction

The coronavirus (SARS-CoV-2) was first detected in Wuhan City, China, in December 2019 and rapidly spread in 2020 and 2021 to most of countries in over the world. To control the spreading of the virus, countries have imposed social distancing which resulted in dramatically decrease in transportation and travelling. Besides, it is reported that people in some cities themselves have avoided unnecessary going out during the pandemic. Clearer skies during the social distancing period were observed with normal eyes in some cities.

Viet Nam recorded the earliest cases on 23 January 2020 and reached 635,000 cases currently [12]. The country now is in the fourth wave of COVID-19 with the longest social distancing period since 27 April 2021. Restrictions

released through dispatches and directions included; (a) people to stay at home, except for limited purposes; (b) suspending schools and promoting online education; (c) closing of all non-essential businesses and public venues; and (c) stopping all gatherings of more than two people in public [5, 6, 7].

Social distancing or lock-down in many countries is considered as a reason changes air quality in cities and industrial zones due to shutting down of power plants, transportation and manufactures. The air quality change during COVID-19 in China [2, 9, 10, 11, 21], USA [15], Brazil [3, 17], Spain [18] and Morocco [14] shows significant improvement in several air pollutants such as particulate matter (PM_{10} , $PM_{2.5}$), nitrogen dioxide (NO_2), carbon monoxide (CO) and SO_2 .

In this study, the air quality of Ha Noi is assessed by six pollutants including PM_{10} , $PM_{2.5}$, NO_x , SO_2 , CO and O_3 collected from 11 stations in Ha Noi. The VN_AQI index is also calculated following Decision No.1459/QD-TNMT [4] at

Corresponding author: Ngo Thi Thuy
E-mail: tide4586@gmail.com

Nguyen Van Cu, Kim Lien, Tan Mai and Tay Mo stations to assess the composite air quality in Ha Noi. A comparison between air quality measurements during social distancing months and observation in previous periods is also implemented to retrieve the impact of COVID-19 pandemic on air pollution.

2. Data and Methodology

2.1. Study area

Ha Noi, the capital of Viet Nam, is located in the Red River Delta. The city occupies an area of 3,358.6 km² [12] and being the second largest city in Viet Nam. Ha Noi consists of 12 urban districts, 1 district-level town and 17 rural districts. Population of Ha Noi is about 8,053,700, including 49.2% of population living in urban areas and 50.8% in rural areas [8]. The city has experienced a construction boom with numerous skyscrapers and roads connecting citadel areas with industrial zones and rural areas.

The city has a humid subtropical climate with a plentiful rainy season from May to October. The average annual rainfall is 1,612 mm with around 85% of rainfall in rainy season. The mean temperature in Ha Noi is 23.6°C accompanying with relative humidity of more than 80%. The hottest month is July and the coldest month is January.

In recent years, the problem of air pollution has been becoming an attention of not only scientific researchers but also authorities and local residents. The danger, potential harm to health and the impact on daily life hit the top news. At air quality monitoring stations located in Ha Noi, the air quality index (AQI) frequently fluctuates around the unhealthy threshold. Most recently, the Global Air Quality Report by IQAir AirVisual in cooperation with Greenpeace in Southeast Asia shows that, in the data collected in some cities at some time, Ha Noi is the second most polluted city in Southeast Asia, as shown by the index of substances that adversely affect the air, exceeding the level recommended by WHO [10, 20]. Although this information was later inaccurately confirmed by the Viet Nam Environment Administration due to the representativeness of the samples, the air pollution in Viet Nam and especially Ha Noi is

undoubtable and is getting worse, shown in many reports such as the National Environmental Report on the air environment (2013), the National Environmental Report on the urban environment (2016).

2.2. Status of COVID-19 pandemic and lockdown periods in Ha Noi

According to the data from Ha Noi CDC, Ha Noi has 3,695 COVID-19 cases in the third and fourth waves of COVID-19 in 2021 (up to 9th September, 2021). In which, there were 35 cases in the third wave from 28 January to 17 February and 3,660 cases in the fourth wave lasting from 29th April to 9th September. To control the covid pandemic and promote socio-economic development, the Ha Noi People Committee released many documents that restrict activities of local residents. The critical documents are summarized as follows.

- 4 May 2021: Ha Noi Department of Education and Training were temporarily suspended all schools and education at all levels following the direction of the Ha Noi People's Committee at Official Dispatch No. 04/CD-UBND dated April 29, Dispatch No. 05/CD-UBND dated May 2 and Dispatch No. 06/CD-UBND dated May 3.

- 00h 5 May 2021: Temporarily suspending operations at cinemas, movie centers, massage service facilities, spas, gyms, stadiums, etc., to minimize crowded events, large parties and meals (weddings, anniversaries, birthdays, grand openings...);

- 12h 25 May: Temporarily suspending operation of some business and services such as restaurants, on-site food and beverage service establishments (only for take-out sales), do not organize meals and festivals with large crowds; Barber shops and hairdressers. Completely stop playing, exercising, and gathering at parks, flower gardens and public places.

- 13 July 2021: Dispatch No. 14/CD-CTUBND stops non-essential business activities" Restaurants, on-site food service establishments, only for takeout, stop thoroughly hair shops, enjoy activities at public and public places.

- 14 July 2021: Vehicles traveling from 14 provinces and cities with epidemics include: Ho Chi Minh City, Binh Duong, Dong Nai, Khanh Hoa,

Phu Yen, Dak Lak, Quang Ngai, Quang Nam, Da Nang, Hue, Ha Tinh, Nghe An, Thanh Hoa, Ha Nam requested to turn back, not to move into Ha Noi.

- From 24 July 2021: All unnecessary services are restricted, moving allowance is required with all citizens.

2.3. Data

By 2016, there are 12 automatic air quality monitoring stations in Ha Noi including 10 stations under the management of the Ha Noi Department of Natural Resources and Environment (started in 2017), 01 station under the management of the Viet Nam Environment Administration (since 2010), and 01 monitoring stations managed by the US Embassy (Figure 1). By July 2019, the French Embassy installed

an air monitoring station, measuring $PM_{2.5}$ concentration at the embassy campus. By May 2020, THT Co., Ltd. (Korea) sponsored and handed over to Ha Noi 24 automatic air monitoring sensor stations. Up to this point, the total number of monitoring stations in the city is 37 [22]. Nevertheless, due to the lack of data availability, only 11 stations' data (Table 1) are analyzed in this report. In this study, the air quality of Ha Noi city is assessed using the six components including PM_{10} , $PM_{2.5}$, CO , O_3 , NO_x and SO_2 . Among 11 stations, there are 3 stations observe all of six air pollution components others do not have data of SO_2 and O_3 . The stations and observation data used in this study from ground stations are listed in Tables 1 and 2.

Table 1. Air pollution stations in Ha Noi city

No.	ID	Station	Address
1	CCBVM	Ha Noi Environmental Protection Department	Trung Hoa, Cau Giay district
2	MKhai	Minh Khai	People's Committee of Minh Khai Ward, Bac Tu Liem District
3	HDau	Hang Dau	Police Department of Hang Ma Ward
4	HKiem	Hoan Kiem	Police Department of Hoan Kiem district
5	KLien	Kim Lien	Kim Lien Kindergarten
6	MDinh	My Dinh	Nam Tu Liem Power Company
7	PVD	Pham Van Dong	36A Pham Van Dong street
8	TCong	Thanh Cong	Thanh Cong lake park
9	TMai	Tan Mai	People's Committee of Hoang Van Thu Ward
10	TMo	Tay Mo	Tay Mo commune, Nam Tu Liem district
11	NVC	Nguyen Van Cu	556 Nguyen Van Cu street

Table 2. Availability of air pollution data in Ha Noi city

No.	Stn ID	PM_{10}	$PM_{2.5}$	NO_x	SO_2	O_3	CO
1	CCBVM	2017 - 2018	2018				
2	MKhai	2017 - 2018, 2021	2018, 2021				
3	HDau	2017 - 2018	2018	-	-	-	2018
4	HKiem	2017 - 2018	2018	-	-	-	2018
5	KLien	2017 - 2018, 2021	2018, 2021	-	-	-	2018
6	MDinh	2017 - 2018	2018	-	-	-	2018
7	PVD	2017 - 2018	2018	-	-	-	2018
8	TCong	2017 - 2018	2018	-	-	-	2018
9	TMai	2017 - 2018, 2021	2018, 2021	-	-	-	2018
10	TMo	2017 - 2018, 2021	2018, 2021	-	-	-	2018
11	NVC	2010 - 2019, 2021					

Sine the data is not synchronous, the observation before 2021 is used to assess the air quality before COVID-19 pandemic while

the data observed from January to August 2021 is representative for air quality during COVID-19.

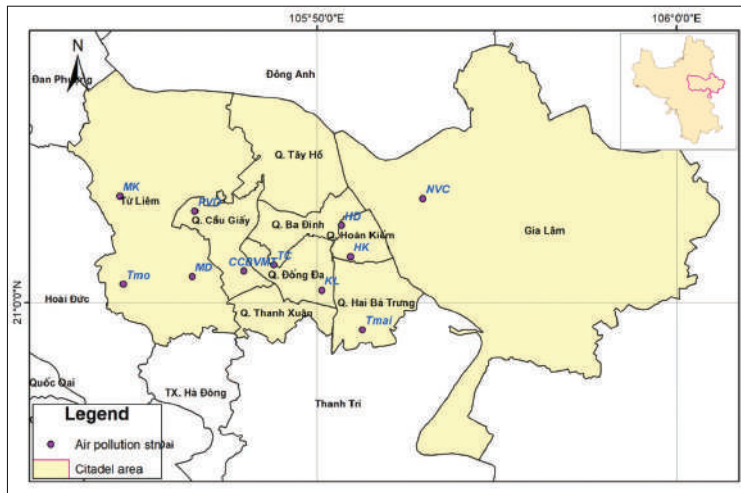


Figure 1. Map of the air pollution stations in the core area of Ha Noi city

2.4. Air quality index calculation

According to Decision No. 1459/QĐ-TCMT, Viet Nam Air Quality Index (abbreviated as VN_AQI) is an index calculated from monitoring parameters of pollutants in the air in Viet Nam, in order to indicate air quality status and its impact on human health, expressed through a scale. In

this guidance, AQI is applied to two types: The daily AQI is a representative value of air quality in a day; the hourly AQI is the AQI value representing the air quality for 1 hour. The Air Quality Index is calculated on a scale (6 ranges of AQI values) corresponding to icons and colors to warn of air quality and its impact on human health.

Table 3. AQI Quality Index Score Scale

AQI range	Air quality category	Color	Color code RGB
0 - 50	Good	Green	0;228;0
51 - 100	Moderate	Yellow	255;255;0
101 - 150	Unhealthy for sensitive groups	Orange	255;126;0
151 - 200	Unhealthy	Red	255;0;0
201 - 300	Very unhealthy	Purple	143;63;151
301-500	Hazardous	Maroon	126;0;35

In this study, the daily VN_AQI is calculated using the hourly and daily observation of SO₂, CO, NO₂, O₃, PM₁₀, and PM_{2.5}. VN_AQI calculation method requires at least 01 of 02 parameters PM₁₀, PM_{2.5} in the calculation formula. Specifically, the daily AQI value is calculated based on the following values:

- PM_{2.5} and PM₁₀ parameters: 24-hour average value.
- Parameter O₃: The maximum 1-hour average value of the day and the maximum 8-hour average value of the day.
- Parameters SO₂, NO₂ and CO: The maximum 1-hour average value of the day.

3. Results and Discussion

3.1. General distribution of air quality in Ha Noi

Since the collected data is nonsynchronous the assessment is implemented for PM_{10} at 10 stations from May 2017 to Dec 2018 and for all six mentioned components at Nguyen Van Cu (NVC) station from 2010 to 2019. The results are illustrated in Figure 2.

The average PM_{10} concentration in 24 hours at most of station in Ha Noi city is under the threshold indicated in Viet Nam Technical Standard (QCVN 05:2013/BTNMT). However, the concentration is far higher than the guideline of WHO [20]. When consider hourly distribution of PM_{10} , the analysis shows peaks at 8 am and 7 pm at most of station through Ha Noi city (Figure 3).

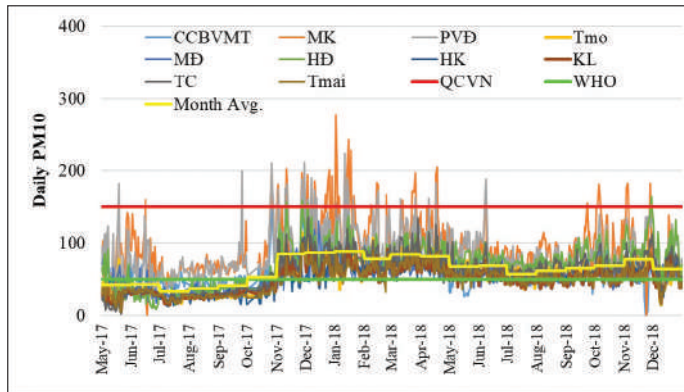


Figure 2. Change in daily PM_{10} concentration at stations from May 2017 to Dec 2018

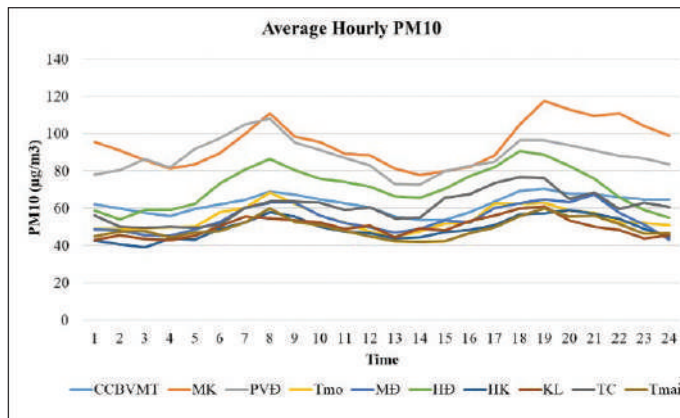


Figure 3. Distribution of PM_{10} concentration in a day

The analysis at NVC station in 10 years of observation shows an improvement trend of air

pollution in VN_AQI (Figure 4) from relatively unhealthy in 2010 to moderate level in 2019.

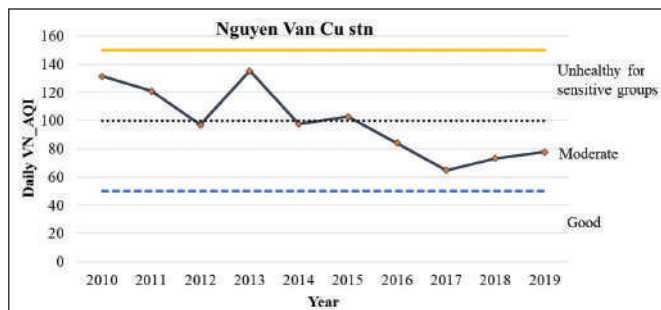


Figure 4. Change in PM_{10} concentration at NVC over time

3.2. Changes of air quality during COVID-19

Due to social distancing in 2021, the air quality of Ha Noi is significantly improved. The analysis of PM_{10} and $PM_{2.5}$ concentration at most stations in Ha Noi show a remarkable decrease from March to August 2021, except at Minh Khai station (Bac Tu Liem district)

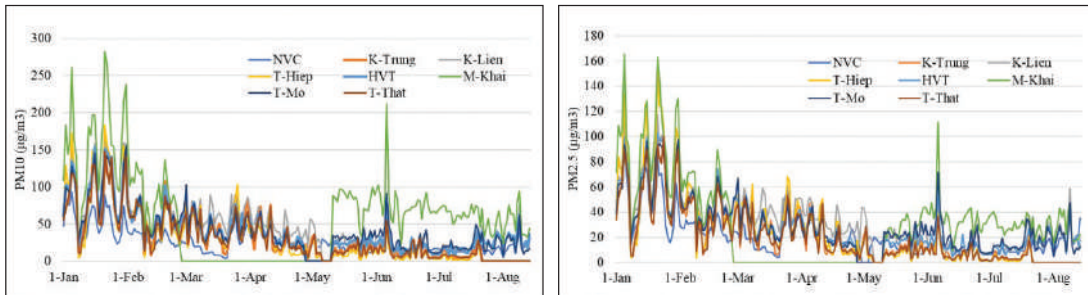


Figure 5. The change of PM_{10} (left) and $PM_{2.5}$ (right) at Ha Noi's stations in 2021

To analyze the change of VN_AQI during social distancing periods of 2021, the observation of six pollutant components at four stations inside Ha Noi citadel area including Nguyen Van Cu (NVC), Kim Lien (KLiен), Tan Mai (TMai) and Tay Mo (TMo) are collected (detailed in Table 2). From January 2021, the VN_AQI at these stations were around moderate to good quality. In monthly scale the average daily VN_AQI in 2021 was improved much more than before (Figure 6). Specifically, the monthly average AQI in 2021 (orange solid line) is lower than mean monthly average (red dash line). At the beginning 2021, Ha Noi experienced the 3rd wave of COVID-19 that corresponding to the start of AQI decrease. The index dropped from around 100 to 50 during Lunar New Year break and maintained in next months. After the 3rd wave of COVID-19 cases, the economic activities in Ha Noi had been recovering before facing the 4th wave from 27th April, 2021. In this period, the average AQI in Ha Noi (black solid line) fluctuated between 50 to 100 corresponding to moderate grade. At NVC, the AQI during this two month was in a slightly increasing episode.

In the 4th wave of COVID-19, the daily routine changed a lot. Schools at all levels were temporarily suspended, entertainment activities and on-site restaurants were not allowed. The

(Figure 5). Even though containing a peak concentration in Jun, the general trend at Minh Khai station represents remarkable decrease comparing to before pandemic. The overall PM_{10} and $PM_{2.5}$ in all stations are far lower than the threshold according to QCVN 05:2013/BTNMT.

partial social distancing was applied in Ha Noi city to restrict unessential activities. The average VN_AQI in May and June were at the good level and far smaller than multi-year mean average VN_AQI at most of considered stations except for Minh Khai station (Bac Tu Liem ward). At this station, the VN_AQI during social distancing period was lower than before and similar to the mean average. From the 4th wave of COVID's cases, a slight decrease of VN_AQI was recorded in most of stations comparing to the 3rd wave and the period after the 3rd wave as well (Figure 6). When comparing to the average trend in same period (red dash line), the VN_AQI during the 4th wave (orange line) illustrates a significant decrease in all months from May to August.

From 24 July a full social distancing was implemented in Ha Noi city, people were recommended stay home and the moving allowance reports are required. More specific, the 1st social distancing is from 24th July to 7th August, the 2nd is to 22nd August, the 3rd is to 6th September and the fourth until 21st September. In the 1st social distancing period (from 24 July) The VN_AQI present a slightly increase compared to preceding months. Even though this abnormal trend might be local, the delivery exploration should be considered as one of reasons.

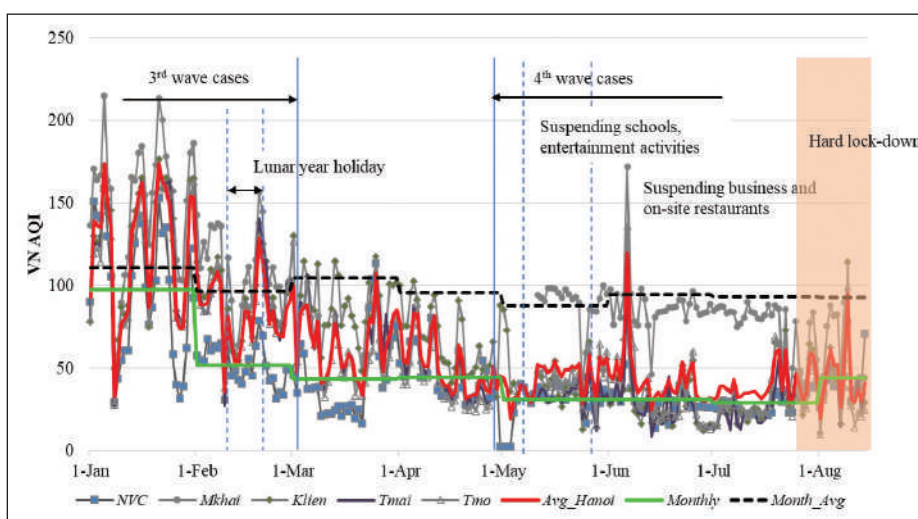


Figure 6. The change of daily AQI at some stations during COVID-19 pandemic

4. Conclusion

The study assessed the change of air quality at eight monitoring stations in Ha Noi during social distancing periods in 2021. The PM_{10} and $PM_{2.5}$ concentration at these stations show obvious decrease from January to August 2021. The comparison of VN_AQI at four stations inside Ha Noi during eight early months of 2021 also present dropping down between 2021

with multi-year average trend and between the first two months (January and February) with the remaining of the collection. This change of VN_AQI presents a close relation with restrictions in social distancing. The paper utilizes measurements at 11 stations in Ha Noi, however, the data collected is quite short and not synchronously. Due to this, local finding might be retrieved.

Acknowledgement: The study was supported by a grant from the project TNMT.2019.05.03, funded by the Viet Nam Ministry of Natural Resources and Environment (MONRE).

References

1. Berman, J. D. & Ebisu, K. (2020), *Changes in US air pollution during the COVID-19 pandemic*. Sci. Total Environ. 739, 139864.
2. Chen, L. W. A., Chien, L. C., Li, Y. & Lin, G. (2020) *Nonuniform impacts of COVID-19 lockdown on air quality over the United States*. Sci. Total Environ. 14110 5.
3. Dantas, G., Siciliano, B., França, B., da Silva, C. M. & Arbilla, G. *The impact of COVID-19 partial lockdown on the air quality of the city of Rio de Janeiro*. Brazil Sci. Total Environ. 729, 139085.
4. Decision No. 1459/QĐ-TCMT of Viet Nam Environment Administration *on the issuance of Technical Guidelines for calculation and publication of Viet Nam Air Quality Index (VN_AQI)*.
5. Directive No. 15/CT-TTg of the Prime Minister: *On drastically implementing the peak period of COVID-19 epidemic prevention and control*.
6. Directive No. 16/CT-TTg dated March 31, 2020 *on the implementation of urgent measures to prevent and control the COVID-1 epidemic*.
7. Directive 17/CT-UBND of the Ha Noi People's Committee *on social distancing in the city to prevent COVID-19 epidemic*.
8. General Statistics Office of Viet Nam (2019). *"Completed Results of the 2019 Viet Nam Population and Housing Census"* (PDF). Statistical Publishing House (Viet Nam). ISBN 978-604-75-1532-5.
9. He, G., Pan, Y. & Tanaka, T. (2020), *The short-term impacts of COVID-19 lockdown on urban air*

pollution in China. Nat. Sustain.

10. IQAir AirVisual and Greenpeace ASEAN, (2018), "Global air quality report".
11. Li, L. et al. (2020), *Air quality changes during the COVID-19 lockdown over the Yangtze River Delta Region: An insight into the impact of human activity pattern changes on air pollution variation*. Sci. Total Environ. 13928 2.
12. Ministry of Natural Resources and Environment (Viet Nam). Act No. 2908/QĐ-BTNMT of 13 November 2019 Announcements of area statistics for the whole country in 2018]. (in Viet Namese).
13. Nie, D. et al. (2020), *Changes of air quality and its associated health and economic burden in 31 provincial capital cities in China during COVID-19 pandemic*. Atmos. Res.10532 8.
14. Otmani, A. et al. (2020), *Impact of COVID-19 lockdown on PM₁₀, SO₂ and NO₂ concentrations in Salé City (Morocco)*. Sci. Total Environ. 735, 139541. <https://doi.org/10.1016/j.scitotenv.2020.139541>.
15. Parker, H. A., Hasheminassab, S., Crouse, J. D., Roehl, C. M. & Wennberg, P. O. (2020), *Impacts of traffic reductions associated with COVID-19 on Southern California air quality*. Geophys. Res. Lett. 47, e2020GL090164. 64.
16. Shi, X., & Brasseur, G. P. (2020), *The response in air quality to the reduction of Chinese economic activities during the COVID-19 outbreak*. Geophysical Research Letters, 47, e2020GL088070. 70.
17. Siciliano, B. et al. (2020), *"The impact of COVID-19 partial lockdown on primary pollutant concentrations in the atmosphere of Rio de Janeiro and São Paulo Megacities (Brazil)"*. Bull. Environ. Contam. Toxicol. 105, 2-8.
18. Tobías, C. et al. (2020), *"Changes in air quality during the lockdown in Barcelona (Spain) one month into the SARS-CoV-2 epidemic"*. Sci.Total Environ. 726(1-4).
19. Viet Nam Ministry of Health (MOH) <https://covid19.gov.vn/> assess date 15 Sep 2021
20. WHO (2005). *WHO Air quality guidelines for particulate matter, ozone, nitrogen dioxide and sulfur dioxide*.
21. Yuan, Q. et al. (2020), *Spatiotemporal variations and reduction of air pollutants during the COVID-19 pandemic in a megacity of Yangtze River Delta in China*. Sci. Total Environ.
22. <https://moitruongthudo.vn/>.



VIETNAM INSTITUTE OF METEOROLOGY, HYDROLOGY AND CLIMATE CHANGE

No.23 Lane 62 Nguyen Chi Thanh, Ha Noi, Viet Nam

Email: imhen@imh.ac.vn

Website: www.imh.ac.vn